2013

Phenotypic and Genotypic Models of Streptococcal Colonization of the Human Tonsil

Dennis J. Spencer

PHENOTYPIC AND GENOTYPIC MODELS OF STREPTOCOCCAL COLONIZATION OF THE HUMAN TONSIL

A Thesis Presented to the Faculty of

The Rockefeller University

in Partial Fulfillment of the Requirements for

the degree of Doctor of Philosophy

by

Dennis J. Spencer

June 2013

PHENOTYPIC AND GENOTYPIC MODELS OF STREPTOCOCCAL COLONIZATION OF THE HUMAN TONSIL

Dennis J. Spencer, Ph.D.

The Rockefeller University 2013

Pharyngitis due to oropharyngeal infection with *Streptococcus pyogenes* is most commonly treated by using penicillin-derived antibiotics.While treatment failure in the 1950's was reported in 4-8% of children, more recent studies have alarmingly found antibiotic failure as high as 20-40% providing the impetus to study this important pathogen. The contiguous mucosa along neighboring oropharyngeal surfaces is classically unaffected during Strep "Throat" suggesting pathogen specificity for palatine tonsil epithelium. While recent studies are advancing the premise of pathogen-host microenvironment effects on streptococcal virulence, the specific interaction between *S. pyogenes* and the human tonsillar surface relative to neighboring tissues remains insufficiently understood.

This thesis investigates the unique interaction between the Group A Streptococcus, GrAS, and the human tonsil surface. We were particularly interested in the transcriptional response exhibited by the bacterium during co-culture with this tissue epithelium compared to epithelium from an anatomically neighboring sight to determine if phenotype might be informed by the genotypic

profile. During the course of this work, we introduce new palatine tonsil tumor-derived cell lines for their novel usefulness as a model for studying pharyngitis. Using primary tonsil epithelial cells from non-malignant patient samples to confirm our studies with the cancer cell line, we were successful in demonstrating a tissue-specific phenotype and have begun the process of elucidating the genotypic nuances that an M1 strain exhibited in direct response to the tonsillar environment. These and further studies should allow us to better understand the pathogenic adaptions exhibited by this bacterium at its preferred target niche for infection.

"It must be borne in mind that the tragedy in life doesn't lie in not reaching your goal. The tragedy lies in having no goal to reach. It isn't a calamity to die with dreams unfulfilled, but it is a calamity not to dream. It is not a disaster to be unable to capture your ideal, but it is a disaster to have no ideal to capture. It is not a disgrace not to reach the stars, but it is a disgrace to have no stars to reach for. Not failure, but low aim is sin."

Dr. Benjamin Elijah Mays – 6th President of Morehouse College

I dedicate this dissertation to those who I try to be the best Me I can be for…

To the Blue Nile Rites of Passage. To the Explorer mentorship program. To the members of the Student National Medical Association. To the members of the NYC Minority Graduate Student Network. To the BNGAP initiative. To Dione. To Aqil.

To my FAMILY (Dennis, Judie, Taneka, Jinae, Alijah, Asaiah, Anastacia, Herbert, Alice, Frank, Justine, Marjorie…) I hope I've done you proud.

I Love You all so much!

Acknowledgements

First and foremost, I must thank my advisor, Dr. Vincent Fischetti for welcoming me into his laboratory and providing this amazing opportunity. I have grown so much, both scientifically and as a person. I do hope to continue to glean from your wisdom and experience as I continue on in my career. The Fischetti lab "experience" is one that I will always treasure…and I am grateful.

I also must thank my faculty advisory committee, Drs. Sanford Simon, Emil Gotschlich, and Dirk Schnappinger for their willingness to provide great insight during my committee meetings, and their patience with me. I am additionally grateful to Dr. Jon Heinrichs, my mentor from Merck & Co., who has gone above and beyond the call of duty. His decision to join my committee, enduring travel from out of state on each occurrence leaves me truly humbled. I would be remiss to not acknowledge my indebtedness to Dr. Edward Kaplan for his willingness to read my dissertation and serve as an outside examiner within the "short window" of dates we offered him.

I would also like to thank the surgeon physicians in the Department of Otorhinolaryngology at Weill Cornell Medical College (Drs. Max April, Robert Ward, Vikash Modi, and Jacquelyn Jones) for their continued support throughout this work, providing me with fresh tonsil samples. I must thank in particular Dr. Michael Stewart, Department Chairman, and Dr. Erich Voigt for their particularly extraordinary support and taking an interest in my success with this work.

Finally I would like to thank the members of the Laboratory of Bacterial Pathogenesis. In particular, I must thank Dr. Patricia Ryan for both mentorship and friendship. She too has been patient with me and has helped me throughout this process. I do not know what I would've done without her. I also thank Drs. Barbara Juncosa and Chad Euler for welcoming me into the "cool" Group A Strep Group. I MUST also thank Mrs. Clara Eastby 1000X over for her indispensable tissue culture support. She NOW has my blessing to retire.

Finally, I must thank the Weill Cornell / Rockefeller / Sloan-Kettering Tri Institutional MD-PhD program for their continued support and guidance. Dr. Olaf Anderson's ever-insightful conversations have surely been crucial to my success to this point.

Table of Contents

LIST OF FIGURES

LIST OF TABLES

§1. INTRODUCTION

1.1 Genus Streptococcus

Streptococcus is a genus of facultative anaerobic bacteria that consists of over 100 recognized species. Named for it's morphology, "Strep" from the Greek word στρεπτος "streptos" which translates to mean "twisted" or "chained", and the word "kokhos" meaning a "berry" or "seed", it is among the most studied gram positive pathogens. Early observations by such historic investigators as Van Leeuwenhoek in the 17th century and Louis Pasteur in the 19th century identified this pathogen in the context of its interaction with human host. Pasteur also proposed that these "rounded granules (microorganisms) arranged in the form of strings of beads" found in the bodies of diseased women in the maternity wards as being the infective cause. In this regard, streptococcus served as one for the first microbes identified as a contagious agent.

1.2 Classification System

Gram Positive bacteria are characterized by a thick cell wall matrix composed of peptidoglycan (PG), teichoic acid, polysaccharides (PS), and a cadre of cell wall associated proteins (CWPs) (Figure 1.1). Identification of unique cell surface antigens have provided some of our earliest understanding of streptococcal pathogenesis as well as providing a convenient means for organizing the genus into classification schemes of related species.

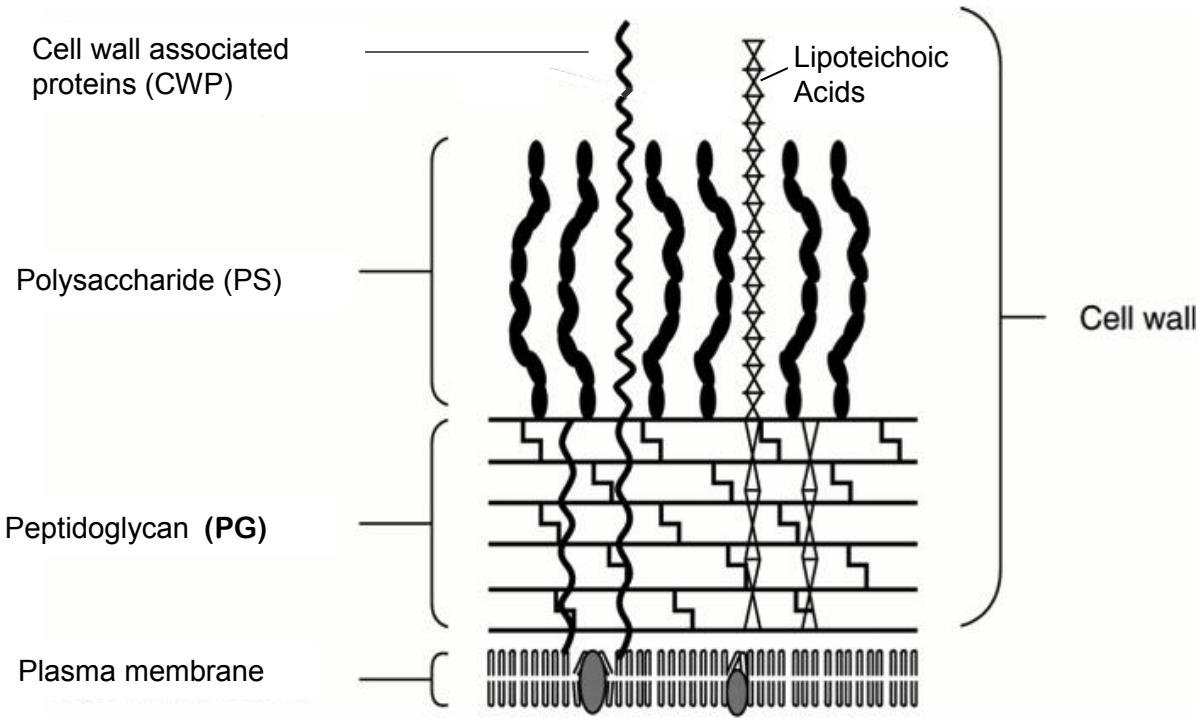

Figure 1.1. Gram positive bacterial cell wall contains mainly peptidoglycan (PG), polysaccharide (PS), and cell wall associated proteins (CWPs). The CWPs outside the PS and PG layers can be removed by proteolytic enzymes, whereas the proteins inside the PG layer are difficult to remove without breaking the PG structure. PS binds covalently to the PG layer, and protects PG polymers from the degrading enzymes. PG consists of several of sugar chains composed of N-acetylglucosamine and N-acetylmuramic acid alternately linked each other. Short peptides bound to the N-acetylmuramic acid (muramyl peptides) connect the sugar chains.

Image modified from Zhang *et al* 2001

1.2.1 Lancefield Classification

Despite Leeuwenhoek and Pasteur's important morphologically descriptive accounts on Streptococcal bacteria, a widely accepted classification system for this historic bacterium was not adapted until hundreds of years later in the 20th century. Developed by Dr. Rebecca C Lancefield at the Rockefeller University, this system of grouping related streptococcal species was based on serologically active polysaccharides associated with the bacteria's cell wall (Cunningham 2000). These aptly named "Lancefield Groups" were stratified by "group specific antigens" or C –substances such as polysaccharides (ie. groups A, B, C, E, F, and G), techoic acids (ie. groups D and N), and lipoteichoic acids (ie. group H). Notably, Group A carbohydrate is composed of *N-acetylglucosamine* linked to a rhamnose polymer backbone. The Lancefield typing system remains a cornerstone of the diagnosis of many streptococcal diseases, including the identification of *S. agalactiae* using rapid test kits for the detection of the Lancefield Group B carbohydrate (GBC) (Sutcliffe 2008). *Streptococcus spp*, may also be grouped using 16s rRNA gene sequence analysis to produce a grouping scheme based on taxonomic relationship: Pyogenic, Bovis, Salivarius, Mutans, Mitis, and Anginosus. These molecular-based groups in some instances ungroup and regroup related members from disperate Lancefield Groups. For instance, the "Pyogenic" group includes respective members representing Lancefield Groups A, B, C, G, and L (Figure 1.1). *Streptococcus pyogenes* constitutes the sole species in the Lancefield Group A of Streptococci. The

name “pyogenes” comes from the word pyogenic, which served to distinguish this it’s association with pus formation.

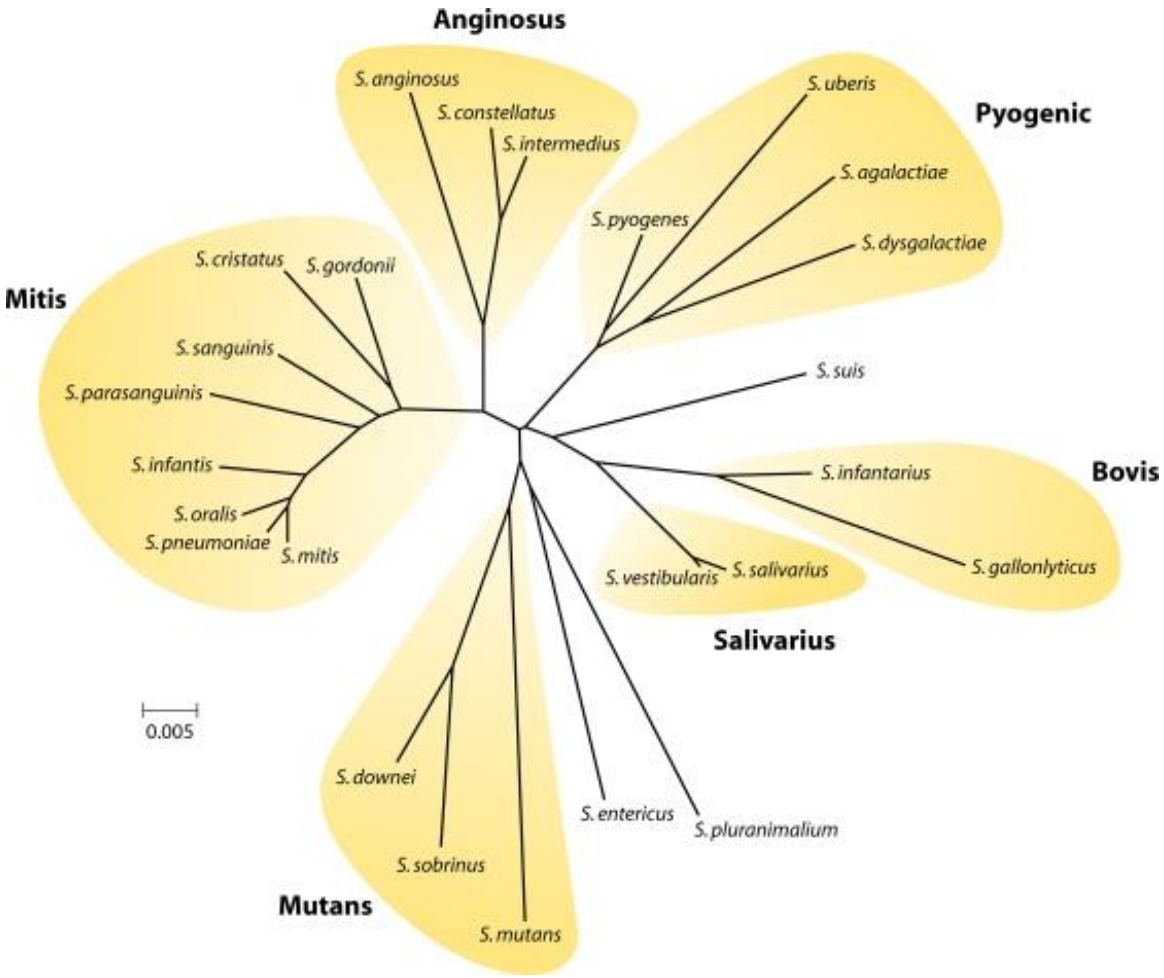

Figure 1.2. Taxonomic relationship tree for *Streptococcus* based on 16S rRNA gene sequence comparisons showing positions of selected species.

Nobbs *et al* 2009

1.2.2 R and T typing

Further classification systems within this group have historically been delineated by the surface antigen expressed by the streptococci, including the R, M and T proteins.

R proteins were initially identified in *S. pyogenes* by Rebecca Lancefield in the early1950's (Lancefield 1952). Later, groups would identify, four immunologically distinct R proteins (R1, R2, R3, and R4) occurring in various combinations in streptococci of groups A, B, and C. The R protein sequence has yet to be elucidated (Paoletti 2000).

The R, T and M antigens were found to uniquely participate in the serological reactions of group A streptococci. In the laboratory, the T typing assay is performed as an agglutination test. The T typing of group A streptococci has been important in the investigation of epidemiology of group A streptococcal infections and has identified strains associated with outbreaks when the M type was not identifiable (Cummingham 2000). It was also found that strains designated by M antigen may have serologically distinct T types (Lancefield 1946). Notably, the T protein was not present in streptococcal groups C and G (Cunningham 2000). Falugi *et al* also indicte one of the major drawbacks of the T-typing sera is that different centers have reported discrepant results This same group has recently described that pili, and in particular the backbone protein (BP) subunits, correspond to these Lancefield T antigens, and that the 15 BP variants account for all but 4 of the 21 T serotypes (Falugi 2008).

1.2.3 M typing / *emm* sequencing

Most commonly, GrAS typing is based on M protein gene (*emm*) sequence. The *emm* gene encodes streptococcal M protein, a surface exposed protein considered the the primary virulence factor of the organism. Variation within this gene's unique 5'sequence enables researchers to determine distinct "emm-"or "M-" types. Before this molecular approach was introduced, M protein serotyping was based on M precipitin reactions in capillary pipettes (Swift 1943). More than 200 *emm*/M-types have been identified (Bessen 2011, Johnson 2006) among Group A Streptococcal isolates.

1.3. Specialists vs Generalists

The primary ecological niches for GrAS are the epithelial surfaces of the upper respiratory tract and skin of the human host, and the vast majority of GrAS infections involve one of these two tissues, namely pharyngitis and impetigo, as aforementioned. Robust historical epidemiological evidence has demonstrated the causative strains for a respective tissue-specific infective phenotype have discrete sets of M or emm types. Five major *emm* chromosomal patterns were identified based on the number and arrangement of emm subfamily genes (Bessen 2010). According to this system, emm pattern groups A–D, are considered "specialist" and are all serum-opacity factor (SOF)-negative. *S. pyogenes* strains preferentially isolated from throat (ie. M1, M3, M6, and M18) belong to patterns A–C. Pattern D is composed of strains preferentially isolated

from skin sites. Bessen and colleagues provide a review of epidemiologic surveys on population-based collections of GrAS causing superficial throat or skin infections between1989 – 2009. Their robust analysis strongly supported the conclusion that GrAS strains harboring the emm pattern A-C genotype are better equipped to fill the superficial throat infection niche, as compared to emm pattern D (Bessen 2011). Global molecular analysis between groups have also revealed three accessory gene regions (AGR) may account for all statistical significant difference in genotypic biomarkers separating the throat vs skin specialists. Conversely, strains recovered readily from both tissues and are SOF-positive (ie. M49) are considered “generalists” and belong to Pattern E. (Bessen 1996, Klenk 2007). Significantly, emm pattern A-C genotypes are highly diverse in AGR content, suggestive of multiple genetic pathways associated with adaptation to their narrow niche (Bessen 2011).

Table 1.1Chromosomal *emm* patterns and related serotypes

Chromosomal Pattern	Infection	*emm* gene subfamily	M class[b]	Opacity factor reaction	Usual tissue site of isolation	Typical M serotype(s)
A	Pharyngitis[a]	SF1	I	Negative	Throat	1,3,6,12,17,19
B	Pharyngitis[a]	SF1-SF1	I	Negative	Throat	,24
C	Pharyngitis	SF1-SF3	I	Negative	Throat	1,5,14
D	Impetigo	SF4-SF1-	I	Negative	Skin	18
E	Pharyngitis or impetigo	SF3 SF4-SF2-SF3	II	Positive	Throat or skin	33,41,42,52,53,70 2,4,11,22,28,49,75

[a]All of the studies conducted that will be discussed in this dissertation will be of Chromosomal *emm* patterns A-B.
[b]Class I M proteins were identified by reactivity with anti-M protein Mabs 10.B6 and 10.F5; class II M proteins do not react with these Mabs.

Table contents originally modified from (Cunningham 2000)

1.4 Virulence Factors

The pathogenicity of Group A Streptococci is exhibited by the structure and function of proteins in their arsenal with such roles in virulence as adhesion to host cells, stimulation of host responses, binding of soluble factors, and immune evasion. The number of virulence factors that GrAS encodes varies, even between strains of the same phenotype (Cunningham 2000).

1.4.1 Adhesins

A key characteristic expected for a tissue-specific GrAS adhesin is differential binding to throat versus skin-derived cells or tissues of human origin (Bessen 2010). These microbial surface components recognizing adhesive matrix molecules (MSCRAMMs) represent a particular class of proteins expressed on the GrAS surface (Nobbs 2009). MSCRAMMs mediate bacterial binding to host serum- and extracellular matrix proteins, leading to firm attachment and in some cases also to internalization into host cells or paracellular translocation (as later described). MSCRAMMs are usually anchored covalently to the peptidoglycan of Gram-positive species by the transpeptidase activity of sortase enzymes recognizing a specific LPXTG amino acid motif located at the C terminus of these proteins (Nobbs 2009). Other important adhesin proteins, however, have been found to be either anchorless at the cell surface or linked to the streptococcal

surface other non-LPXTG motifs. List 1.2 elaborates on the known adhesins expressed by *S. pyogenes.*

1.4.1.1 M protein

M protein is one of the classical virulence determinants of *S. pyogenes* and is an important adhesin, This abundant protein appears as hair-like fibrils at the bacterial surface. Some of the 50 kDa α-helical coiled-coil M1 protein is spontaneously shed from the surface but some is also actively released through cysteine protease (SpeB) secreted by the bacteria. M1 protein contains fibrinogen-, IgG- and albumin-binding regions, properties that are important for adhesion and its overall virulence. In addition, M1 protein is important for the adhesion of *S. pyogenes* to epithelial cells via glucosaminoglycans (GAGs) and sialic acid containing cell surface proteins (Ryan 2001).

1.4.1.2 Pilli

The recent discovery of pili in gram-positive bacteria and their role as a major factor in adherence to host cells have been proposed by numerous investigators (Abbot 2007, Yeates 2007, Olsen 2008, Ryan 2007, Manetti 2007). Abbot and colleagues have used apiliated mutants to demonstrate that early adherence events are drastically impaired across multiple epithelial cell types if pili are not present or produced (Abbot 2007). The genes for such pili are encoded by the pathogenicity island known as the fibronection-binding, collagen-binding, T-antigen (FCT) region, which has been identified in all sequenced group A

streptococcal isolates to date (Manetti 2007, Falugi 2008). The pili are encoded within this region by a multi-gene loci. Recently the actual pilus subunit t that serves as the epithelial cell adhesin has been proposed to be encoded by locus tag *Spy0125,* although recombinantly expressed minor pilus subunit *Spy0130* has also been shown to adhere to human pharyngeal cells in vitro (Smith 2010). Importantly, biofilm formation is a characteristic lifestyle feature of *S. pyogenes* during colonization, and it has been suggested that pili mayplay and particularly pivotal role in facilitating biofilm formation (Manetti 2007).

Table 1.2. Cell wall-anchored or surface-associated adhesins

Protein group	Protein(s)	Species	Cell surface linkage	Function(s) and/or substrate(s)
Agl/II family	Spy1325	*S. pyogenes*	LPxTz	Coaggregation; multiple substrates
Alp family	R28/Alp3	*S. pyogenes, S. agalactiae*	LPxTz	Multiple substrates
	R proteins (R1–R4)	*S. pyogenes, S. agalactiae,* S. dysgalactiae	LPxTz	Host glycosaminoglycans
Pili / fimbriae / fibrils	PI	*S. pyogenes*	LPxTz	Coaggregation, biofilm formation, phagocyte resistance; multiple substrates
Saliva-binding proteins	AgI/II family	*S. mutans, S. sobrinus, S. gordonii, S. oralis, S. intermedius*	LPxTz	Salivary components (gp340, salivary glycoproteins, proline-rich proteins)
	Pili, fimbriae, fibrils	*S. pyogenes, S. parasanguinis, S. intermedius, S. salivarius, S. gordonii*	LPxTz	gp340
Fn-binding proteins	SfbI/PrtF1	*S. pyogenes*	LPxTz	Fn
	FbaA	*S. pyogenes*	LPxTz	Fn
	FbaB/PFBP/PrtF2	*S. pyogenes*	LPxTz	Fn
	SOF/SfbII	*S. pyogenes*	LPxTz	Fn
	SfbX	*S. pyogenes*	LPxTz	Fn

Table 1.2 (continued)

	Fbp54	*S. pyogenes*	Anchorless	Fn
	ScpA (C5 peptidase)	*S. pyogenes*	LPxTz	Fn
	GAPDH/SDH	*S. pyogenes*	Anchorless	Fn
	M proteins	*S. pyogenes*	LPxTz	Fn
	M-like proteins	*S. pyogenes*	LPxTz	Fn
	Shr	*S. pyogenes*	Anchorless	Fn
Collagen-binding proteins	Cpa	*S. pyogenes*	LPxTz	Collagen
	Enolase	*S. pyogenes, S.pneumoniae, S. oralis, S. anginosus, S. mutans, S. salivarius, S. sanguinis*	Anchorless	Plasminogen, plasmin
Plasminogen-binding proteins	M protein	*S. pyogenes*	LPxTz	Plasminogen
	PAM	*S. pyogenes*	LPxTz	Plasminogen
	GAPDH/Plr	*S. oralis, S. anginosus, S. agalactiae, S. pyogenes, S. pneumoniae, S. gordonii, S. dysgalactiae*	Anchorless	Plasminogen, plasmin
	Streptokinase (Ska)	*S. pyogenes*	None	Plasminogen
Laminin-binding proteins	Lbp	*S. pyogenes*	LXXC/XXGC	Laminin
	Lsp	*S. pyogenes*	LXXC/XXGC	Laminin
	SpeB	*S. pyogenes*	Anchorless/none	Laminin
	Lmb	*S. agalactiae, S. pyogenes*	LXXC/XXGC	Laminin
Fibrinogen-binding proteins	M protein	*S. pyogenes*	LPxTz	Fibrinogen
	SOF/SfbII	*S. pyogenes*	LPxTz	Fibrinogen
	Fbp54	*S. pyogenes*	Anchorless	Fibrinogen
	Mrp	*S. pyogenes*	LPxTz	Fibrinogen
Ig-binding proteins	SfbI/PrtF	*S. pyogenes*	LPxTz	IgG
	Sib35	*S. pyogenes*	Anchorless	IgG
	SibA	*S. pyogenes*	None	IgG, IgA, IgM

Table 1.2 (continued)

	Sir	*S. pyogenes*	LPxTz	IgA, IgG
	Enn protein	*S. pyogenes*	LPxTz	IgA
	M protein	*S. pyogenes*	LPxTz	IgG, IgA
	M-like proteins	*S. pyogenes*	LPxTz	IgG, IgA
	Mrp	*S. pyogenes*	LPxTz	IgG
	FcRA	*S. pyogenes*	LPxTz	IgG

Table 1.2 (continued)

	Lzp	*S. pyogenes, S. agalactiae*	Anchorless	IgG, IgA, IgM
Complement-binding proteins	M protein	*S. pyogenes*	LPxTz	Factor H, factor H-like protein 1
	M-like proteins	*S. pyogenes*	LPxTz	Factor H, factor H-like protein 1
	FbaA	*S. pyogenes*	LPxTz	Factor H, factor H-like protein 1
Host cell-binding proteins	ScpA	*S. pyogenes*	LPxTz	Complement C5a
	Shr	*S. pyogenes*	Anchorless	Epithelial cells
	ScpA	*S. pyogenes*	LPxTz	Epithelial cells
	Lbp	*S. pyogenes*	LXXC/XXGC	Epithelial cells
	R28	*S. pyogenes*	LPxTz	Epithelial cells
	M protein	*S. pyogenes*	LPxTz	Epithelial/endothelial cells ($\alpha_5\beta_1$ integrin, Fn bridge)
	SfbI/PrtF	*S. pyogenes*	LPxTz	Epithelial/endothelial cells (α5β1 integrin, Fn bridge)
	SclA, SclB (Scl1, Scl2)	*S. pyogenes*	LPxTz	Epithelial cells ($\alpha_2\beta_1$, $\alpha_{11}\beta_1$ integrins)
	Pili, fimbriae, fibrils	*S. agalactiae, S. pyogenes, S. pneumoniae, S. salivarius*	LPxTz	Epithelial/endothelial cells
Enzymes	HtrA	*S. mutans, S. pneumoniae, S. pyogenes*	Anchorless	Serine protease
	GAPDH, α-enolase, PGK, PGM, TPI	*S. pyogenes, S. oralis, S. anginosus*	Anchorless	Glycolytic enzymes
	GAPDH/SDH	*S. pyogenes*	Anchorless	Lysozyme, cytoskeletal proteins, CD87/uPAR
	PulA	*S. pyogenes*	LPxTz	Pullulanase
	GRAB	*S. pyogenes*	LPxTz	α_2-Macroglobulin; protects against proteolysis

(Adadpted from Nobbs 2009)

1.4.2 Invasins

In order to cause invasive diseases as myositis and necrotizing fasciitis, *S. pyogenes* must invade deep tissue through either a paracellular route between adjacent cells, or by traversing epithelia through intracellular movement. It is now established that the streptococcal M-protein and fibronectin-binding protein

(Protein F) serve as invasins, since latex beads coated with either protein will efficiently become internalized by epithelial cells (Fluckiger 1998, Jadoun 1998).

1.4.3 Secreted Factors

Secreted proteins can include degradative enzymes (SpeB, DNases, hyaluronidases), toxins (streptolysins and superantigens), and proteins for immune evasion (antibody-degrading factors) (Hynes 2004). The streptococcal pyrogenic exotoxins (Spes) have likely been most studies of any of the pathogen's secreted products. Principally, Spes have been shown to induce fever as its name implies, among a cadre of other symptoms of disease. The Spes have been defined in four distinct antigenic groups, A to D. Types A, B, and C are well defined, while type D is not well characterized (Cunningham 2000).

1.4.3.1 SpeA

The nucleotide sequence of the streptococcal pyrogenic exotoxin A gene was reported by Weeks and Ferretti (Weeks 1986) and the gene has been found to be expressed in most streptococcal strains isolated from cases of streptococcal toxic shock syndrome (Hauser 1991). In this study, 85% of the patients who manifested toxic streptococcal syndrome had strains which produced pyrogenic exotoxin A. Nucleotide sequencing of the streptococcal pyrogenic exotoxin A (speA) gene in strains associated with various outbreaks has revealed that there are four naturally occurring alleles of *speA* (Cunningham 2000). The *speA1, speA2,* and *speA3* alleles encode toxins, which differ in a single amino acid,

while *speA4* encodes a toxin which is 9% divergent from the other three and has 26 amino acid substitutions. The *speA2* and *speA3* alleles are expressed in most of the recent isolates from toxic streptococcal syndrome (Nelson 1991).

1.4.3.2 SpeB

SpeB (streptococcal cysteine protease, streptococcal exotoxin B) is a cardiotoxic virulence factor of *S. pyogenes*). The *speB* gene is carried by all strains of *S. pyogenes*, but the degree of expression varies from strain to strain. Its protease activity has the ability to degrade the human extracellular matrix protein fibronectin and vitronectin, release inflammatory mediators such as interleukin 1β and bradykinin from their precursors, cleave or degrade immunoglobulins and complement factors, and also bind to the human cell surface receptors integrins (Cunningham 2000). Its expression is directly under the reglation of mg. In addition to *ropA*, the presence of M-protein on the streptococcal surface is needed for the maturation of SpeB. The secreted SpeB has an important role in *S. pyogenes* virulence. It degrades host extracellular matrix proteins activates interleukin-1β and releases fragments of proteins from the *S. pyogenes* surface (Nelson 2011).

1.5 Genetics of Virulence

1.5.1 Chromosomal and Bacteriophage-encoded Virulence Factors

Streptococcal virulence factors can be encoded on the streptococcal chromosome or located on lysogenic bacteriophage. Integrated phages not

only contribute to the genetic diversity of GrAS strains, but they can also introduce virulence factors that alter the phenotype of a particular strain in the infection setting. Although strain SF370 encodes for extracellular DNases, hyaluronidases, and superantigens within its bacterial chromosome, additional proteins from each category have been introduced by phage transduction as evidenced by the four integrated prophage sequences in the SF370 genome (Ferretti 2001). It is important to also note that these factors are often strain and serotype-specific. For example, skin- tropic M type strains are often distinguished from throat-tropic M type isolates by the presence of the chromosomally encoded serum opacity factor (sof) on the former (Cunningham 2000, Bessen 2010). Tables 1.2 and 1.3 provide the known annotated known virulence factors for the M type 1 strain SF370 with accompanying locus tag and gene name. We exclusively use this strain in all of microarray experiments presented later in section 6.

Table 1.3 Chromosomally Encoded Virulence Factors

Locus Tag[1]	Gene Name	Protein Function and/or Recognized Role in Virulence	Reference[2]
spy0019	*sibA*	Secreted immunoglobulin binding protein; Binds IgG, IgA, IgM	Fagan, *et al.* 2001
spy0125[3]	*cpa.1*	Minor pilin subunit protein (AP1); Binds collagen	Ferretti, *et al.* 2001; Smith, *et al.* 2010
spy0127	*sipA1*	Pilin-specific signal peptidase; Plays chaperon-like function in pilus polymerization	Zahner & Scott 2008
spy0128		Major pilin subunit protein (Lancefield T antigen); Responsible for pilus length and stability	Mora, *et al.* 2005; Abbot, *et al.* 2007
spy0129	*srtC1*	Sortase; Polymerizes the pilus structure	Barnett, *et al.* 2004; Mora, *et al.* 2005
spy0130		Minor pilin subunit protein; Links pilus to cell wall (AP2)	Abbot, *et al.* 2007; Smith, *et al.* 2010
spy0165	*nga*	NAD-glycohydrolase; Reduces host cell energy stores	Ferretti, *et al.* 2001
spy0167	*slo*	Streptolysin O; Cytolysin that forms pores in host cell membranes and induces apoptosis in phagocytes	Ferretti, *et al.* 2001
spy0212	*speG*	Pyrogenic exotoxin; Nonspecifically stimulates T cells	Ferretti, *et al.* 2001
spy0274	*sdh/plr*	Surface dehydrogenase (GAPDH); Binds to plasminogen and fibronectin; Regulates host cell signaling	Pancholi & Fischetti 1992
spy0378	*hlyX*	Hemolysin	Ferretti, *et al.* 2001
spy0380		Exopolyphosphatase; Possible adhesin	Ferretti, *et al.* 2001
spy0390	*ideS*	Secreted cysteine protease; Cleaves the IgG heavy chain	von Pawel-Rammingen, *et al.* 2002
spy0416	*scpC/spyCEP*	Secreted protease; Degrades IL-8 and other host chemokines	Hidalgo-Grass, *et al.* 2006
spy0428	*spyA*	Surface-bound ADP-ribosyltransferase; Function in virulence not understood	Coye & Collins 2004
spy0436	*speJ*	Pyrogenic exotoxin; Nonspecifically stimulates T cells	Ferretti, *et al.* 2001
spy0470	*mcrA*	Myosin cross-reactive antigen; Antigenic mimicry	Ferretti, *et al.* 2001
spy0591		Possible proteinase (collagenase)	Ferretti, *et al.* 2001
spy0605	*bsa/gpoA*	Glutathione peroxidase; Involved in antioxidant defense during suppurative disease	Brenot, *et al.* 2004
spy0731	*eno*	Alpha-enolase; Binds plasminogen	Pancholi & Fischetti 1998
spy0737	*epf*	Surface protein; Binds plasminogen	Ferretti, *et al.* 2001
spy0738-0746	*sagA-sagI*	Streptolysin S; Hemolysin that kills neutrophils and interrrupts host intercellular junctions for dissemination	Ferretti, *et al.* 2001
spy0747	*spnA*	Cell-surface nuclease; Destroys neutrophil extracellular traps	Hasegawa, *et al.* 2010
spy0861	*sib35/mac*	Secreted protein that mimics a host cell receptor; Binds & degrades IgM, IgA, IgG; Blocks phagocytosis and ROS production by PMNs	Lei, *et al.* 2001; Kawabata, *et al.* 2002
spy1013	*fbp/fbp54*	Fibronectin-binding protein	Courtney, *et al.* 1994
spy1032	*hylA*	Hyaluronidase	Ferretti, *et al.* 2001
spy1054	*sclB/scl2*	Collagen-like protein	Ferretti, *et al.* 2001
spy1159	*hlyIII*	Hemolysin III	Ferretti, *et al.* 2001
spy1273	*cfa*	CAMP factor; Helps lyse erythrocytes; Binds Fc regions of Ig	Ferretti, *et al.* 2001
spy1302	*cdg/amyA*	Amylase/cyclomaltodextrin glucanotransferase; Important for epithelial translocation	Ferretti, *et al.* 2001
spy1312-1309	*dltA, dltB, dltC, dltD*	D-alanylation of surface lipoteichoic acids (LTA); Insertion of positively charged residues protects against cationic antimicrobial peptides and lysozyme killing; Enhances host cell adherence & invasion	Kristian, *et al.* 2005

Table 1.3 (continued) Chromosomally Encoded Virulence Factors

spy1357	*grab*	G-related α-2-binding protein; Binds a human protease inhibitor, which prevents degradation of bacterial surface-bound adhesins & recruits SpeB to surface for defense against antimicrobial peptides	Ferretti, *et al.* 2001
spy1361	*slr*	Histidine triad protein (surface-bound lipoprotein); Recruits collagen type I to surface	Reid, *et al.* 2003
spy1497	*hylA1*	hemolysin	Ferretti, *et al.* 2001
spy1600	*hyl*	O-GlcNAse; Used on eukaryotic modified glycoproteins (role possibly limited to sugar foraging)	Ferretti, *et al.* 2001
spy1798	*shr*	Heme acquistion and adhesin; Binds fibronectin and laminin	Fisher, *et al.* 2008
spy1801	*isp2*	Immunogenic secreted protein; Function unknown	Ferretti, *et al.* 2001
spy1813	*endoS*	Secreted IgG glycan hydrolase; Inhibits function of IgG Fc region	Collin & Olsen 2001
spy1851		C3-degrading proteinase; Inhibition of complement	Ferretti, *et al.* 2001
spy1896	*ropA/tig*	Trigger factor; Chaperone essential for SpeB secretion and maturation	Ferretti, *et al.* 2001
spy1911	*salY*	ABC transporter permease; Intracellular survival in macrophages	Phelps & Neely 2007
spy1915	*salA*	Salivaricin A; Lantibiotic	Ferretti, *et al.* 2001
spy1972	*pulA*	Pullulanase; Binding to carbohydrates on host cells	Shelburne, *et al.* 2011
spy1979	*ska*	Streptokinase; Activates plasmin to degrade blood clots and ECM components	Ferretti, *et al.* 2001
spy1983	*sclA/scl1*	Collagen-like protein; Binds to host LDL (lipoprotein in blood plasma), collagen, and laminin	Ferretti, *et al.* 2001
spy1357	*grab*	G-related α-2-binding protein; Binds a human protease inhibitor, which prevents degradation of bacterial surface-bound adhesins & recruits SpeB to surface for defense against antimicrobial peptides	Ferretti, *et al.* 2001
spy1361	*slr*	Histidine triad protein (surface-bound lipoprotein); Recruits collagen type I to surface	Reid, *et al.* 2003
spy1497	*hylA1*	hemolysin	Ferretti, *et al.* 2001
spy1600	*hyl*	O-GlcNAse; Used on eukaryotic modified glycoproteins (role possibly limited to sugar foraging)	Ferretti, *et al.* 2001
spy1798	*shr*	Heme acquistion and adhesin; Binds fibronectin and laminin	Fisher, *et al.* 2008
spy1801	*isp2*	Immunogenic secreted protein; Function unknown	Ferretti, *et al.* 2001
spy1813	*endoS*	Secreted IgG glycan hydrolase; Inhibits function of IgG Fc region	Collin & Olsen 2001
spy1851		C3-degrading proteinase; Inhibition of complement	Ferretti, *et al.* 2001
spy1896	*ropA/tig*	Trigger factor; Chaperone essential for SpeB secretion and maturation	Ferretti, *et al.* 2001
spy1911	*salY*	ABC transporter permease; Intracellular survival in macrophages	Phelps & Neely 2007
spy1915	*salA*	Salivaricin A; Lantibiotic	Ferretti, *et al.* 2001
spy1972	*pulA*	Pullulanase; Binding to carbohydrates on host cells	Shelburne, *et al.* 2011
spy1979	*ska*	Streptokinase; Activates plasmin to degrade blood clots and ECM components	Ferretti, *et al.* 2001
spy1983	*sclA/scl1*	Collagen-like protein; Binds to host LDL (lipoprotein in blood plasma), collagen, and laminin	Ferretti, *et al.* 2001

Table 1.3 (continued) Chromosomally Encoded Virulence Factors

spy1998	*smeZ*	Pyrogenic exotoxin; Nonspecifically stimulates T cells	Ferretti, *et al.* 2001
spy2006	*htpA*	Surface-bound histidine triad protein; Immunogenic in mice	Kunitomo, *et al.* 2007
spy2007	*lmb/lsp*	Suface lipoprotein; Zn acquisition from host; Binds to human basal lamina glycoprotein laminin	Ferretti, *et al.* 2001
spy2009	*fbaA*	Fibronectin-binding adhesin; Controlled by Mga; Required for adherence and invasion	Terao, *et al.* 2001
spy2010	*scpA*	C5a peptidase; Inhibits complement	Ferretti, *et al.* 2001
spy2016	*sic*	Streptococcal inhibitor of complement; Inactivates lysozyme, LL-37, and host defensins	Ferretti, *et al.* 2001
spy2018	*emm1*	M protein; Dominant GrAS virulence factor; Binds fibronectin; Mediates phagocytosis resistance	Ferretti, *et al.* 2001
spy2025	*isp*	Immunogenic secreted protein; Function unknown	Ferretti, *et al.* 2001
spy2039	*speB*	Exracellular cysteine protease; Mediates immune modulation, ECM hydrolysis, and release of GrAS surface antigens	Ferretti, *et al.* 2001
spy2043	*speF/spd*	Pyrogenic exotoxin; Nonspecifically stimulates T cells; DNase	Ferretti, *et al.* 2001
spy2200-2202	*hasA, hasB, hasC*	Hyaluronate capsule synthetase; Mediates phagocytosis resistance and cytoskeletal rearrangements in host cells for intercellular translocation	Ferretti, *et al.* 2001
spy2216	*degP/htrA*	Membrane associated protease; Role in defenses against oxidative stress & maturation of SpeB	Jones, *et al.* 2001

Table 1.4 Phage Encoded Virulence Factors

Locus Tag	Gene Name	Protein Function and/or Recognized Role in Virulence	Reference[2]
spy0701	*hylP1*	Hyaluronidase	Ferretti, *et al.* 2001
spy0711	*speC*	Pyrogenic exotoxin; Nonspecifically stimulates T cells	Ferretti, *et al.* 2001
spy0712	*spd1/mf2*	Extracellular DNase	Ferretti, *et al.* 2001
spy0997	*hylP2*	Hyaluronidase	Ferretti, *et al.* 2001
spy1007	*speI*	Pyrogenic exotoxin; Nonspecifically stimulates T cells	Ferretti, *et al.* 2001
spy1008	*speH*	Pyrogenic exotoxin; Nonspecifically stimulates T cells	Ferretti, *et al.* 2001
spy1436	*spd3/mf3*	Extracellular DNase	Ferretti, *et al.* 2001
spy1445	*hylP3*	Hyaluronidase	Ferretti, *et al.* 2001

[1] Locus tag in the SF370 genome.

[2] For genes identified as virulence factors during the initial SF370 sequencing project, the reference indicates the original publication of the genome (Ferretti, *et al.* 2001). For genes not annotated as virulence factors at the time of publication for the genome, the reference signifies the initial description of the virulence gene or the first association of a previously characterized ORF with a function in streptococcal virulence.

[3] ORF not represented on the SF370 microarray used for this work.

1.5.2 Regulation of Virulence

Regulation of virulence in *S. pyogenes* is widely considered to be executed at the transcriptional level. Studies that have examined the correlation between mRNA levels and protein production in *S. pyogenes* have found good agreement (Lyon 2001, Chaussee 2002, Ryan 2007, Juncosa 2012).

1.5.2.1Stand-alone Regulators

Stand-alone regulators can positively or negatively affect virulence factor expression in response to environmental signals communicated by unknown sensory elements (Kreikemeyer 2003). SF370 encodes over 40 stand-alone regulators (Ferritti 2000).

1.5.2.1.1 Mga

Mga has been so named as the multiple gene regulator of group A streptococcus. The *mga* gene lies immediately upstream of *emm,* which encodes M protein. ga is ubiquitous in GrAS and, due to its regulation of a vast array of genes implicated in GrAS pathogenesis, is often referred to as a global regulator of virulence (Nobbs 2009). It is now established that Mga activates the transcription of several additional genes, including those for C5a peptidase (scpA), M-like proteins (mrp, *enn,* and *fcR),* serum opacity factor (sof), and secreted inhibitor of complement (sic). Mga feeds back to positively regulate itself and functions as a 62-kDa protein to bind to the promoter region of the genes that it regulates (Cunningham 2000).

1.5.2.1.2 amrA

The *amrA* locus corresponds to Spy0797 in the serotype M1 GrAS. Based on mutation experimental screens, it received its name for activation of Mga regulon expression locus A. As *amrA* is strongly conserved across the sequenced streptococcal M types, and inactivation of *amrA* in an M3 serotype also resulted in reduction of *emm* transcripts. Ribardo *et al* asserted that the original role the noted during their screen identifying *amrA* does not appear to be serotype specific. Although the specific function of AmrA is unknown, its putative membrane localiza- tion and homology to transporters involved in cell wall synthesis suggest a link between growth and virulence gene expression in GrAS (Ribardo 2003).

1.5.2.2 Two-Component Systems

Working in conjunction with stand-alone regulators, two-component systems (TCS) offer GrAS the ability to integrate extracellular signals directly into regulatory circuits (Kreikemeyer 2003).The sequenced genomes of *S. pyogenes* have been found to encode 13 two-component systems (Ferritti 2000).

1.5.2.2 .1 CovR / CovS

Levin and Wessels identified *csrR / csrS (*CovR / CovS*),* a pair of genes in group A streptococci that encode a two-component regulatory system. It's name stem from "control of virulence" genes. Inactivation of CovR resulted in a striking increase in transcription of the capsule synthesis genes of the *has* operon and a

corresponding increase in hyaluronic acid capsule production (Cunningham 2000). The CovR / CovS is now know to be responsible for negative regulation of capsule production, streptokinase, SpeB and streptolysin S, and appears to influence the transcription of up to 15% of the genes in GrAS (Ribardo 2003).

1.5.2.2.2 SptR / SptS

Named for its role in Streptococcal persistence in Saliva, the SptR/SptS TCS plays a crucial role during the host–pathogen interaction in saliva. It has been proposed that SptR/S links central metabolic processes with the production of a broad range of putative and known virulence factors Interestingly, one of the major roles of the SptR/SptS is to coordinate expression of genes involved in acquisition and processing of complex carbohydrates, with little to no effect on the use of simple sugars like glucose (Shelburne 2005). SptR regulates 20% of GrAS ORFs during growth in saliva including transcription of *spd* (DNase), *spd3* (DNase), *sic, speB,* and *hasA* (capsule) (Shelburne 2008). These genes have been associated with colonization and infection of the oropharynx. (Fig.1.3).

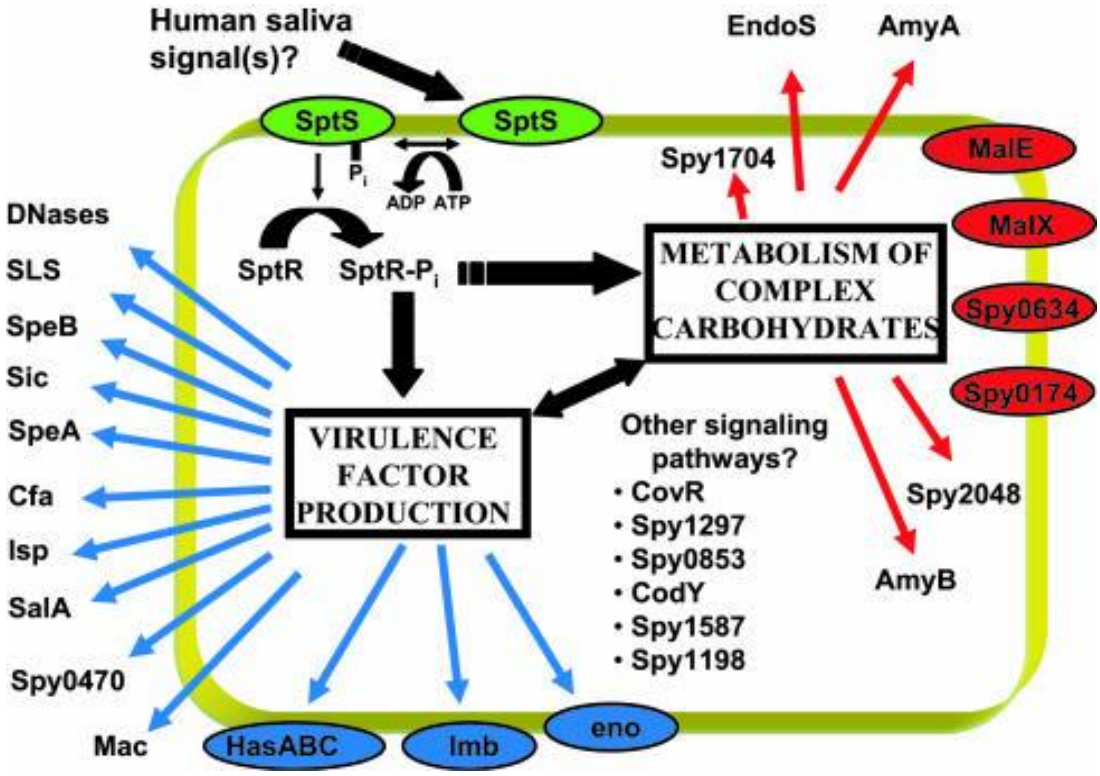

Figure 1.3 Proposed mechanism for how the SptR/S TCS contributes (directly or indirectly) to persistence of GrAS in human saliva.

Adapted from Shelburne *et al* 2005

1.6 Pathogenesis

1.6.1 Adhesion

The dominant theory describing streptococcal colonization of pharyngeal and dermal epithelia is via a two-step adherence mechanism (Hasty 1999, Nobbs 2009). The first step involves a weak electrostatic interaction likely mediated by lipotechoic acid (LTA) in the bacterial cell wall. This amphipathic molecule contains a lipid moiety attached to a negatively (-) charged polyglycerol phosphate backbone, which reacts with positively (+) charged residues on host epithelial surface proteins, such as fibronectin. This electrostatic attraction may account for up to 60% of the pathogen's adhesion to epithelial cells (Cunningham 2000).

The second stage of adherence occurs by a mechanism that confers tissue specificity (Bessen 2010) and involves high-avidity binding that is mediated by multiple bacterial adhesins and their associated host cell epitopes, often extracellular matrix proteins (Cunningham 2000, Nobbs 2009).

1.6.2 Invasion

In order to cause invasive diseases as myositis and necrotizing fasciitis, *S. pyogenes* must invade deep tissue through either a paracellular route between adjacent cells, or by traversing epithelia through intracellular movement. LaPenta *et al.* were the first to demonstrate *in vitro* that group A streptococci are able to invade (or become internalized by) immortalized cells (LaPenta 1994). These

initial findings have been confirmed and expanded by other groups demonstrating that streptococci can invade certain cell lines as efficiently as certain obligate intracellular pathogens such as *Listeria* and *Salmonella* (Greco 1995, Cunningham 2000). It is now established that the streptococcal M-protein and fibronectin-binding protein (Protein F) serve as invasins, since latex beads coated with either protein will efficiently become internalized by epithelial cells (Fluckiger 1998, Jadoun 1998). The mechanism for fibronectin-mediated invasion has been extensively studied. A leading theory proposes streptococci bind host serum fibronectin with one of multiple fibronectin-binding proteins (e.g. FnBP, Sfb1) and is subsequently engaged by the α5β1 integrin as a consequence of it being the host cell fibronectin receptor. Once bound to the integrin, propagation of phosphoinositide 3-kinase and integrin-linked kinase-dependent intracellular signals induce cytoskeletal rearrangement and internalization of the streptococci (Wang 2006a, Wang 2006b). Integrin ligands frequently posses the tripeptide sequence RGD, which serves as the integrin recognition or binding site. Other peptides with RGD amino acid sequences appear to stimulate uptake without either M-protein or serum. Another factor potentially important for invasion is laminin, which binds group A streptococci and induce epithelial internalization also without serum (Cunningham 2000).

The evolution of presumably many routes to the interior of human epithelial cells implies that this otherwise extracellular bacterium might be able to survive, at least transiently, intracellularly. Osterlund *et al* were among the first to

convincingly demonstrate that streptococcal internalization may not be an *in vitro* laboratory artifact when they recognized that excised tonsil tissue contained viable intra- and extracellular streptococci (Osterlund 1997). This observation led to the suggestion that the tonsil may contain an intracellular reservoir of *S. pyogenes* that mediates recurrent infection (Osterlund 1997). Mammalian epithelial cells are not well penetrated by β-lactam antibiotics. Multiple groups propose that streptococci may persist intracellularly and evading killing by antibiotics prescribed to treat pharyngotonsillits. (Cue 2000, Osterlund 1997). We further explore the mechanisms of epithelial internalization as well as it's consequence to the host and bacterium in section 7.

1.7 Streptococcal Disease Burden

This pathogen causes a wide variety of diseases including acute pharyngitis, impetigo, scarlet fever, and puerperal sepsis. In many cases, these diseases have been attributed to particular M serotypes. For example, M types 2, 49, 57, 59, 60, and 61, are associated with pyoderma and acute glomerulonephritis while M types 1, 3, 5, 6, 14, 18, 19, and 24 arep found associated with throat infection and rheumatic fever. More recently, studies have also linked post-streptococcal infection sequelae to such neurologic conditions as Tourette's syndrome, Tics, Attention Deficit Disorder (ADD), and Pediatric Autoimmune Neurosychiatric Disorders Associated with Streptococcal infections (PANDAS) (Cunningham 2000, Pavone 2006, Hahn 2005). Significant outbreaks of streptococcal infections and their sequelae have historically occurred in densely populated

settings, such as schools and in the military (Kaplan 2009). The annual global burden of *S. pyogenes* related diseases is staggering and includes greater than 100 million cases of pyoderma, and over 600 million cases of pharyngitis (Bisno 2000). An increased global incidence of severe invasive diseases due to *S. pyogenes* has been observed over past decades (Kaplan 1996), often associated with bacteremia, streptococcal toxic shock syndrome (STSS), and high mortality. It was estimated that nearly 500,000 deaths due to invasive diseases occurred in 2005 (Carapetis 2005).

1.7.1 Acute Rheumatic Disease and Sydenham Chorea

Molecular mimicry is proposed to be an important mechanism in the pathogenesis of Acute Rheumatic Fever (ARF). Human monoclonal antibodies derived from rheumatic heart disease have provided evidence supporting the hypothesis that crossreactive autoantibodies that target the dominant group A streptococcal epitope of the group A carbohydrate, N-acetyl-beta-D-glucosamine (GlcNAc), and heart valve endothelium, laminin and laminar basement membrane. This cross reactivity may then lead to the initiation of carditis and rheumatic heart. Similarly, Antineuronal antibodies in Sydenham chorea may cross the blood–brain barrier and trigger antibody-mediated neuronal cell signaling induction of calcium calmodulin- dependent protein kinase II (CaMKII) and subsequent dopamine release in the caudate putamen region of the brain, which may lead to the movement disorder (Cunningham 2012).

1.7.2 Pharyngitis

1.7.2.1 Healthcare Burden

The superficial infection of the pharyngeal mucosa is among the important primary infections of the throat specialist streptococcal serotypes. M type 1 has been of particular importance as it remains the most commonly isolated serotype associated with pharyngeal and invasive disease (Bessen 2010). Notably, however, there have been an increasing number of adults and children hospitalized annually for throat infections over the past decade in the industrialized world. In Australia, 4% of all symptomatic presentations to general practitioners from 2000 – 2001 were for throat complaints, second only to cough at 7%. Sore throat consultations resulted in an antibiotic prescription in 89% of cases (WHO 2005). In England from 2000 – 2001, there were 30,942 tonsil related admissions for medical treatments. By 2008 – 2009, the figure had risen to 43,641 medical admissions for throat symptoms, an increase of over 41% (12,700 admissions) in 8 years [http://www.hesonline.nhs.uk], (Vincent 2004). The Ambulatory Medical Care Utilization in the United States (AMCUS), estimates for 2007 found that acute pharyngitis accounts for 1.1 percent of visits in the primary care setting and is ranked in the top 25 reported primary diagnoses resulting in office visits (Schappert 2011).

1.7.2.2 Antibiotic Failure

While treatment failure in the 1950's was reported in 4-8% of children, more recent studies have alarmingly found antibiotic failure as high as 20-40%

(Pichichero 1991, 2007). Treatment failure has been attributed to reasons inlcluding: 1) carrier state, 2) lack of compliance, 3) recurrent exposure, 4) *in vivo* copathogenicity of beta-lactamase–producing normal pharyngeal flora, 5) *in vivo* bacterial coaggregation, 6) poor antibiotic penetration to tonsillopharyngeal tissue, 7) *in vivo* eradication of normal protective flora, 8) early initiation of antibiotic therapy resulting in suppression of an adequate host immune response, 9) intracellular localization of GrAS, 10) GrAS tolerance to penicillin, 11) contaminated toothbrushes or orthodontic appliances, and 12) transmission from the family pet (Pichichero 2007).

1.7.2.3 GrAS Pharyngitis Clinical Appearance

The clinical presentation for group a streptococcal pharyngotonsillits on physical examination may be atypical with non-descript physical symptoms or more commonly reveals well confined pharyngeal erythema with palatine tonsil swelling, an edematous uvula, and anterior cervical lymphadenopathy (figure 1.4). Ebell and colleagues' literature review of physical exam findings in strep throat cases concluded the signs and symptoms that help rule in GABHS pharyngitis include tonsillar exudates (positive likelihood ratio [LR+]: 3.4), pharyngeal exudates (LR+: 2.1), and exposure to strep throat in the previous two weeks (LR+: 1.9) (Ebell 2000). The presence of a scarlatiniform rash or palatine petechiae is uncommon but very specific for the diagnosis of GABHS pharyngitis As previously described, more outspread symptoms may increase the likelihood of an alternative pathogen (Ebell 2000).

1.7.2.4 Differential Diagnosis of Non-GrAS Pharyngitis

Group A streptococcus remains the most common bacterial cause and is estimated to account for 15-30% of cases of pharyngitis in children (<18 y.o.) and 5-10% of cases in adults. The differential diagnosis is generally a distinction between bacterial and viral, since the treatment course between bacterial etiologies may not differ dramatically. Among the other bacterial causes, *Neisseria gonorrhea* pharyngitis occurs in sexually active patients18 presents with fever, severe sore throat, dysuria, and a characteristic greenish exudate. *Corynebacterium diphtheria* pharyngitis is assumed if examination reveals a serosanguineous nasal discharge. Other diphtheria related symptoms may include a grayish-white pharyngeal membrane where exudative and extending to the uvula and soft palate in association with the pharyngitis, tonsillitis, and cervical lymphadenopathy Table 1.5 provides a non-exhaustive review of the alternate causes of pharyngitis (Vincent 2004, Bisno 2001).

Table 1.5 Viral versus bacterial causes of pharyngeal infection

PATHOGEN	SYNDROME OR DISEASE	ESTIMATED PERCENTAGE OF CASES
Viral		
Rhinovirus (100 types and 1 subtype)	Common cold	20
Coronavirus (3 or more types)	Common cold	>5
Adenovirus (types 3,4,7,14, and 21)	Pharyngoconjunctival fever, acute respiratory disease	5
Herpes simplex virus (types 1 and 2)	Gingivitis, stomatitis, pharyngitis	4
Parainfluenza virus (types 1 and 4)	Common cold, croup	2
Influenza virus (types A and B)	Influenza	2
Coxsackie virus A (types 2, 4-6, 8, and 10)	Herpangina	<1
Epstein-Barr virus	Infectious mononucleosis	<1
Cytomegalovirus	Infectious mononucleosis	<1
HIV virus type 1	Primary human deficiency virus infection	<1
Bacterial		
Streptococcus pyrogenes (group A B-hemolytic streptococci)	Pharyngitis and tonsillitis, scarlet fever	15-30
Group C B-hemolytic streptococci	Pharyngitis and tonsillitis	5
Neisseria gonorrhea	Pharyngitis	<1
Corynebacterium diphtheria	Diphtheria	<1
Arcanobacterium haemolyticum	Pharyngitis, scarlatiniform rash	<1
Chlamydial		
Chlamydial pneumonia	Pneumonia, bronchitis, and pharyngitis	Unknown
Mycoplasmal		
Mycoplasma pneumonia	Pneumonia, bronchitis, and pharyngitis	<1

The list is not exhaustive.Estimates are of the percentage of cases of pharyngitis in persons of all ages that are due to the indicated organism.

(Adapted from Bisno 2001)

1.7.2.5 Surgical Indications

Tonsillectomy remains the most common operation in Ear, Nose and Throat units (Little 1996). While hypertrophy increasingly has become the most common indication for this procedure in recent years, recurring tonsillitis continues to be an important predisposing factor, creating a significant financial burden with potential complications, especially in the very young (Spencer 2012). Indication for tonsillectomy relates to surgeon preference as well as effect on the overall quality of life for the patient. One longstanding recommendation shared by the American Medical Association and the American Academy of Pediatrics, is that tonsillectomy be indicated for patients who have four or more documented cases of pharyngitis over one year (Gates 1986).

Figure 1.4. Clinical presentation of “Strep Throat”.

*Arrows indicate white exudate on the palatine tonsil. Patient was cultured to be positive for Group A Streptococci and was treated with 1.2 million units of penicillin G benzathine intramuscularly with benzocaine spray for topical analgesia.

Image adapted from Nimishikavi *et al* 2005.

1.8 Human Oropharynx anatomy

The tonsils are secondary lymphoid organs that form a first line of defense in protecting the oropharyngeal isthmus. Collectively referred to as Waldeyer's Ring (Figure 1.5), humans uniquely have numerous "tonsils", namely: palatine, nasopharyngeal (or adenoids), lingual, and tubal tonsils.). Similar to Peyers patches and the vermiform appendix, the tonsils belong to the mucosa-associated lymphoid tissue (MALT) system and are constantly exposed to antigens. In contrast to the material in contact with the intestinal MALTs, however, these antigens are in their native form having not been modified by gastric acid or digestive enzymes. An additional unique quality is that unlike most lymphoid organs/nodes (with the exception of the spleen), tonsils do not have afferent lymph vessels (Perry 1998). The palatine tonsils' anatomic placement within Waldeyer's ring is ideally situated for antigen sampling but are themselves more vulnerable to damage and infection than many of the less exposed members of this lymphoidal network. Accordingly, tonsillitis caused by bacterial and viral infections is usually localized to the palatine tonsils (Clark 2000), with occasional involvement of the adenoids. Diseased tonsils are associated with decreased antigen transport, decreased antibody production above baseline levels, and chronic bacterial infection.

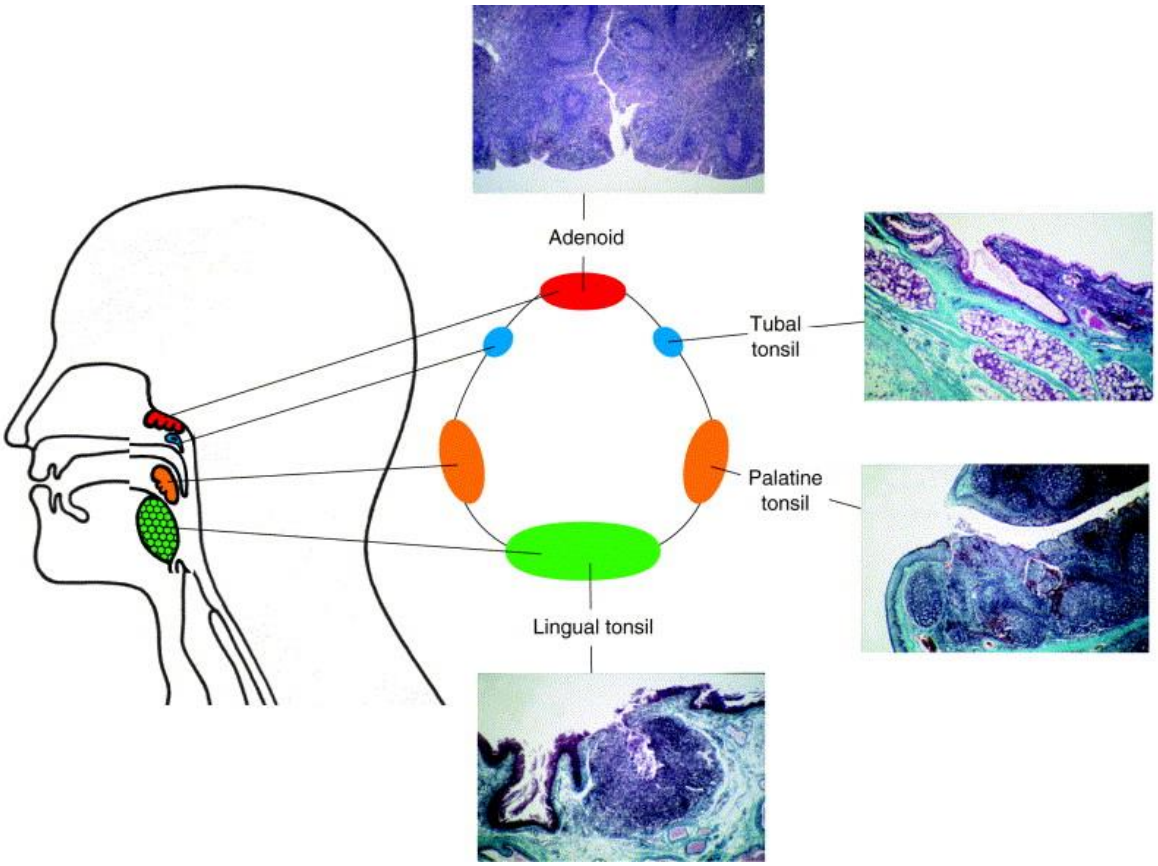

Figure 1.5 Waldeyer's Ring. Pharyngeal lymphoid tissue of Waldeyer's ring comprises the nasopharyngeal tonsil or adenoid (NT), the paired tubal tonsils (TT), the paired palatine tonsils (PT) and the lingual tonsil (LT). All four micrographs show that the surface of the tonsils is in each case covered with pharyngeal epithelium. Note the branching crypt arrangement in the NT and the PT, and the single crypt in the LT. The intimate relationship of tonsils with salivary glands is especially obvious in the TT.

Adapted from Perry *et al* 1998

Although healthy tonsils offer immune protection, diseased tonsils are less effective at serving their immune functions. Diseased tonsils are associated with decreased antigen transport, decreased antibody production above baseline levels, and chronic bacterial infection.

Of note, the pharyngeal surface of the nasopharyngeal tonsil is covered mainly with a ciliated respiratory epithelium. The surface epithelium (or outer capsule) of the palatine tonsils, however, is essentially a continuation of the non-keratinized or parakeratinized stratified squamous of the surrounding oropharyngeal mucosa (Perry 1998). Heterogeneity within both the nasopharyngeal and palatine tonsil architectures becomes apparent at the tonsil crypts as epithelia becomes increasingly reticulated and often desquamated (Perry 1994). In an average adult, it has been estimated that the stratified squamous epithelium of the superficial oropharyngeal aspect accounts for $45cm^2$ of total palatine tonsil surface area while the morphologically non-uniform epithelium of the tonsillar crypts accounts for $295cm^2$ of total surface area (Perry 1994, 1998).

Antigen sampling in this lymphoepithelial organ occurs at specialized tonsillar crypts either through direct contact with infiltrated immune cells or via follicle-associated epithelium (FAE). FAE refers to the epithelium lining the crypts, and includes reticulated specialized M-cells, which are able to sample antigen and

translocate them to underlying lymphoid tissue (Perry 1994, Perry 1998). (Figure 1.6)

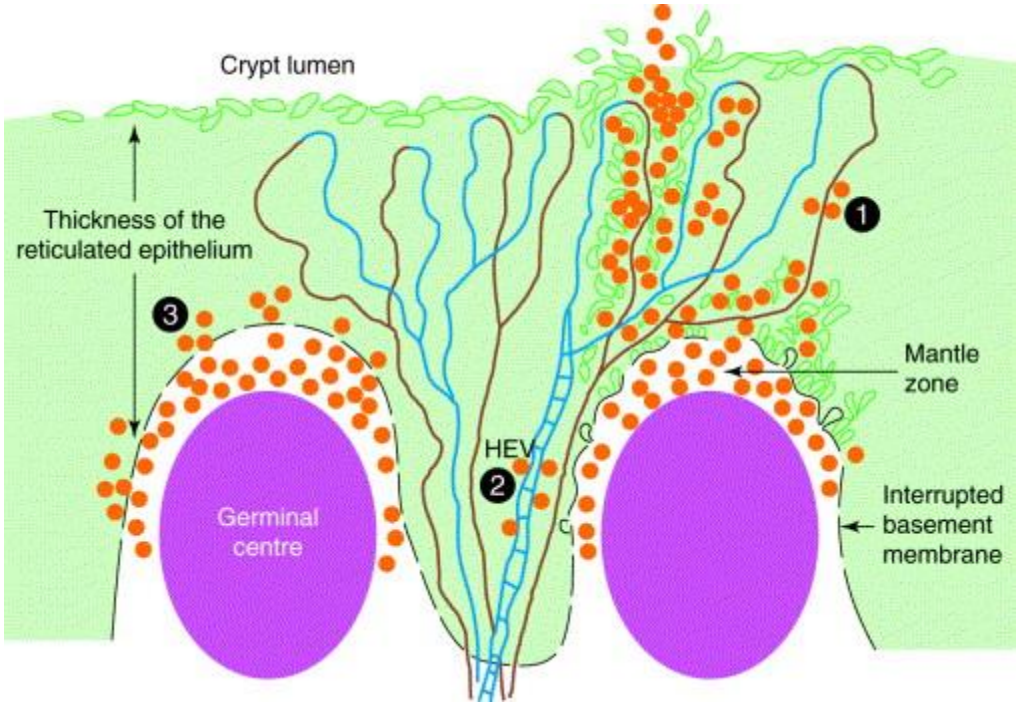

Figure 1.6. The lymphoepithelium of the palatine tonsil. The nonepithelial cells, mainly lymphocytes, can enter the reticulated epithelium either via vascular (1 and 2) or nonvascular routes (3). Routes 1 and 2 involve direct homing into the lymphoepithelium through the walls of capillaries and high endothelial venules (HEVs), whereas route 3 involves entry from the subepithelial lymphoid compartments through the disrupted basement membrane.

Image adapted from Perry *et al* 1998

While the uniqueness of the specialized epithelium of the palatine tonsil provides a functional capacity to sample antigens for immunoprotection, it is well documented that this organ is a prudent area for pathogen entry. Various investigators have shown a pathogenic focus for oral HIV transmission, EBV transmission, and a putative route for prion entry concentrated in tonsillar crypt reticulated epithelium (Perry 1998, Pegtal 2004, Maher 2005, Moutsopoulos 2007).

1.9 Experimental Models of Pharyngitis

In an animal model, rabbits infected with aerosolized group A streptococci revealed streptococci and cell debris-like masses mainly within the micropores of the palatine tonsillar crypt while the pharynx, larynx, trachea, bronchi, and lungs appeared mostly resistant (Hokonohara 1988).

The rabbit model offers insight that is likely applicable to humans, but potentially significant anatomic and pathologic inconsistencies exist between the two species. Rabbit palatine tonsils are monocryptic, as compared to polycryptic tonsils of humans (Effat 2006). Infected rabbits also do not present symptoms of pharyngitis as do infected humans. Tissues equivalent to those of Waldeyer's ring are actually present in all mammals (except rodents), but tonsil crypt distribution and epithelial lining differs greatly amongst mammals. These differences include the few short wide-tonsil crypts of camels, the few deep crypts of the cow, and the many deep crypts of dogs (Effat 2006). Interestingly,

the clinical features of acute pharyngitis is absent in all aforementioned mammals, and are even not seen in baboons and rhesus macaques that are infected with group a streptococci. *Cynomolgus macaques* however, do reliably mimic the clinical features of the human infection (Sumby 2008), but this model is prohibitively expensive and therefore could not be used in routine studies. Additionally, while numerous studies have used nonhuman primate models for pharyngeal colonization and/or infection by GrAS, high inoculating doses of bacteria are consistently employed, ranging from more than 3×10^5 to 10^8 CFU. Nonetheless, transcription of several GrAS genes that are upregulated in organisms recovered from pharyngitis patients are also expressed at elevated levels during infection in the macaque model (Virtaneva 2003, Shumby 2008, Shea 2010).

In vitro studies remain a useful alternative to animal models for elucidating basic features of complex infection mechanisms. We discuss existing epithelial cell *in vitro* models along with some of their benefits and set backs in section 4.

§2.0 OBJECTIVES

As more is understood about *Streptococcus pyogenes* pathogenesis, the complexity of its adaptive capacity is further revealed. The anatomical predisposition of the tonsil makes it an organ prone to streptococcal infections although this phenomenon is not well understood from a mechanistic perspective. Putative virulence factors appear to guide S*. pyogenes* infective capacity in a serotype specific and environment-dependent manner. The growing appreciation of the relationship between streptococcal virulence factors, environmental conditions, and surface anatomic architecture necessitate the development of systems that better mimic the natural host. Additionally, our current ability to investigate mechanisms of pathogenesis by cellular and genetic tools may further allow us to understand a simple clinical observation that Group A streptococci appears to preferentially infect tonsillar tissue in the oropharynx leading to acute tonsillitis.

The overarching aim of this study was to better understand the tissue-/niche-specificity that has been attributed to “throat specialists” strains of Group A streptococci, GrAS. While during the process of this investigation, however, we successfully established techniques for cultivating primary tonsil epithelial cells, as well as characterized two palatine tonsil-derived tumor cell lines for their novel use as an *in vitro* model for tonsillitis. Armed with these new tools, we were able to specifically test the bacterium’s ability to discern from its proximate environment: tonsil vs non-tonsil epithelium. Using established measures of pathogenesis, we observed epithelial cell type-specific phenotypic and genotypic

responses by our representative M type 1 strain, SF370, a member of the earlier ascribed “throat tropic” group of streptococci. This study has extended our lab’s continued work on the transcription shifts observable in *S. pyogenes* from initial contact with host factors in suspension (conditioned media), to transient contact / association with neighboring epithelial cells (Detroit 562), to transient contact / association with palatine tonsil epithelium (UT-SCC-60B), to adherence with nasopharyngeal (Detroit 562) surface. It is clear that, *in vivo*, the GrAS must experience to some extent every step within our model’s continuum. The bacteria also may adhere to non-tonsil tissues in the pharynx, particularly during asymptomatic carriage of the pathogen in the nasopharynx. While we have observed unique qualities that are stage-specific throughout the course of an infection, improvements in models and annotation will only produce even greater opportunities to ask more precise questions. Our UT-SCC-60A and UT-SCC-60B tonsil epithelial model mirrored many of the *in vitro* effects exhibited by the more precious HPTE cells, offering an affective surrogate for determining anatomically significant mechanisms underlying streptococcal pharyngotonsillitis.

§3.0 MATERIALS AND METHODS

3.1 ***Bacterial Strains and Growth Conditions.*** Group A Streptococcus (GrAS) strain SF370 (M type 1) was provided by J. Ferretti, University of Oklahoma Health Sciences Center. Unless otherwise stated, the spontaneous streptomycin-resistant derivative of SF370 will be referred to as SF370 Wild Type or $SF370SM^R$. The isogenic KO mutant SF370∆0129 was derived from this GrAS background. GrAS strain D471 (M type 6), and the isogenic M-negative mutant JRS75 were from the Rockefeller University culture collection. All GrAS strains were grown at 37°C supplemented with 5% $C0_2$ in Todd Hewitt broth + 1%Yeast Extract (BD, Becton, Dickinson and Company) and on protease peptone blood agar (ie. supplemented with 4% defribinated sheep blood (Cleveland Scientific)) or Columbia Blood Agar plates (Thermo Scientific). When required, media was supplemented with antibiotics at the following concentrations: erythromycin at15 µg/ml or streptomycin at 200 µg/ml. *E. coli* strain One Shot DH5α (Invitrogen) was cultured in Luria-Bertani (LB) broth and on LB agar supplemented with erythromycin at 200 µg/ml at 37°C.

3.2 ***Human Immortalized Epithelial Cell Lines and Growth Conditions*** Detroit 562 (ATCC CCL-138) human nasopharyngeal epithelial cell line obtained from the American Type Culture Collection (Manassas, Va.) was maintained at 37°C in minimal essential medium (MEM) (Gibco-BRL, Life Technologies, Grand Island, NY) supplemented with 10% fetal bovine serum (FBS), 5 mM L-

Glutamine, and 1mM Na pyruvate. Human immortalized epithelial cell lines UT-SCC-60A (palatine tonsil primary tumor-derived) and UT-SCC-60B (donor paired secondary / metastatic tumor-derived) were generously provided to us for this study by Dr. Reidar Grenman (University of Turku, Turku, Finland) (Lange, et al 2009) (Takebayashi 2004). UT-SCC cell types were maintained at 37°C in Dulbecco's Modified Essential Medium (DMEM) (Gibco-BRL) supplemented with 5% fetal bovine serum (FBS) 2 mM L-glutamate.

3.3 *Adherence and invasion assay* GrAS strains SF370, SF370Δ0129, D471 and JRS75 cultures were grown to early log phase (OD600 ~0.6) in THY, washed twice with 0.1 M Phosphate Buffered Saline (PBS, pH 7.4), collected by centrifugation (3000 g, 10 min), and resuspended in Minimum Essential Medium (MEM, Invitrogen, Carlsbad, CA) at a concentration of ~1x108 CFU/mL and incubated for 1 h at 37°C. Glycerol (10% vol/vol) was added and cultures were flash frozen in liquid N_2. Culture suspensions were kept at -80°C until the day of assay experiment when frozen suspensions were thawed in a 37°C waterbath for 1h. Thawed bacterial suspensions were diluted with warm MEM (without serum). A Falcon® 24-well tissue culture plate with respective human epithelial cell type(s) grown as a monolayer to approximately 90% confluency was washed twice with PBS. Approximately 10^6 bacteria were added per well and plates were infected for 2 h at 37°C in a 5% CO_2 atmosphere. The wells were then washed twice with PBS, and parallel tests were performed to assess bacterial adherence and internalization.

The presence of intracellular viable intracellular bacteria was quantified by the standard antibiotic protection assay as previously described (Ryan 2007). Briefly, the extracellular bacteria after 2 h of infection were killed by adding prewarmed MEM without serum containing 600mg l^{-1} penicillin (Sigma) and 100 mg l^{-1} gentamicin (Sigma). After 1 h of further incubation, the monolayers were rinsed twice with PBS. Purified phage lytic enzyme, PlyC (0.05U / well) (Fischetti 1971, Nelson 2001) was then added to monolayers and incubated for 5 min at 37° and washed three times with PBS. Cells were detached from the plate by treatment with 100µl of 0.25% trypsin−0.02% EDTA (Life Technologies) and then lysed by the addition of 400µl of Triton X-100 (0.025% in H_2O). Appropriate dilutions were plated on blood agar to determine the number of viable bacteria. Antibiotic sensitivity was demonstrated in control experiments with equivalents numbers of bacteria and under the same conditions as in the invasion assay except that no epithelial cells were present in the well. Internalization results were expressed as the average number of bacteria recovered per well for three independent determinations in a single assay and the invasion efficiency (% invasion) was calculated using the following equation: bacteria recovered (cfu ml^{-1}) time 3 hrs in the presence of antibiotics/bacteria inoculated (cfu ml^{-1}) × 100.

To measure bacterial adherence the monolayers were further incubated with fresh media for 1 h. Then, cells were dispersed and lysed, and bacteria were plated for enumeration. The numbers of cfu recovered from these wells represent total associated bacteria (attached plus internalized), and for simplicity named as adherence. Adherence results were expressed as the average number of

bacteria recovered per well for three independent determinations in a single assay and the percentage of adherence was calculated using the following equation: bacteria recovered (cfu ml^{-1}) after 3 h (2 h infection + 1 h incubation) / bacteria inoculated (cfu ml^{-1}) × 100.

Tests were repeated four times and results are expressed as the averages + SD for a representative experiment performed in triplicate.

3.4 ***Bacterial Intracellular Viability.*** Mid- late log phase ($O.D._{600}$ ~0.6) bacteria were co-cultured with human epithelial monolayers as described previously for the Invasion Assay. After extracellular bacteria were killed by antibiotic solution (600mg/mL penicillin and 100 mg/mL gentamicin) with subsequent PlyC treatment (0.05U / well), monolayers were overlaid with anti-reemergence medium consisting of DMEM with 10% FBS, diluted PlyC solution (0.005U/mL), and Tannic acid) (Nakagawa 2004). At specified time intervals, post initial antibiotic treatment (T_0= 0hrs, T_2=2hrs, T_3= 16hrs, and T_4=24hrs), designated monolayers were enzymatically detached and lysed to quantify viable intracellular bacteria by cfu counts on blood agar plates as previously described

3.5 ***Human Primary Tonsil Epithelium*** At the present time, there remains no ATCC deposited human tonsil epithelial cell line. Human palatine tonsils were obtained from otherwise healthy patients undergoing routine tonsillectomy by surgeons affiliated with NewYork-Presbyterian (NYP) Department of Otorhinolaryngology or the National Cancer Institute's Cooperative Human

Tissue Network (CHTN) Eastern, Midwestern, and Western Divisions. Only specimens from traditional “full” tonsillectomy (FT) performed either by cold dissection (conventional scalpel), electrocautery, laser, the harmonic scalpel, or coblation was used for culturing. Specimens from “partial” tonsillectomy techniques such as Powered Intracapsular Tonsillectomy with Adenoidectomy (PITA) were rejected due to the procedure’s inherent tissue pre-masceration.

The experimental protocol received Institutional Review Board approvals from both the Rockefeller University (VAF-0621-1207) and the Weill Cornell Medical College [nos. 0803009695 and 0806009857and individual patient consent for the use of tissue in research applications was obtained prior to the surgical procedure. Other investigators may have received specimens from the same subjects. Specimens were never refrigerated and unless otherwise noted, all subsequent processing was performed using reagents pre-warmed to 37° C. Tonsils were transported within 6 h of surgery at room temperature (RT) in “transport antibiotic solution” consisting of sterile 0.1M phosphate-buffered saline (PBS) (pH 7.4) supplemented with 0.5% bovine serum albumin (SIGMA) and antibiotic / anti-mycotic cocktail (Gentamicin [50 μg mL^{-1}], Penicillin [1000 U mL^{-1}], Streptomycin [10 mg mL^{-1}], Fungizone [25 μg mL^{-1}], and Nystatin [240 U mL^{-1}])(SIGMA) or shipped overnight at ambient temperature in DMEM supplemented with fetal bovine serum (10%) and antibiotic / anti-mycotic cocktail (Penicillin [100μg mL^{-1}], Streptomycin [100μg mL^{-1}], Amphotericin B [2.5μg mL^{-1}].

Acquired tonsil specimens were carefully dissected about the surface of the tonsil capsule under a sterile cell culture hood using surgical tools in a glass Petri dish. Investigator visual inspection was used to separate the exterior (epithelial) tissues from underlying follicular lymphocytes and connective tissues as best as possible and resulting capsular tissues were further cut into small explants measuring ~1-3 mm^3. Explants were transferred to a conical tube containing fresh, pre-warmed transport antibiotic solution and washed twice by briefly vortexing to liberate potentially associated non-epithelial cell types (including lymphocytes, innate immune cells, and low density fat), allowing the explants to settle by gravity at the bottom of the tube and aspirating off resulting supernatant. Explants were then washed an additional two times in pre-warmed "high Ca^{++} media" consisting of Dulbecco's modified Eagle's medium (DMEM) supplemented with 10% fetal bovine serum, F12, 0.1mM Na Pyruvate, 1mM calcium, and antibiotic / anti-mycotic cocktail (Gentamicin [50 µg mL^{-1}], Penicillin (1000 U mL^{-1}], Streptomycin [10 mg mL^{-1}], Fungizone [25 µg mL^{-1}], and Nystatin [240U mg mL^{-1}]). After final wash, explants were placed in a 100-mm-diameter petri dish, submerged in high Ca^{++} media, and incubated overnight at 37° C in 5% CO_2. The next day, explants were washed twice with transport antibiotic solution before being transferred to a Costar 100-mm-diameter tissue culture plate (Figure 3.1).

Culturing the explants was done in three phases. In the first phase, Costar® 24-mm-diameter transwell devices (3 per culture plate) was placed on

top of tissue explants (~10 pieces) with high calcium media added into and around each transwell. Inert sterile glass beads were (~5-8) were added inside of each transwell to provide a weight to aid explants adhere to the tissue culture dish and stimulate the outward migration of epithelial cells from the tissue. Explants with weighted transwells were incubated at 37° C in 5% CO_2 for approximately 8 days with daily media changes. In the second phase, the transwells were removed and the remaining adherent explants were assessed for migrating epithelial colonies extending from the tissue. Keratinocyte serum-free medium with keratinocyte growth factor (KGF) (Invitrogen) supplemented with 0.1 mM Ca^{++} and antibiotic / anti-mycotic cocktail (Gentamicin [50 µg mL^{-1}], Penicillin [1000 UmL^{-1}], Streptomycin [240 µg mL^{-1}], Fungizone [240 µg mL^{-1}], and Nystatin [240 U mL^{-1}]). The low calcium "keratinocyte medium" supported outgrowth of epithelial cells, and kill both fibroblasts and lingering lymphocytes. Keratinocyte media was changed daily for 10 days. For the third phase, the explants were gently removed leaving only attached epithelial cells. Subsequent epithelial cells were then transferred to Falcon PRIMARIA® tissue culture flasks (BD) at ~60% confluency in the UT-SCC cell media (MEM).

Tonsil media was switched to a basal media with serum 5-12 hrs before human primary tonsil epithelial cell monolayers were used for co-culturing experiments with bacterial pathogen.

Figure 3.1. Schematic of Human Primary Tonsil Epithelial Cell Culture technique

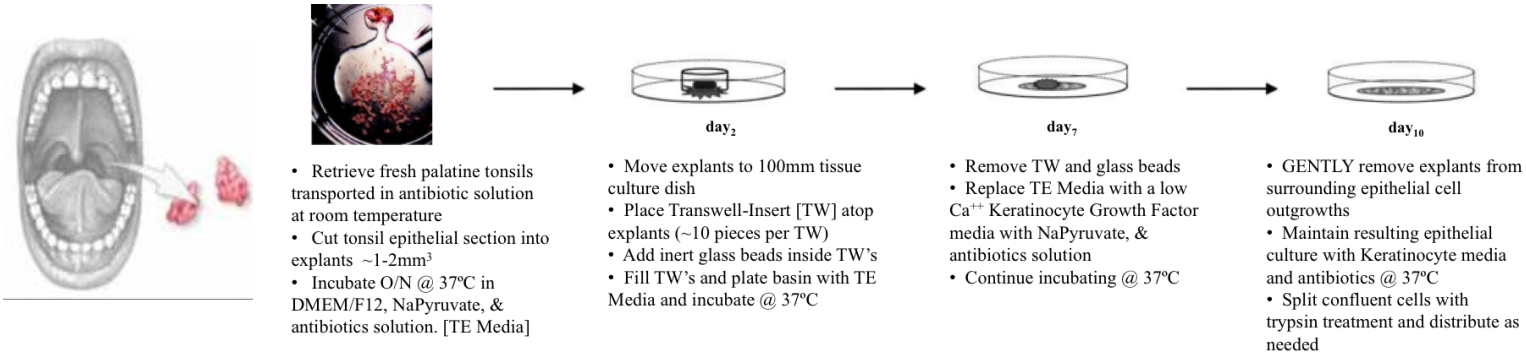

Protocol modified from Pegtal et al 2004

3.6 *Recombinant M- protein preparation*

E. coli bearing plasmid pJRS42.13 (Coli M6) was cultured to amplify recombinant M type 6 protein in the host bacteria's periplasmic space. This material was extracted and purified essentially as described by Fischetti *et al* 1984.

3.7 *Bacterial cell wall preparation* *S. pyogenes* cells were fractionated by two separate methodological protocols as indicated in the results. The first method is modified from a protocol described by Linke *et al* 2009. *S. pyogenes* serotype strain SF370 was grown in Todd-Hewitt broth supplemented with 1% yeast extract (THY) overnight at 37°C and harvested by centrifugation at 4000 rpm for 5 min. The cell pellet was resuspended in cold lysis buffer (100mM KH_2PO_4, pH 6.2, 40% sucrose, 10mM $MgCl_2$) supplemented with Complete EDTA-free protease inhibitor cocktail tablets (Roche), 4 mg/ml lysozyme, and 5U/ml amidase enzyme, PlyC, and incubated at 37°C for 2.5 h with gentle rotation.

Cells and debris were sedimented by centrifugation at 12,900 × *g* for 15 min at 4°C); the supernatant containing proteins covalently attached to the cell wall such as the pili was kept as the cell wall fraction.

As second method for extracting the bacterial cell fraction, a 50mL culture of *S. pyogenes* SF370 was grown overnight in THY media at 37°C, and harvested by centrigugation at 3000 rpm. The pellet was washed three times in PBS and resuspended to 1/50 (v/v) in lysis buffer (30% raffinose, 5mM DTT, EDTA-free protease Inhibitor [Roche®] in PBS, pH 6.1). PlyC stock (5.0 U/mL) was added to the buffer solution at 1/100 (v/v) and the mixture was incubated at 37°C for 1.5h. Following incubation, lysed material was centrifuged 10 min at 3000rpm separating protoplasts, membrane, cytoplasmic proteins. The supernatant, containing cell wall proteins, was then dialyzed against 50mM Tris-HCl, pH7.5 for 24h at 4°C. Resulting dialysate was concentrated using Centricon® filter devices (Millipore Corp, Bedford, MA).

3.8 *Conditioned media extraction and LC/MS* Fresh DMEM was applied to Detroit 562, UT-SCC-60A, UT-SCC-60B, or HPTE cell monolayers for 3h (37°C at 5% CO_2). After 3h, the cells were removed from the media by centrifugation and filtration. This supernatant or control media (20mL) was then extracted with 30mL of chloroform:methanol (7:3). The resulting emulsion was resolved by centrifugation (3200G, 15min), the aqueous layer was aspirated and the organic layer was dried down in a speed vac. This crude organic extract was resuspended in methanol (100mL) and analyzed by analytical LC/MS (XBridge

C-18, 20min linear gradient from 20:80 methanol/water with 0.1% formic acid to 100% methanol).

3.9 *Co-Immunoprecipatation (whole bug)* *S. pyogenes* grown to mid-log phase were Mitomycin C-killed using [25μg/mL] in THY for 2h at 37°C. These cells were then washed twice in PBS and used to capture natural binding partners from fractionated epithelial cell membrane proteins in suspension. Briefly, human epithelial cell monolayers were seeded to approximately 60% confluency. Adherent cells were then briefly washed of serum with pre-warmed PBS, and fed methionine-free / serum-free DMEM (Gibco) for 60 min to deplete monolayer epithelial cell methionine reserves. Cells were then l fed methionine free - MEM supplemented with ~40μM L-Azidohomoalanine (AHA), a synthetic amino acid, as well as for ~4 – 8 h to incorporate AHA in newly synthesized mammalian surface proteins. Epithelial cells were fractionated as previously described (Linke 2009) to achieve a final suspension of mammalian cell membrane associated surface proteins. Using fractionation and ultracentrifugation techniques to isolate epithelial membrane fractions, this protein suspension was exposed to killed bacteria, treated with a cross-linker, dithiobis[succinimidylpropionate] (DSP) (Pierce Biotechnology, Rockford, IL) to create a covalent bond between the human protein and pathogen, then washed to eliminate unbound debris. The pathogen-host binding partners will be un-cross-linked with dithiothreitol (DTT) (Hoefer Inc., San Francisco, CA) and the liberated human proteins will be eluted off in RIPA buffer and salt. Subsequently, the bacteria were lysed and the *S.*

pyogenes cell membrane protein fractions were collected. Bacterial fractionation was performed by method described by Linke et al mentioned above. Both eluted and membrane associated protein samples were then reacted to alkaline-Rhodamine using Cu1-catalyzed azide-alkyne cycloaddition (CuAAC) or “Click Chemistry” reaction as described previously by (Grammel 2010). Proteins were separated by SDS PAGE and bands containing human epithelial proteins cross-linked to bacterial cell wall fractions were identified by in gel fluorescence directly by scanning the gel on a GE Healthcare Typhoon 9400 variable-mode imager. Rhodamine-associated signal was detected at excitation 532 nm / emission 580nm.

3.10 ***Phase contrast microscopy*** Detroit 562, UT-SCC-60A, UT-SCC-60B, and human primary tonsil epithelial cell monolayers were grown to > 90% confluence in Falcon® or Falcon PRIMARIA® 24-well tissue culture plates. Entire plate visualized at room temperature using an Olympus IX71 inverted microscope with phase contrast optics using 20X and 40X objectives. Images were captured using a Hamamatsu Orca ER B/W digital camera with MetaMorph acquisition software (Molecular Devices, Sunnyvale, CA).

3.11 ***Streptococcal transformation with GFP expression plasmid pCM18).***

The pCM18 plasmid vector (Figure 3.2) was a generous gift from Michael Kehoe (University of Newcastle, UK). A transformation procedure described by Hansen, et al 2001 was performed with minor modification. The plasmid pCM18 was

amplified and purified by adding 5µL of pCM18 [3ng/µL] to 80µL *E. coli* One Shot TOP10 and subjected to one freeze / thaw cycle (1h on ice, then 40 seconds at 42°C, and 2min on ice) immediately followed by adding 1mL SAC media and incubation for 2 h at 37°C. After transformed *E. coli* was plated onto selective Luria-Bertani agar and incubated overnight, resistant colonies were selected and used to inoculate a 2mL culture in LB for 8h. The purification was then completed using the Qiagen HiSpeed™ Plasmid Purification Midi Kit (QIAGEN, Valencia, CA) as described by the manufacturer's protocol, finally eluting in 200µl TE. An overnight culture of *S. pyogenes* strain SF370 grown in Todd–Hewitt broth supplemented with 1% yeast extract was diluted 33 fold and incubated for 3h at 37°C until when an OD_{600} = 0.3 was reached. The culture harvested by centrifugation and washed five times in chilled electroporation medium (10% glycerol) for 15 min, rendering the streptococci competent. The pellet was then suspended in 1mL of electroporation medium to the mixture and incubated at 37°C for 2.5h. The cells were then spread on protease peptone blood agar plates with 5 µg/mL erythromycin, and transformants were scored after 2d incubation at 37°C.

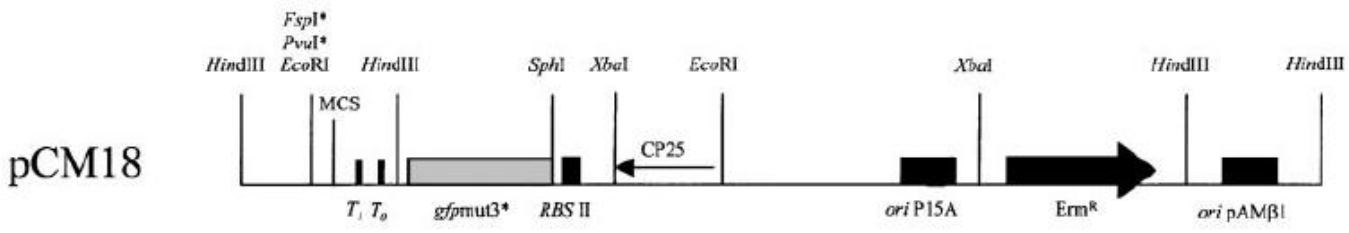

Figure 3.2 Genetic and physical map of pCM18.

Adapted from Hansen *et al* 2001

3.12 ***PlyCB purification and Alexa Fluor labeling.*** PlyCB purification and labeling was performed as previously described by Nelson *et al* 2006. Briefly, PlyCB was induced with 0.5% arabinose overnight from *E. coli* XL-1 blue (Stratagene) transformed with pBAD24 vector containing *plyCB* gene construct. Cells were washed in 20 mM phosphate buffer at pH 7.0 and lysed with 20% wt / vol chloroform to yield crude PlyCB. Lysate was then run over a hydroxyapatite (MacroPrep Typell 40µm, BioRad) column, undergoing a stepwise elution from 200mM to 1M phosphate buffer to elute PlyCB. The enzyme was then dialyzed extensively against phosphate buffer with 1mM DTT and 50mM NaCl. Protein quantification was determined with the BCA method (Sigma, St. Louis, MO). Five hundred micrograms of purified PlyCB was reacted with the carboxylic acid, succinimidyl ester of Alexa Fluor 568, or Alexa Fluor 488 (Molecular Probes) according to the manufacturer's instructions. Unreacted dye was removed from the labeled protein by application to a 5-ml HiTrap Desalting column (GE Healthcare), equilibrated with PBS.

3.13 ***Fluorescence microscopy*** Bacterial cultures were grown overnight, washed in PBS, mixed with 50 µg of labeled PlyCB (PlyCB-Alexa568), washed two times in PBS, and wet mounted on a glass microscope slide. For experiments to differentiate internalized from adherent bacteria on human epithelial monolayers, Detroit 562, UT-SCC-60B, and UT-SCC-60B cells were seeded onto coverslips placed at the bottom of wells in Falcon® 24-well plates and grown to 90% confluence. The adherence and internalization assays were

performed on coverslips as described. Wells were co-cultured with streptococci constitutively expressing GFP for 1.5h. After final wash of the ascribed assay, the monolayer wells were inoculated with 1mL vol MEM supplemented with PlyCB-Alexa568 for 5 minutes at 37°C. The wells were then washed an additional 2 times with PBS. The streptococci and pharyngeal monolayers were fixed in 4% paraformaldehyde at room temperature for 15 min, washed 3 times in PBS for 5 min each wash, and inverted onto 10µL of Prolong® Antifade (Molecular Probes, Eugene, OR) mounting media on a glass microscope slide. An Eclipse E400 microscope with a Plan Apo -100 objective (both from Nikon) was used to visualize all fluorescence samples, and digital images were obtained by using a Retiga Exi camera with Q CAPTURE PRO® software (both from QImaging, Burnaby, BC, Canada)

3.14 ***Immunofluorescence microscopy*** Cell lines (Detroit 562, UT-SCC-60A, UT-SCC-60B, and THP-1) were seeded onto coverslips placed at the bottom of wells in Falcon® 24-well plates and grown to 90% confluence. For HPTE and THP-1 cells, coverslips were pre-treated with 0.1% poly-L-lysine solution (Sigma) for 10 minutes at room temperature, washed one time in sterile water, and allowed to completely air dry before seeding. For Streptococcal internalization fate experiments, monolayers were co-cultured with *S. pyogenes* in MEM supplemented with PlyCB-Alexa568 for 1hr.

All monolayers were fixed in 4% paraformaldehyde at room temperature for 15 minutes, washed 3 times in PBS for 5 minutes each wash. For intracellular

immunolabeling, monolayers were permeabilized with 0.05% Tween in PBS$^-$ solution for 1 minute, then washed 3 times in PBS for 5 min each wash. Antibodies were diluted in 5% Normal goat serum (in PBS$^-$) as shown in table3.1. The coverslips were then distributed 200µL of their appropriate primary antibody(s) and incubated at room temperature for 1 hr or overnight at 4°C. Following incubation, excess antibiotic solution was aspirated off and coverslips were washed 3 times in PBS for 5 minutes each wash. Secondary antibodies diluted in 5% Normal goat serum (in PBS$^-$) as described (Table 3.1) were distributed to appropriate coverslips if indicated for 1h at room temperature, followed by 3 washes in PBS for 5 minutes each wash. The coverslips were then inverted onto 10µL of Prolong® Antifade (Molecular Probes, Eugene, OR) mounting media on a glass microscope slide.

Fluorescence microscope, camera, and image software was used as described earlier.

Table 3.1 Primary and secondary antibodies used for immunofluorescence

Name/Target Epitope	Host	Species Reactivity	Antibody concentration	Dilution of Antibody in %5 NGS[a]	Fluorophore label	Clone	Source
Primary Ab's							
Anti-Vimentin	Mouse	Human, Pig, Rat, Chicken, Cow, Cat, Dog	1.0mg mL^{-1}	1:100	N/A		Abcam
Anti-Cytokeratin 19	Rabbit	Human, Mouse	0.2mg mL^{-1}	1:200	N/A		Abcam
Keratin 8 /18 Ab-1	Mouse	Humans	Unavailable	1:50	N/A	5D3	NeoMarkers
Keratin, Pan Ab-1	Mouse	Human, Monkey, Cow, Rabbit, Mouse, Rat, Chicken	0.2mg mL^{-1}	1:50	N/A	AE1/AE3	NeoMarkers
Human CD44	Mouse	Human	0.1mg mL^{-1}	1:100	Fluorescein (FITC)	F10-44-2	Southern Biotech
Early Endosome Antigen-1	Mouse	Human	0.25mg mL^{-1}	1:100	Fluorescein (FITC)	14/EEA1	BD Biosciences
Phalloidin[b]	N/A	N/A	~6.6μM	1:200	Alexa Fluor 555		Invitrogen / Molecular Probes
Secondary Ab's							
F(ab')2 fragment of goat anti-rabbit IgG	Goat	Rabbit	2.0mg mL^{-1}	1:200	Alexa Fluor 488		Invitrogen / Molecular Probes
Goat Anti-Mouse IgG (H+L)	Goat	Mouse	2.0mg mL^{-1}	1:200	Rhodamine Red™-X		Invitrogen / Molecular Probes

[a] Normal Goat Serum (Vector Laboratories, Burlington, CA)
[b] Not an Antibody, but rather a fuorophore-conjugated water soluble "toxin" that is extremely used to stain F-actin at nanomolar concentrations. Unlike antibodies, the binding affinity does not change appreciably with actin from different species or sources.

3.15 ***Spotted oligonucleotide microarrays*** Sense strand oligonucleotides (primarily 55-mers), representing the 1769 open reading frames (ORF) in the genome of *Streptococcus pyogenes* strain SF370 were designed by Invitrogen and produced by Eurofins MWG Operon (Huntsville, AL) . Oligonucleotides were spotted onto Corning Epoxide Coated Slides (Corning Inc., Life Sciences, Acton, MA) by Microarrays Inc (Huntsville, AL). Slides were post-processed by Microarrays Inc, and adequate oligonucleotide deposition was verified using their quantitative Veriprobe QC assay (http://www.microarrays.com/mi-quality.php). Each oligonucleotide was spotted six times in a well-spaced configuration to generate in-slide replicates.

3.16 ***Epithelial cell association assay (for microarray).*** Assays on streptococcal association with the human pharyngeal cells were performed, as described previously (Ryan 2007), with the following modifications. Human Pharyngeal (Detroit 562) and palatine tonsil-derived (UT-SCC-60B) epithelial cell lines were grown to confluence (5×10^6 cells/well) in 6-well Falcon® plates. Intact monolayers were washed three times with 2ml PBS to remove serum. Streptococcal stock cultures in MEM and glycerol were pre-incubated at 37°C for 1 hour, and aliquots (1mL) were added to each well of 6-well plates containing confluent monolayers at a multiplicity of infection (MOI) of 100 (5×10^8 CFU/well). Streptococci in co-culture with their respective epithelial cell line in MEM were incubated for 2.5 hours at 37°C in 5% CO_2. Associated (non-adherent)

streptococci were harvested from the monolayer wells by aspiration. One PBS wash (1ml volume) was performed to ensure collection of all associated bacteria.

3.17 ***RNA isolation.*** Streptococci from the pharyngeal association assays were washed twice in PBS, resuspended in 0.1X TE (pH 6.0), and flash frozen in a bath of ethanol and dry ice. Bacteria were lysed with the amidase enzyme lysin PlyC (Fischetti 1971, Nelson 2001). Lysin was added to the bacterial samples ($2U/10^8$ cfu) and incubated for 1 minute at room temperature, which was determined to be optimum for complete streptococcal lysis in preliminary experiments. RNA was isolated immediately after lysis with a modified phenol-chloroform protocol, as described previously (Juncosa 2012), substituting acid phenol (Invitrogen) to reduce genomic DNA contamination.

RNA was digested with DNase I (TURBO DNA-*free*, Invitrogen). Removal of contaminating genomic DNA was confirmed by the absence of any PCR product using ethidium-bromide gel visualization following 40 cycles of PCR. Primers specific for the ORF *spy0930* were used as this gene was previously reported in our laboratory to be constitutively expressed in the host cell environment (unpublished observations). RNA quantity was determined with the NanoDrop 1000 spectrophotometer (Thermo Scientific, Wilmington, DE), and RNA quality was assessed with the Nucleic Acid Bioanalyzer 2100 (Agilent Tech., Palo Alto, CA).

3.18 ***Synthesis of cDNA and labeling.*** DNase-treated streptococcal total RNA (2.5 µg) was reverse transcribed using the Superscript Indirect cDNA Labeling System (Invitrogen). Random hexamers (Invitrogen) primed the reverse transcription reaction that incorporated a 5-(3-aminoallyl)-dUTP into the first synthesized cDNA strand. cDNAs from experimental streptococci and control streptococci were indirectly labeled with the N-hydroxysuccinimide activated fluorescent dyes cyanine 3 (Cy3) and cyanine 5 (Cy5), respectively, as outlined in the Superscript kit. Amersham CyDyes were purchased for this use from GE Healthcare Life Sciences (Piscataway, NJ). Labeled cDNA samples were purified following Superscript kit instructions. cDNA yield and dye incorporation rates were assessed using the NanoDrop 1000 spectrophotometer to ensure high-quality labeled probes.

3.19 ***Microarray hybridization and image acquisition.*** Biological replicate experiments incorporating dye swaps were performed to account for both biological and technical variability (Yang & Speed 2002). To determine transcriptional differences between streptococci co-cultured with human pharyngeal versus tonsillar epithelial cells, eight biological replicate experiments were prepared for both Detroit 562 and UT-SCC-60B cell lines. For microarray analysis, 4 replicates for each data set were labeled in the standard dye orientation, and 4 replicates were labeled in the flip orientation (total of 16 separate hybridizations).

Microarray slides were blocked with a prehybridization solution containing 10 mg/ml bovine serum albumin (Sigma). Labeled cDNA samples were hybridized to the arrays under standard glass microscope coverslips in a hybridization buffer containing 50% deionized formamide (Sigma), 10X SSC, and 0.2% SDS for 16 h at 55°C in a stationary hybridization oven. Slides were washed with agitation as follows: one wash with 0.2X SSC, 0.1% SDS at 55°C for 15 minutes and two washes with 0.1X SSC at room temperature for 15 minutes.

Slides were dried via centrifugation (1000 rpm, 3 minutes) and then scanned with the Agilent High-Resolution C Microarray Scanner (Agilent Technologies, Santa Clara, CA) at 5 μm per pixel resolution. The resulting images were processed using the GenePix Pro program (version 4.0, Axon, Union City, CA).

3.20 ***Data filtering, normalization, statistical significance analysis, and calculation of P values for individual genes*** *Following* image analysis, low level processing of microarray data included probe and array quality filtering to remove probes that were saturated, displayed a low signal to noise ratio, and/or produced signal in only one dye channel. Lowess standardization was performed for data normalization, and a modified *t*-test (based on CyberT software) was implemented to calculate a *P* value of the $\log_2$-fold change (expression ratio in the experimental sample to the appropriate control) for each gene, as previously described (Ryan 2007).

The *t*-test statistics and *P* values generated in this analysis were used to rank genes undergoing statistically significant changes in expression ($P < 0.05$) during association with UT-SCC-60B tonsil as compared to Detroit 562 monolayers in MEM.

No cutoff values were set for the magnitude of the expression change necessary to be included in the set of genes undergoing statistically significant fold changes. Although researchers often disregard expression changes that are less than 2-fold ($\log_2$ value of ± 1) between the experimental and control conditions, gene expression changes as low as 1.5-fold ($\log_2$ value of ± 0.6) have been demonstrated to be physiologically relevant (Hughes 2000).

The GenomeCrawler algorithm, written in the statistical language R (http://www.R-project.org), stepped through the expression date and identified adjacent gene grouping s that exhibited similar expression fold changes. The algorithm then calculated statistical significance of all putative resulting neighbor clusters using a permutation algorithm with the sum of the t-test statistics (generated by Cyber-T) from each gene within a given cluster as the metric for comparison. The output was then inspected visually and groupings were disqualified that violate the neighbor cluster definition based on established guidelines for functionally coupled gene pairs: (1) genes occur on the same DNA strand and (2) adjacent genes are separated by ≤300 bp.

Since a specified gene could be a member of many different clusters, only the cluster that generated the lowest P_K value < 0.05 and met all of the defined conditions of a neighbor cluster (as detailed in the text) was reported. The

GenomeSpyer algorithm, also written in R, provides a method to view the GenomeCrawler output and to visualize clusters and their respective gene members (Ryan 2007).

§4.0 CULTIVATION AND CHARACTERIZATION OF HUMAN PALATINE TONSIL-DERIVED EPITEHELIAL CELLS

4.1.0 Introduction:

Epithelial cell monolayers remain the standard *in vivo* model of pharyngitis for the study of basic pathology and mechanisms for infection. Group A Streptococci strains belonging to *emm* pattern groups A-C are referred to as “throat specialists”, as epidemiologic evidence demonstrate their collective predilection for this specific ecologic niche (Bessen 2009).

4.1.1 *Relevant clinical anatomy at times incongruent with cell type of convenience*

As the throat specialists GrAS strains come in contact with oramucosa, they must come in contact and may even adhere to surface along the way. Indeed, it has been reported that *S. pyogenes* can be found to bind buccal, tongue and other non-tonsillar surfaces *in vivo* (Ellen1974*).* Clinically, however, the sites of typical streptococcal disease during acute infection tend to occur posterior to the hard palate within the pharynx. Thus, clinically informed *in vitro* models should reflect disease pathology with anatomic context. For instance, A549 cells are derived from carcinomatous tissue of human alveoli (Lieber 1976), and have been used in numerous studies modeling GrAS infections of the oropharynx despite it not being an anatomic site that is normally colonized by this bacterium outside the the extraordinary rare cases of *S. pyogenes* pneumonia. Furthermore, most cases of GrAS pneumonia are not associated with concurrent or recent

pharyngitis infections, drawing into question sebseqent conjecture regarding oropharyngeal disease processes from these cells (Barnham 1999).

Another important example of an existing epithelial monolayer model that has been revisited recently is the commonly utilized HEp-2 cells to model laryngeal disease. Despite previous reports, this line was not derived from an epidermoid carcinoma of the larynx, but rather originated from a HeLa cell contamination [American Type Culture Collection (ATCC) website: http://www.atcc.org] (Abbot 2007). Additionally, many cell lines in common use for in vitro studies contain an undefined set of mutations and chromosomal abnormalities of undetermined effect on cell physiologic properties.

Detroit 562 is a permanent heteroploid human cell line that is similar to HeLa and other heteroploid cell lines in morphology, growth, and virus infectibility (Peterson 1971). The cell line was derived from a metastatic pleural lesion of an adult female with nasopharyngeal carcinoma (Brock 2002). It differs from similar permanent human cell lines in having G-6-PD type B isozyme (Peterson 1971). The Detroit 562 naspharyngeal cell line has been reported to more faithfully display the carbohydrate epitopes, however, which are more representative of the native nasopharyngeal cell than certain other transformed cell lines (Ryan 2001). The well characterized nature of this cell type, along with it's relative proximity to the normal site of clinically observed pharyngotonsillitis has made

the Detroit 562 an attractive cell line to model GrAS pathogenesis (Bartelt 1978, Ryan 2001, Pancholi 2003).

The extent to which the *in vivo* microenvironment can be reproduced *in vitro* may likely be of particular importance when modeling tissue-tropic or niche specific disease processes. There are currently no “commercially” available immortalized tonsil epithelial cell lines.

4.1.2 UT-SCC-60A / B Epithelial Cell Lines

Palatine tonsil squamous cell carcinoma tumor explants were recently dissected and cultivated from a 59 year old male patient in Finland who presented with stage IV primary disease to Dr. Reidar Grenman and colleagues from the Department of Otolaryngology and Medical Biochemistry at the University of Turku (Turku, Finland). A cell line was established using a technique whereby malignant outgrowing epithelial cells were harvested from 1 x 1 mm tissue explants attached to tissue culture flasks in DMEM supplemented with NEAA, FBS and antibiotics as previously described (Grenman 1992). The resulting cells were designated University of Turku Squamous Cell Carcinoma line 60A (UT-SCC-60A). The same patient donor had a metachronous tumor (relative to the primary) 3 months later following the onset of radiation treatment. This well-differentiated secondary tumor was surgically resected from the patient’s neck lymph node, also underwent subsequent culturing, and is designated UT-SCC-60B. The UT-SCC-60B cell line exhibited a loss of heterozygosity in an allele on

chromosome arm 18, which has been hypothesized as a common marker for growth regulation and enhanced cancer cell survivor in head and neck malignant disease (Takebayashi 2004). Pries and colleagues further noted a constitutive expression of CD44 on the cell surface of these cells as they noted of nearly all head and neck cancers reviewed in their study to differences between tumor lines and non-malignant epithelia (Pries 2008).

4.1.3 Tumor derived cell lines and Toll-Like Receptors expression

Lange et al demonstrated that UT-SCC-60A and UT-SCC-60B cell lines are similar to primary tonsil epithelial cells in Toll Like Receptor (TLR) expression. Of note, while primary and UT-SCC-60A/B lines all express mRNA for TLR and TLR-4, neither the primary or UT-SCC-60A cells were observed to actually exhibit TLR2 protein expression. UT-SCC-60B, however, was found to produce TLR2 protein following Poly I:C stimulation (Lange 2009). UT-SCC-60B's inducibility is significant as TLR-2 has been previously shown to mediate intracellular NF-KB activation in epithelial cells following stimulation by soluble peptidoglycan and lipoteichoic acid derived from oral pathogens like gram-positive streptococci (Schwandner 1999). M-protein is also recognized by TLR-2, which has been shown by oral epithelia. TLR-2 is also detected on the surface of resting Detroit 562 cells and can be further induced to increased expression after stimulation with IFN-γ (Eliasson 2007).

Relatively few protocols are available in the literature from investigators who have attempted to recreate the heterogeneous palatine tonsil epithelial cell population in vitro (Cue 2000, Pegtal 2004, Maher 2005, Abbot 2007). The heterogeneity in vivo was underscored by visual inspection of tonsillar epithelium as reported by Clark *et al (*Clark 2000). They observed localized irregularities, including lymphocyte invasion of the stratified squamous epithelium covering the external surface of the palatine tonsil in 10 of 11 randomly selected tonsils. Furthermore, in examining tonsil pieces by SEM, they recognized abrupt transition in the topographical structure of the surface. One shortcoming of many early primary tonsil epithelial cell culturing protocols is the potential mesenchymal influence that may inform the differentiating of epithelial cells to be representative of the in vivo heterogeneity (Pegtal 2004),

Work on protocols for harvesting and culturing epithelial cells from human palatine tonsils continues to be necessary given the growing evidence for the niche specificity of pathogenesis (Wannamaker 1970, Bessen 2010, Bessen 2011). Developing a standardized method becomes further complicated by the variety of tonsillectomy procedural techniques, which can alter the quality of organ samples.

In this chapter, four pharyngo-tonsillar epithelial cell monolayers are described and compared for the purpose of contributing to the existing repertoire of *in vitro* model systems for tonsillitis. A cell culturing method was implemented to isolate

and culture human primary tonsil epithelial cells (HPTEC) from fresh human palatine tonsil specimens. The HPTEC culture method utilized a staged strategy, employing both serum-containing and serum-free media to preferentially stimulate epithelial growth while mitigating contamination by fibroblast and lymphoid organ-associated immune cell types. Preliminary comparative characterization studies include visualizing relative cellular morphology, confirming epithelial nature of cell cultures, identifying surface expression of a known binging receptor, and gross comparison of surface protein banding patterns on gel electrophoresis.

4.2 Results:

4.2.1Human primary epithelial (HPTE) cell cultivation

Human primary tonsil epithelial cells were cultivated from fresh clinical patient samples post-tonsillectomy. Patients ranged in age and disease indication for the surgical procedure, although the majority (>90%) of the de-identified patient reports list hypertrophy and disordered breathing (i.e., Obstructive Sleep Apnea) as the primary complaint. Using a three-phase primary culturing system switching between serum-containing and serum-free media, primary epithelial cell populations were proliferated outwards from the edges of tonsil tissue explants.

At approximately 15-18 days after receiving the tonsil, the epithelial cells usually will have expanded adequately, such that the cells can be split and cultured into new tissue flasks or petri dishes. The stability of our attained monolayer was not as robust as reported by other researchers creating primary epithelial cell systems (Ropke 1997, Pegtal 2004), exhibiting stability only up to a maximum of 3 – 4 trypsin treatments before significant apoptosis would ensue as observed by light microscopy and cell viability staining (*not shown*).

In general, epithelial cells spread out from the tonsil explants as a carpet mainly consisting of flattened cells. The resulting cell populations were often not homogeneous in shape and size. As has been reported, it was typical to see both small (10-20μm) and large (20-100μm) cells from the start of the culture. Additionally, cytoplasmic extensions were frequently observed between adjacent

cells (Figure 4.1*F*). Previous researchers have linked this morphologic presentation in *ex vivo* tonsil cultures to the secretion of lymphokines and mediators from infiltrating lymphocytes. Perry *et a*l purports that secretions are made that may induce neighboring epithelium to undergo changes specifically in cytokeratin expression (Perry 1998). Whether cytokeratin-mediated rearrangements or by some other mechanisms, a subpopulation of the stratified squamous epithelia in the tonsil appears to undergo this unique morphologic transition of undetermined purpose. Based on a similar protocol and their observations, Pegtal *et al* suggested that by virtue of the achieved proliferative cells stemming from tissue explants, these tonsil epithelial cells are likely to be derived from the basal epithelial layer and/or tonsillar reticulated epithelium (Pegtal 2004).

Figure 4.1 Human Primary Tonsil Epitheliium

A-F Light photomicrograph of tissue explants (T) on Day 7 post tonsillectomy. **A. "**Low" magnification (10X objective) view of tonsil explant surrounded by outgrowth of migrating epithelial cells. **B-E**. "High" magnification (25X objective) view of adherent primary epithelial cells. **F**. Image E was digitally zoomed an additional x4 on area demarcated in E by white box. White arrow indicates a representative cytoplasmic extension

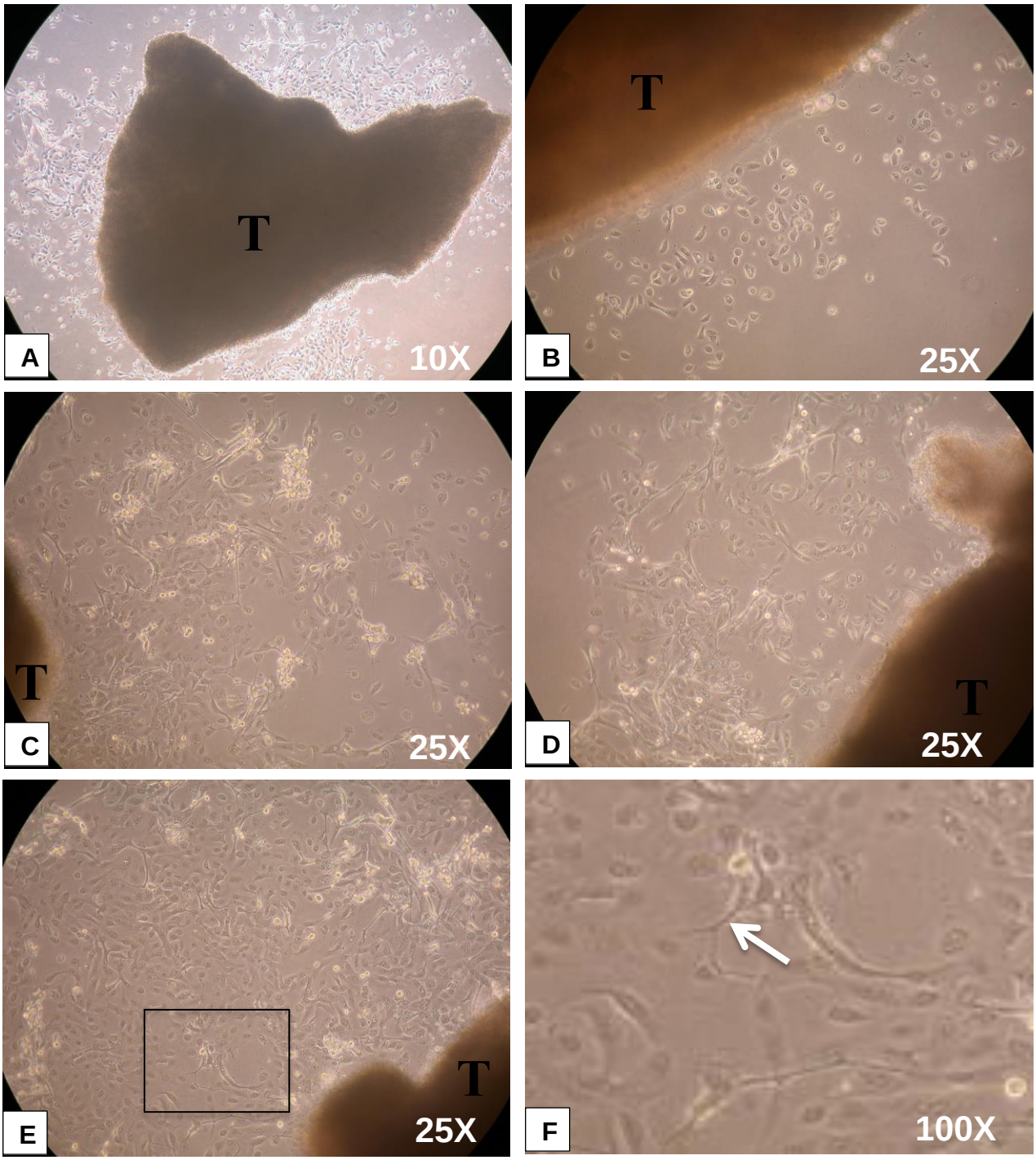
T
A
10X
T
B
25X
T
C
25X
T
D
25X
T
E
25X
F
100X

4.2.2 *Comparative light microscopy of confluent monolayers*

Epithelial cell monolayers could be distinguished based on morphology by visual inspection using microscopy. The Detroit 562 and the UT-SCC-60B cells appear similar in size when visualized as a confluent monolayer on a tissue culture flask. When compared with UT-SCC-60A and HPTE cells, the Detriot 562 and UT-SCC-60B cells are smaller. Notably, the cultured UT-SCC-60B cells grow with a distinctly dichotomous morphologic distribution throughout the monolayer. Soon after seeding these cells to ~40% confluence, patches of cells quickly adhere to the tissue culture surface and assume a flattened morphology. As the remaining "late" cells in suspension settle to fill in the patches, their adherent morphology assume a more columnar shape on visual inspection. The appearance of these "early" adhering patches seems independent of their starting cell concentration. To test this, wells were seeded heavily. While the size of the gaps between patches declined, excess cells tended to grow on top of one another at the patches rather than necessarily filling open areas remaining on the flask surface (*not shown*). No obvious differences were detected in cytokeratin expression (or in any of the other markers) stained for in our study between the "early" adhering flat cells and columnar "late" cells. This growth pattern was UT-SCC-60B-specific as it was not observed in the UT-SCC-60A monolayer.

Since the UT-SCC-60A tumor line was originally cultivated from a tissue explant taken from the primary site of the squamous cell palatine tonsillar cancer, soon after diagnosis (and in advance of chemotherapeutic treatments), there is likely

significant similarities between this and our cultured HPTC. By extension, it may not be surprising that similar characteristics are shared between these cells in culture. The relative size similarities between the lines were additionally relevant when determining the multiplicity of infection calculations for our *in vitro* studies. Detroit 562 and UT-SCC-60B monolayers both reached 100% confluency on Falcon 24-well plates at ~ 1.2 x 10^6 cells / well, while UT-SCC-60A and HPTEC reached confluence at ~2.8 x 10^5 cells / well and ~1.1 x 10^5 cell / well, respectively.

Figur4.2. Morphology of human oropharyngeal epithelial cells as a monolayer

Phase contrast microscopy images of non-fixed (A) Detroit 562, (B) UT-SCC-60A, (C) UT-SCC-60B, and (D) Human Primary Tonsil Epithelial Cell [HPTE] monolayers. Cells were grown to ~95% confluence as previously described (see methods). Images taken at original magnification 100X.

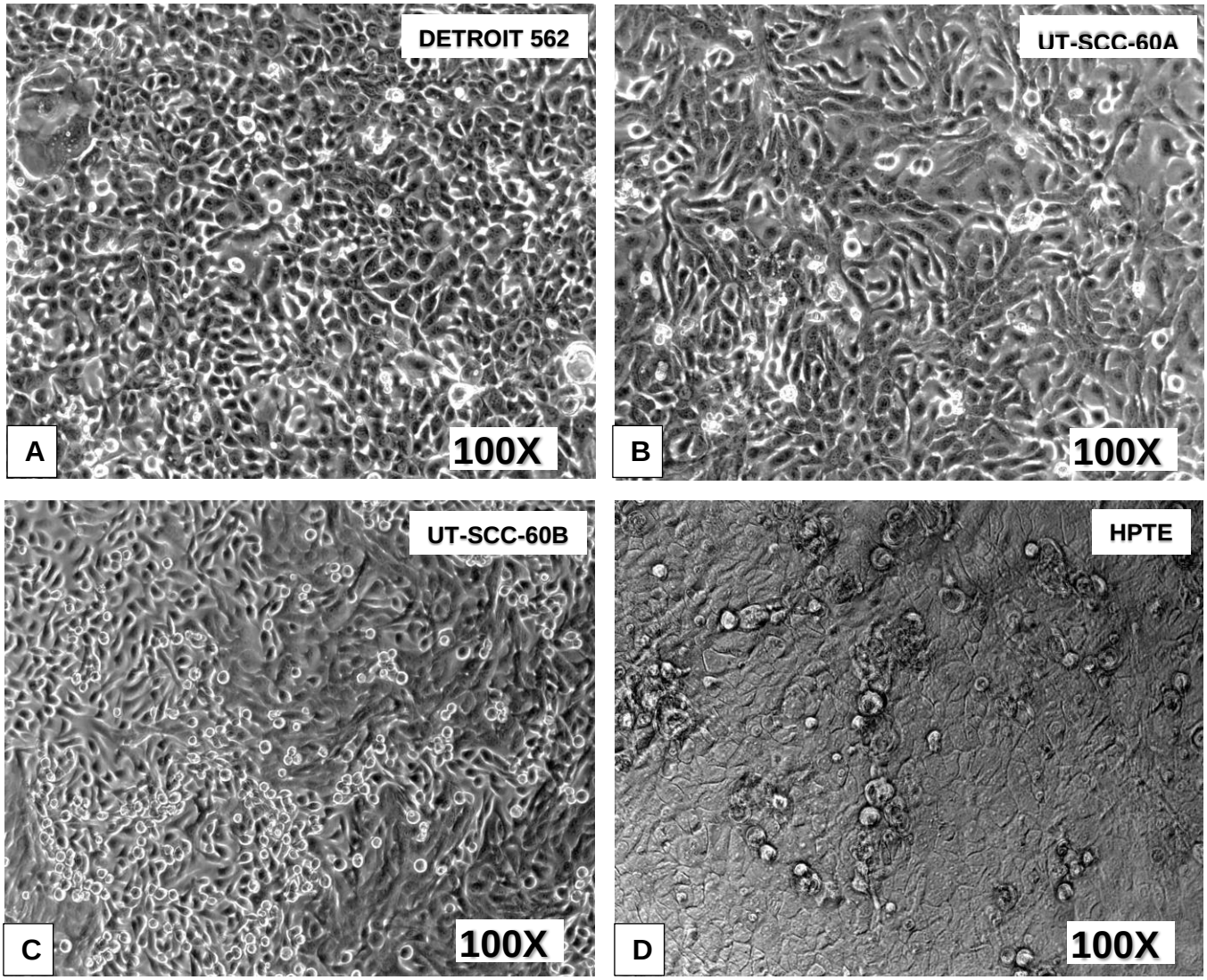
DETROIT 562
A
100X
UT-SCC-60A
B
100X
UT-SCC-60B
C
100X
HPTE
D
100X

4.2.3 Immunofluorescence staining for epithelial and fibroblast markers

In order to verify tonsil derived cell cultures were free of non-epithelial cell types, Immunofluorescence (IF) staining for epithelial (pankeratin, keratins 8 [K8], K18, and K19) and fibroblast (vimentin) markers was performed on Detroit 562, UT-SCC-60A, UT-SCC-60B, and HPTEC lines. Tonsil epithelium is comprised of stratified surface and reticulated crypt epithelia. Clark *et al* determined pan-epithelial tonsil markers and demonstrated that surface and reticular crypt epithelia may be differentiated by the expression of particular cytokeratins. Their *in situ* staining of tonsil epithelium demonstrated expression of the simple epithelial keratins K8 and K18 were mostly limited to the crypt epithelial cells, along with K19 (Clark 2000). Pancytokeratins represent a much broader staining pattern that captures numerous cytokeratin markers for both simple keratins (including K8/18) as well as complex. In this this study, variable pankeratin, K8, K18, and K19 (not shown) expression was detected in the HPTE and UT-SCC-60A, UT-SCC-60B monolayers. Interestingly, the Detroit 562 cells stained uniformly across the monolayer for the simple epithelial markers, likely indicative of cell type homogeneity. In contrast, the HPTEC cells were more heterogeneous with some cells staining significantly brighter than neighboring cells. This was less true for UT-SCC-60B cells, which suggests the presence of subpopulations of cells, which may be of crypt epithelial lineage (in appendix A4.1) (Table 4.1).

A non-epithelial cell type of monocyte lineage was used as a negative control and demonstrated the appearance of no keratin staining.

Table 4.1 Summary of Epithelial Cell Markers from ImmunoFluorescence Studies

	Cell Marker			
Epithelial Cell Type	**K8 / K18**	**K19**	**Pan-Keratin**	**Vimentin**
Detroit 562	XXX	XXX	XXX	0
UT-SCC-60A	XXX	XXX	XXX	0
UT-SCC-60B	XXX	XXX	XX	0
HPTE	XX / XXX	XXX	XXX	0 / X

XXX – highly expressing marker
XX – mildly expressing marker
X – lighty expressing marker
0 – Not expressing marker

4.2.4 Secreted metabolites by human epithelial monolayers

As with all living cells, the epithelial surfaces of human tissue require nutrients for energy production during growth and maintenance of homeostasis. Adherent cell types grown *in vitro* as a model of tissue undergo periods of enhanced proliferation soon after being passaged to artificially stimulate cell turnover using enzymes to detach them from specially treated plastic or glass to then be re-"seeded" at sub-confluent concentrations. Cells become increasingly crowded until complete monolayer confluence is reached. Environmental limitations such as nutrients and dissolved oxygen will decrease the rate of expansion until finally reaching a state of senescence. The senescent cell phenotype is characterized by a decrease in cellular energy expenditure and subsequent metabolite production. The tonsil epithelial surface *in vivo* is constantly undergoing cell turnover, since this site is subject to injury by inhaling antigens. This is a consequence of its anatomic placement at the isthmus of the digestive and upper respiratory tracts. Given the dynamic state of tonsil epithelium *in vivo*, we have designed an *in vitro* model physiologically reflective of mostly senescent cells with an allowed subpopulation undergoing proliferative growth (~90% confluence). Using this model, we sought to perform a liquid chromatography mass spectrometry (LC/MS)-based metabolomic investigation (Siuzdak 2005) to compare the intrinsic differences in metabolite production between our experimental human pharyngeal epithelial monolayers under pre-infection conditions. Our lab has previously shown how sensing pharyngeal cell soluble factors that are secreted into the mileu may augment bacterial pathogenesis

(Broudy 2001). This screen aimed to establish a baseline for any such differences, which may direct future characterization efforts.

Fresh DMEM was applied to Detroit 562, UT-SCC-60A, UT-SCC-60B, and HPTE cell monolayers and was collected following 3h of unstimulated, bacteria-free, co-culture. The supernatant from each cell line was then extracted with chloroform:methanol (7:3) and the crude extract was analyzed by LC/MS. The LC/MS analysis of the crude extracts revealed few differences between the four tested cell lines and the experimental background when compared to fresh media. Not seeing differences between the cells lines and control media suggests that either the performed LC/MS experiment was not sensitive enough to detect the low titer metabolites produced by cells or that the relatively clean chloroform:methanol extraction does not accurately represent the entire metabolome of the cell line. However, two peaks at 789.03 and 703.87 *m/z* were observed in the HPTE crude extract that were not seen in the extracts of the other cells lines (Figure 4.3).

To further interrogate the identity of these putative metabolites differentially produced by our primary tonsil epithelia, we performed a preliminary search of the Human Metabolome Database, HMDB (available at www.hmbd.ca) (Wishart 2009. Briefly, the HMDB is designed as a comprehensive, web-accessible metabolomics database that brings together quantitative chemical, physical, clinical and biological data about 7,900 experimentally 'proven' or experimentally detected human metabolites. Inputting our spectra informed measurements on molecular weight (789.03 +/- 0.5 *m/z*) (Table 4.2) yielded 210 matches where

80% were either glycerophospholipids (138/210) or diglycerides (22/210). After ruling out unlikely ionization adducts and Diguanosine triphosphate, which is likely too polar to be consistent with the observed hydrophobic retention time, the remaining compounds in the search queue were glycerophospholipids. A hydrophobic glycerophospholipid or diglyceride compound would be consistent with the retention time of the 789.03 *m/z* peak. A diglyceride structure, as suggested from a similar speculative HMDB search, would be consistent with the more polar retention time of the 703.87 *m/z* peak. Phospholipids are ubiquitous in cells and are key components of the lipid bilayer of cells. They are also available to be metabolized as an energy source or as well as signaling intermediates. Diacylglycerols are precursors to triglyceride and, biochemically, function as a 2nd messenger-signaling lipid that directly activates protein kinase C during numerous intracellular signaling pathways.

While particularly crude and speculative, these results demonstrate the potential for differences in metabolites excreted into the conditioned media between our cell lines. For the HPTE monolayer, these differences appear most prominently in liberated lipid products. This finding may have some implications on streptococcal colonization, however, as was observed by Ellen and Gibbson in 1974. Using a throat isolated, M type 12 reference strain STAT628, they noted a relative increase in adherence to oral epithelium by 9% and 25%, respectively, after adding 80µl phosphatidyl serine or phosphatidyl ethanolamine to bacterial suspension (Ellen 1974). A role relating free phospholipids to virulence or persistence at the tonsil has not been previously established, however, so our

“interesting” putative metabolite hit will require much greater context to have meaning, if any.

Figure 4.3. Conditioned "spent" media from primary epithelial cells exhibit unique metabolite production. Detroit 562, UT-SCC-60A, UT-SCC-60B and HPTE cells were grown to near 90% confluency, and subsequently co-cultured with fresh MEM media for 3h. Crude extraction by a chloroform methanol precipitation was performed and analyzed by Liquid Chromatography and Mass Spectrometry. Peak of interest at 789.03 *m/z* circled on bottom panel.

Note: 2nd Peak at 703 *m/z NOT SHOWN*

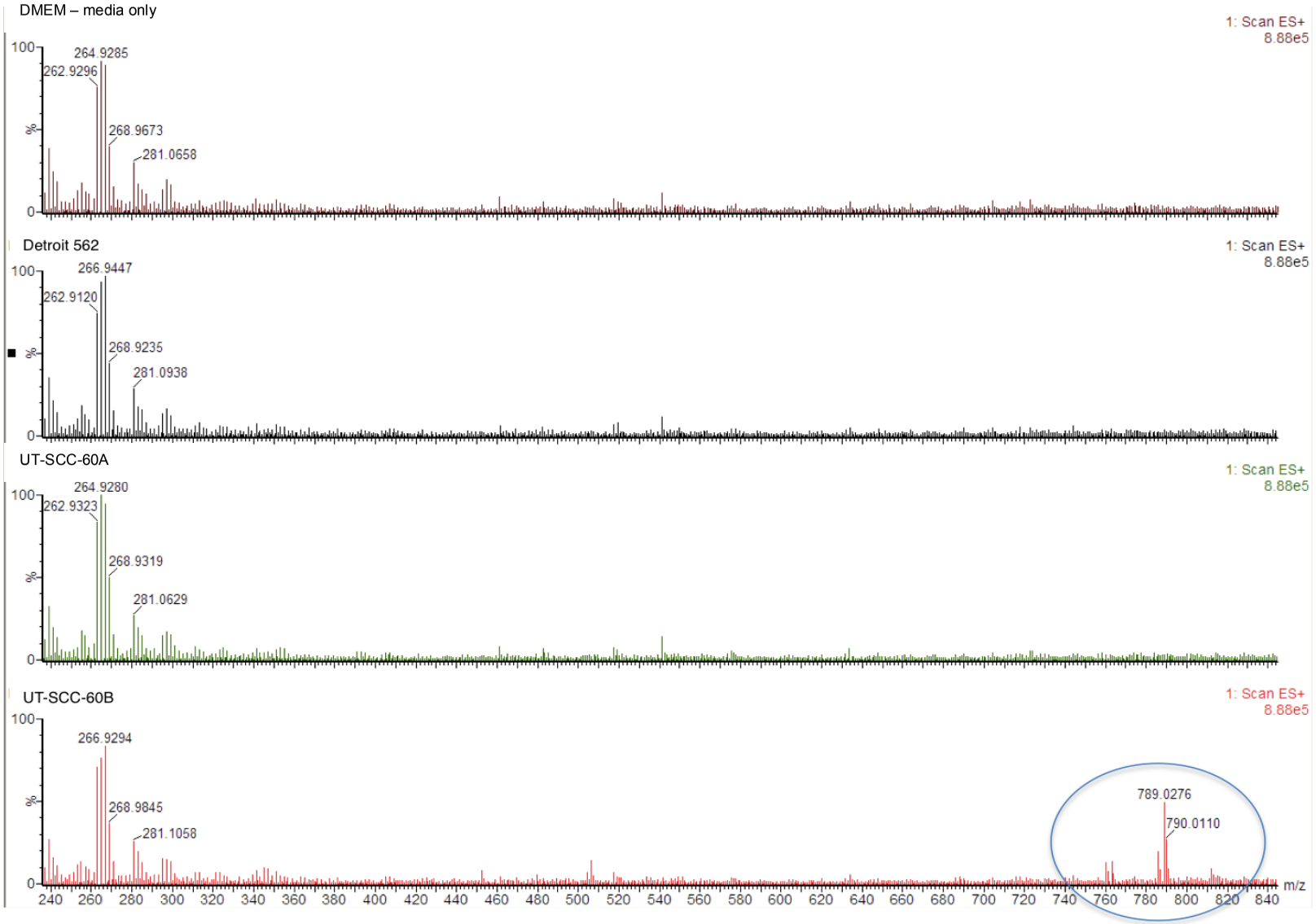
DMEM – media only
1: Scan ES+
8.88e5
100
%
0
264.9285
262.9296
268.9673
281.0658
Detroit 562
1: Scan ES+
8.88e5
100
%
0
266.9447
262.9120
268.9235
281.0938
UT-SCC-60A
1: Scan ES+
8.88e5
100
%
0
264.9280
262.9323
268.9319
281.0629
UT-SCC-60B
1: Scan ES+
8.88e5
100
%
0
266.9294
268.9845
281.1058
789.0276
790.0110
240 260 280 300 320 340 360 380 400 420 440 460 480 500 520 540 560 580 600 620 640 660 680 700 720 740 760 780 800 820 840
m/z

Table 4.2. Summary of preliminary metabolite profile potential biomarkers based on molecular weight

HMDB ID	Common Name	Chemical Formula	Adduct MW (Da) [Matching HMDB MW]	MW Difference (Da) / [QueryMass - AdductMass]	Adduct
HMDB01379	Diguanosine triphosphate	C20H27N10O18P3	789.079041 [788.071777]	0.049011	M+H [1+]
HMDB09741	PE(24:0/P-16:0)	C45H90NO7P	788.652771 [787.645508]	0.377258	M+H [1+]
HMDB09511	PE(22:0/P-18:0)	C45H90NO7P	788.652771 [787.645508]	0.377258	M+H [1+]
HMDB11388	PE(P-18:0/22:0)	C45H90NO7P	788.652771 [787.645508]	0.377258	M+H [1+]
HMDB11362	PE(P-16:0/24:0)	C45H90NO7P	788.652771 [787.645508]	0.377258	M+H [1+]
HMDB08266	PC(20:0/16:1(9Z))	C44H86NO8P	788.616394 [787.609131]	0.413635	M+H [1+]
HMDB08102	PC(18:1(9Z)/18:0)	C44H86NO8P	788.616394 [787.609131]	0.413635	M+H [1+]
HMDB08069	PC(18:1(11Z)/18:0)	C44H86NO8P	788.616394 [787.609131]	0.413635	M+H [1+]
HMDB08038	PC(18:0/18:1(9Z))	C44H86NO8P	788.616394 [787.609131]	0.413635	M+H [1+]
HMDB08037	PC(18:0/18:1(11Z))	C44H86NO8P	788.616394 [787.609131]	0.413635	M+H [1+]
HMDB08010	PC(16:1(9Z)/20:0)	C44H86NO8P	788.616394 [787.609131]	0.413635	M+H [1+]
HMDB09747	PE(24:1(15Z)/15:0)	C44H86NO8P	788.616394 [787.609131]	0.413635	M+H [1+]
HMDB08915	PE(15:0/24:1(15Z))	C44H86NO8P	788.616394 [787.609131]	0.413635	M+H [1+]
HMDB08558	PC(22:1(13Z)/14:0)	C44H86NO8P	788.616394 [787.609131]	0.413635	M+H [1+]
HMDB08526	PC(22:0/14:1(9Z))	C44H86NO8P	788.616394 [787.609131]	0.413635	M+H [1+]
HMDB07978	PC(16:0/20:1(11Z))	C44H86NO8P	788.616394 [787.609131]	0.413635	M+H [1+]
HMDB07919	PC(14:1(9Z)/22:0)	C44H86NO8P	788.616394 [787.609131]	0.413635	M+H [1+]
HMDB07887	PC(14:0/22:1(13Z))	C44H86NO8P	788.616394 [787.609131]	0.413635	M+H [1+]
HMDB08298	PC(20:1(11Z)/16:0)	C44H86NO8P	788.616394 [787.609131]	0.413635	M+H [1+]
HMDB12400	PS(18:2(9Z,12Z)/18:0)	C42H78NO10P	788.543579 [787.536316]	0.48645	M+H [1+]
HMDB12390	PS(18:1(9Z)/18:1(9Z))	C42H78NO10P	788.543579 [787.536316]	0.48645	M+H [1+]
HMDB12380	PS(18:0/18:2(9Z,12Z))	C42H78NO10P	788.543579 [787.536316]	0.48645	M+H [1+]
HMDB11933	Ganglioside GQ1c (d18:0/14:0)	C103H177N5O55	789.047485 [2364.120605]	0.017456	M+3H [3+]
HMDB10243	CL(18:2(9Z,12Z)/18:2(9Z,12Z)/18:1(9Z)/18:1(9Z))	C81H146O17P2	789.048889 [1453.003540]	0.01886	M+3ACN+2H [2+]
HMDB10242	CL(18:2(9Z,12Z)/18:2(9Z,12Z)/18:1(9Z)/18:1(11Z))	C81H146O17P2	789.048889 [1453.003540]	0.01886	M+3ACN+2H [2+]
HMDB10239	CL(18:2(9Z,12Z)/18:2(9Z,12Z)/18:1(11Z)/18:1(9Z))	C81H146O17P2	789.048889 [1453.003540]	0.01886	M+3ACN+2H [2+]
HMDB10238	CL(18:2(9Z,12Z)/18:2(9Z,12Z)/18:1(11Z)/18:1(11Z))	C81H146O17P2	789.048889 [1453.003540]	0.01886	M+3ACN+2H [2+]

HMDB00217	NADP	C21H29N7O17P3	789.054443 [744.083252]	0.024414	M+2Na-H [1+]
HMDB11912	Ganglioside GM2 (d18:1/23:0)	C73H132N2O26	789.000549 [1452.906860]	0.02948	M+3ACN+2H [2+]
HMDB04943	Ganglioside GM2 (d18:1/26:1(17Z))	C75H135N3O26	789.000488 [1493.933350]	0.029541	M+2ACN+2H [2+]
HMDB04917	Ganglioside GD3 (d18:1/24:1(15Z))	C76H135N3O29	788.957275 [1553.918091]	0.072754	M+H+Na [2+]
HMDB11867	Ganglioside GD3 (d18:0/24:1(15Z))	C76H135N3O29	788.957275 [1553.918091]	0.072754	M+H+Na [2+]
HMDB01155	Diadenosine triphosphate	C20H27N10O16P3	789.115417 [756.081909]	0.085388	M+CH3OH+H [1+]
HMDB05017	Pantoprazole	C16H15F2N3O4S	789.139465 [383.075134]	0.109436	2M+Na [1+]
HMDB00912	Succinyladenosine	C14H17N5O8	789.204651 [383.107727]	0.174622	2M+Na [1+]
HMDB06583	Poly-N-acetyllactosamine	C14H25NO11	789.274719 [383.142761]	0.24469	2M+Na [1+]
HMDB06575	Lacto-N-biose I	C14H25NO11	789.274719 [383.142761]	0.24469	2M+Na [1+]
HMDB06535	Beta-1,4-mannose-N-acetylglucosamine	C14H25NO11	789.274719 [383.142761]	0.24469	2M+Na [1+]
HMDB01542	N-Acetyllactosamine	C14H25NO11	789.274719 [383.142761]	0.24469	2M+Na [1+]
HMDB05021	Quetiapine	C21H25N3O2S	789.322693 [383.166748]	0.292664	2M+Na [1+]
HMDB12214	Dihydrozeatin-O-glucoside	C16H25N5O6	789.350159 [383.180481]	0.320129	2M+Na [1+]
HMDB12213	Dihydrozeatin-9-N-glucoside	C16H25N5O6	789.350159 [383.180481]	0.320129	2M+Na [1+]
HMDB12211	Dihydrozeatin-7-N-dihydrozeatin	C16H25N5O6	789.350159 [383.180481]	0.320129	2M+Na [1+]
HMDB06737	CE(22:2(13Z,16Z))	C49H84O2	788.702271 [704.647156]	0.327759	M+IsoProp+Na+H [1+]
HMDB07799	DG(24:0/18:2(9Z,12Z)/0:0)	C45H84O5	788.687012 [704.631897]	0.343018	M+IsoProp+Na+H [1+]
HMDB07658	DG(22:2(13Z,16Z)/20:0/0:0)	C45H84O5	788.687012 [704.631897]	0.343018	M+IsoProp+Na+H [1+]
HMDB07630	DG(22:1(13Z)/20:1(11Z)/0:0)	C45H84O5	788.687012 [704.631897]	0.343018	M+IsoProp+Na+H [1+]
HMDB07602	DG(22:0/20:2(11Z,14Z)/0:0)	C45H84O5	788.687012 [704.631897]	0.343018	M+IsoProp+Na+H [1+]
HMDB07434	DG(20:2(11Z,14Z)/22:0/0:0)	C45H84O5	788.687012 [704.631897]	0.343018	M+IsoProp+Na+H [1+]
HMDB07406	DG(20:1(11Z)/22:1(13Z)/0:0)	C45H84O5	788.687012 [704.631897]	0.343018	M+IsoProp+Na+H [1+]
HMDB07378	DG(20:0/22:2(13Z,16Z)/0:0)	C45H84O5	788.687012 [704.631897]	0.343018	M+IsoProp+Na+H [1+]
HMDB07267	DG(18:2(9Z,12Z)/24:0/0:0)	C45H84O5	788.687012 [704.631897]	0.343018	M+IsoProp+Na+H [1+]
HMDB07239	DG(18:1(9Z)/24:1(15Z)/0:0)	C45H84O5	788.687012 [704.631897]	0.343018	M+IsoProp+Na+H [1+]
HMDB07210	DG(18:1(11Z)/24:1(15Z)/0:0)	C45H84O5	788.687012 [704.631897]	0.343018	M+IsoProp+Na+H [1+]
HMDB07827	DG(24:1(15Z)/18:1(9Z)/0:0)	C45H84O5	788.687012 [704.631897]	0.343018	M+IsoProp+Na+H [1+]
HMDB07826	DG(24:1(15Z)/18:1(11Z)/0:0)	C45H84O5	788.687012 [704.631897]	0.343018	M+IsoProp+Na+H [1+]
HMDB12638	20-hydroxy-E4-neuroprostane	C22H31O5	789.397461 [375.217163]	0.367432	2M+K [1+]
HMDB12601	17-hydroxy-E4-neuroprostane	C22H31O5	789.397461 [375.217163]	0.367432	2M+K [1+]

HMDB12580	14-hydroxy-E4-neuroprostane	C22H31O5	789.397461 [375.217163]	0.367432	2M+K [1+]
HMDB12855	7-hydroxy-D4-neuroprostane	C22H31O5	789.397461 [375.217163]	0.367432	2M+K [1+]
HMDB12777	4-hydroxy-D4-neuroprostane	C22H31O5	789.397461 [375.217163]	0.367432	2M+K [1+]
HMDB04972	Glucosylceramide (d18:1/18:0)	C42H81NO8	788.661499 [727.596191]	0.36853	M+IsoProp+H [1+]
HMDB10709	Galactosylceramide (d18:1/18:0)	C42H81NO8	788.661499 [727.596191]	0.36853	M+IsoProp+H [1+]
HMDB04973	Glucosylceramide (d18:1/20:0)	C44H85NO8	788.661011 [755.627502]	0.369019	M+CH3OH+H [1+]
HMDB10710	Galactosylceramide (d18:1/20:0)	C44H85NO8	788.661011 [755.627502]	0.369019	M+CH3OH+H [1+]
HMDB12643	20-Trihydroxy-leukotriene-B4	C20H31O7	789.403137 [383.206970]	0.373108	2M+Na [1+]
HMDB10705	CerP(d18:1/24:1(15Z))	C42H82NO6P	788.653320 [727.587952]	0.376709	M+IsoProp+H [1+]
HMDB10168	SM(d18:0/16:0)	C39H82N2O6P	788.651428 [705.591064]	0.378601	M+2ACN+H [1+]
HMDB07788	DG(22:6(4Z,7Z,10Z,13Z,16Z,19Z)/ 22:6(4Z,7Z,10Z,13Z,16Z,19Z)/0:0)	C47H68O5	789.425659 [712.506653]	0.39563	M+2K+H [1+]
HMDB09312	PE(20:2(11Z,14Z)/P-16:0)	C41H78NO7P	788.616943 [727.551575]	0.413086	M+IsoProp+H [1+]
HMDB11441	PE(P-18:1(9Z)/18:1(9Z))	C41H78NO7P	788.616943 [727.551575]	0.413086	M+IsoProp+H [1+]
HMDB11440	PE(P-18:1(9Z)/18:1(11Z))	C41H78NO7P	788.616943 [727.551575]	0.413086	M+IsoProp+H [1+]
HMDB09115	PE(18:2(9Z,12Z)/P-18:0)	C41H78NO7P	788.616943 [727.551575]	0.413086	M+IsoProp+H [1+]
HMDB11408	PE(P-18:1(11Z)/18:1(9Z))	C41H78NO7P	788.616943 [727.551575]	0.413086	M+IsoProp+H [1+]
HMDB11407	PE(P-18:1(11Z)/18:1(11Z))	C41H78NO7P	788.616943 [727.551575]	0.413086	M+IsoProp+H [1+]
HMDB09084	PE(18:1(9Z)/P-18:1(9Z))	C41H78NO7P	788.616943 [727.551575]	0.413086	M+IsoProp+H [1+]
HMDB09083	PE(18:1(9Z)/P-18:1(11Z))	C41H78NO7P	788.616943 [727.551575]	0.413086	M+IsoProp+H [1+]
HMDB11376	PE(P-18:0/18:2(9Z,12Z))	C41H78NO7P	788.616943 [727.551575]	0.413086	M+IsoProp+H [1+]
HMDB09051	PE(18:1(11Z)/P-18:1(9Z))	C41H78NO7P	788.616943 [727.551575]	0.413086	M+IsoProp+H [1+]
HMDB09050	PE(18:1(11Z)/P-18:1(11Z))	C41H78NO7P	788.616943 [727.551575]	0.413086	M+IsoProp+H [1+]
HMDB11349	PE(P-16:0/20:2(11Z,14Z))	C41H78NO7P	788.616943 [727.551575]	0.413086	M+IsoProp+H [1+]
HMDB09576	PE(22:2(13Z,16Z)/P-16:0)	C43H82NO7P	788.616394 [755.582886]	0.413635	M+CH3OH+H [1+]
HMDB09313	PE(20:2(11Z,14Z)/P-18:0)	C43H82NO7P	788.616394 [755.582886]	0.413635	M+CH3OH+H [1+]
HMDB09282	PE(20:1(11Z)/P-18:1(9Z))	C43H82NO7P	788.616394 [755.582886]	0.413635	M+CH3OH+H [1+]
HMDB09281	PE(20:1(11Z)/P-18:1(11Z))	C43H82NO7P	788.616394 [755.582886]	0.413635	M+CH3OH+H [1+]
HMDB11447	PE(P-18:1(9Z)/20:1(11Z))	C43H82NO7P	788.616394 [755.582886]	0.413635	M+CH3OH+H [1+]
HMDB11414	PE(P-18:1(11Z)/20:1(11Z))	C43H82NO7P	788.616394 [755.582886]	0.413635	M+CH3OH+H [1+]
HMDB11382	PE(P-18:0/20:2(11Z,14Z))	C43H82NO7P	788.616394 [755.582886]	0.413635	M+CH3OH+H [1+]
HMDB11357	PE(P-16:0/22:2(13Z,16Z))	C43H82NO7P	788.616394 [755.582886]	0.413635	M+CH3OH+H [1+]

HMDB07782	DG(22:6(4Z,7Z,10Z,13Z,16Z,19Z)/22:0/0:0)	C47H80O5	788.616333 [724.600586]	0.413696	M+ACN+Na [1+]
HMDB07754	DG(22:5(7Z,10Z,13Z,16Z,19Z)/22:1(13Z)/0:0)	C47H80O5	788.616333 [724.600586]	0.413696	M+ACN+Na [1+]
HMDB07725	DG(22:5(4Z,7Z,10Z,13Z,16Z)/22:1(13Z)/0:0)	C47H80O5	788.616333 [724.600586]	0.413696	M+ACN+Na [1+]
HMDB07697	DG(22:4(7Z,10Z,13Z,16Z)/22:2(13Z,16Z)/0:0)	C47H80O5	788.616333 [724.600586]	0.413696	M+ACN+Na [1+]
HMDB07669	DG(22:2(13Z,16Z)/22:4(7Z,10Z,13Z,16Z)/0:0)	C47H80O5	788.616333 [724.600586]	0.413696	M+ACN+Na [1+]
HMDB07642	DG(22:1(13Z)/22:5(7Z,10Z,13Z,16Z,19Z)/0:0)	C47H80O5	788.616333 [724.600586]	0.413696	M+ACN+Na [1+]
HMDB07641	DG(22:1(13Z)/22:5(4Z,7Z,10Z,13Z,16Z)/0:0)	C47H80O5	788.616333 [724.600586]	0.413696	M+ACN+Na [1+]
HMDB07614	DG(22:0/22:6(4Z,7Z,10Z,13Z,16Z,19Z)/0:0)	C47H80O5	788.616333 [724.600586]	0.413696	M+ACN+Na [1+]
HMDB07587	DG(20:5(5Z,8Z,11Z,14Z,17Z)/24:1(15Z)/0:0)	C47H80O5	788.616333 [724.600586]	0.413696	M+ACN+Na [1+]
HMDB07839	DG(24:1(15Z)/20:5(5Z,8Z,11Z,14Z,17Z)/0:0)	C47H80O5	788.616333 [724.600586]	0.413696	M+ACN+Na [1+]
HMDB11577	MG(20:3(8Z,11Z,14Z)/0:0/0:0)	C23H40O4	788.608459 [380.292664]	0.42157	2M+3H2O+2H [2+]
HMDB11576	MG(20:3(5Z,8Z,11Z)/0:0/0:0)	C23H40O4	788.608459 [380.292664]	0.42157	2M+3H2O+2H [2+]
HMDB11575	MG(20:3(11Z,14Z,17Z)/0:0/0:0)	C23H40O4	788.608459 [380.292664]	0.42157	2M+3H2O+2H [2+]
HMDB11547	MG(0:0/20:3(8Z,11Z,14Z)/0:0)	C23H40O4	788.608459 [380.292664]	0.42157	2M+3H2O+2H [2+]
HMDB11546	MG(0:0/20:3(5Z,8Z,11Z)/0:0)	C23H40O4	788.608459 [380.292664]	0.42157	2M+3H2O+2H [2+]
HMDB11545	MG(0:0/20:3(11Z,14Z,17Z)/0:0)	C23H40O4	788.608459 [380.292664]	0.42157	2M+3H2O+2H [2+]
HMDB13330	3-Hydroxy-cis-5-tetradecenoylcarnitine	C21H39NO5	788.599487 [385.282837]	0.430542	2M+NH4 [1+]
HMDB00770	N-Glycoloylganglioside GM2	C43H85NO8	788.598633 [743.627502]	0.431396	M+2Na-H [1+]
HMDB10577	PG(16:0/18:3(9Z,12Z,15Z))	C40H73O10P	789.465332 [744.494141]	0.435303	M+2Na-H [1+]
HMDB10576	PG(16:0/18:3(6Z,9Z,12Z))	C40H73O10P	789.465332 [744.494141]	0.435303	M+2Na-H [1+]
HMDB10675	PG(18:3(9Z,12Z,15Z)/16:0)	C40H73O10P	789.465332 [744.494141]	0.435303	M+2Na-H [1+]
HMDB10660	PG(18:3(6Z,9Z,12Z)/16:0)	C40H73O10P	789.465332 [744.494141]	0.435303	M+2Na-H [1+]
HMDB10646	PG(18:2(9Z,12Z)/16:1(9Z))	C40H73O10P	789.465332 [744.494141]	0.435303	M+2Na-H [1+]
HMDB10590	PG(16:1(9Z)/18:2(9Z,12Z))	C40H73O10P	789.465332 [744.494141]	0.435303	M+2Na-H [1+]
HMDB10682	PG(18:3(9Z,12Z,15Z)/18:3(9Z,12Z,15Z))	C42H71O10P	789.467651 [766.478455]	0.437622	M+Na [1+]
HMDB10681	PG(18:3(9Z,12Z,15Z)/18:3(6Z,9Z,12Z))	C42H71O10P	789.467651 [766.478455]	0.437622	M+Na [1+]
HMDB10667	PG(18:3(6Z,9Z,12Z)/18:3(9Z,12Z,15Z))	C42H71O10P	789.467651 [766.478455]	0.437622	M+Na [1+]
HMDB10666	PG(18:3(6Z,9Z,12Z)/18:3(6Z,9Z,12Z))	C42H71O10P	789.467651 [766.478455]	0.437622	M+Na [1+]
HMDB10567	PE-NMe(16:0/16:0)	C38H76NO8P	788.591248 [705.530884]	0.438782	M+2ACN+H [1+]
HMDB08988	PE(18:0/15:0)	C38H76NO8P	788.591248 [705.530884]	0.438782	M+2ACN+H [1+]
HMDB08892	PE(15:0/18:0)	C38H76NO8P	788.591248 [705.530884]	0.438782	M+2ACN+H [1+]

HMDB07965	PC(16:0/14:0)	C38H76NO8P	788.591248 [705.530884]	0.438782	M+2ACN+H [1+]
HMDB07934	PC(15:0/15:0)	C38H76NO8P	788.591248 [705.530884]	0.438782	M+2ACN+H [1+]
HMDB07869	PC(14:0/16:0)	C38H76NO8P	788.591248 [705.530884]	0.438782	M+2ACN+H [1+]
HMDB12868	9'-Carboxy-gamma-chromanol	C23H35O4	789.470215 [375.253540]	0.440186	2M+K [1+]
HMDB08196	PC(18:3(9Z,12Z,15Z)/14:0)	C40H74NO8P	788.580566 [727.515198]	0.449463	M+IsoProp+H [1+]
HMDB08163	PC(18:3(6Z,9Z,12Z)/14:0)	C40H74NO8P	788.580566 [727.515198]	0.449463	M+IsoProp+H [1+]
HMDB08131	PC(18:2(9Z,12Z)/14:1(9Z))	C40H74NO8P	788.580566 [727.515198]	0.449463	M+IsoProp+H [1+]
HMDB08903	PE(15:0/20:3(8Z,11Z,14Z))	C40H74NO8P	788.580566 [727.515198]	0.449463	M+IsoProp+H [1+]
HMDB08902	PE(15:0/20:3(5Z,8Z,11Z))	C40H74NO8P	788.580566 [727.515198]	0.449463	M+IsoProp+H [1+]
HMDB09351	PE(20:3(8Z,11Z,14Z)/15:0)	C40H74NO8P	788.580566 [727.515198]	0.449463	M+IsoProp+H [1+]
HMDB09318	PE(20:3(5Z,8Z,11Z)/15:0)	C40H74NO8P	788.580566 [727.515198]	0.449463	M+IsoProp+H [1+]
HMDB07907	PC(14:1(9Z)/18:2(9Z,12Z))	C40H74NO8P	788.580566 [727.515198]	0.449463	M+IsoProp+H [1+]
HMDB07876	PC(14:0/18:3(9Z,12Z,15Z))	C40H74NO8P	788.580566 [727.515198]	0.449463	M+IsoProp+H [1+]
HMDB07875	PC(14:0/18:3(6Z,9Z,12Z))	C40H74NO8P	788.580566 [727.515198]	0.449463	M+IsoProp+H [1+]
HMDB08199	PC(18:3(9Z,12Z,15Z)/16:0)	C42H78NO8P	788.580017 [755.546509]	0.450012	M+CH3OH+H [1+]
HMDB08166	PC(18:3(6Z,9Z,12Z)/16:0)	C42H78NO8P	788.580017 [755.546509]	0.450012	M+CH3OH+H [1+]
HMDB08134	PC(18:2(9Z,12Z)/16:1(9Z))	C42H78NO8P	788.580017 [755.546509]	0.450012	M+CH3OH+H [1+]
HMDB08006	PC(16:1(9Z)/18:2(9Z,12Z))	C42H78NO8P	788.580017 [755.546509]	0.450012	M+CH3OH+H [1+]
HMDB07975	PC(16:0/18:3(9Z,12Z,15Z))	C42H78NO8P	788.580017 [755.546509]	0.450012	M+CH3OH+H [1+]
HMDB07974	PC(16:0/18:3(6Z,9Z,12Z))	C42H78NO8P	788.580017 [755.546509]	0.450012	M+CH3OH+H [1+]
HMDB07913	PC(14:1(9Z)/20:2(11Z,14Z))	C42H78NO8P	788.580017 [755.546509]	0.450012	M+CH3OH+H [1+]
HMDB08394	PC(20:3(8Z,11Z,14Z)/14:0)	C42H78NO8P	788.580017 [755.546509]	0.450012	M+CH3OH+H [1+]
HMDB08361	PC(20:3(5Z,8Z,11Z)/14:0)	C42H78NO8P	788.580017 [755.546509]	0.450012	M+CH3OH+H [1+]
HMDB08329	PC(20:2(11Z,14Z)/14:1(9Z))	C42H78NO8P	788.580017 [755.546509]	0.450012	M+CH3OH+H [1+]
HMDB07882	PC(14:0/20:3(8Z,11Z,14Z))	C42H78NO8P	788.580017 [755.546509]	0.450012	M+CH3OH+H [1+]
HMDB07881	PC(14:0/20:3(5Z,8Z,11Z))	C42H78NO8P	788.580017 [755.546509]	0.450012	M+CH3OH+H [1+]
HMDB08259	PC(18:4(6Z,9Z,12Z,15Z)/dm18:0)	C44H80NO7P	788.556458 [765.567261]	0.473572	M+Na [1+]
HMDB08228	PC(18:3(9Z,12Z,15Z)/P-18:1(9Z))	C44H80NO7P	788.556458 [765.567261]	0.473572	M+Na [1+]
HMDB08227	PC(18:3(9Z,12Z,15Z)/P-18:1(11Z))	C44H80NO7P	788.556458 [765.567261]	0.473572	M+Na [1+]
HMDB08195	PC(18:3(6Z,9Z,12Z)/P-18:1(9Z))	C44H80NO7P	788.556458 [765.567261]	0.473572	M+Na [1+]
HMDB08194	PC(18:3(6Z,9Z,12Z)/P-18:1(11Z))	C44H80NO7P	788.556458 [765.567261]	0.473572	M+Na [1+]

HMDB11312	PC(P-18:1(9Z)/18:3(9Z,12Z,15Z))	C44H80NO7P	788.556458 [765.567261]	0.473572	M+Na [1+]
HMDB11311	PC(P-18:1(9Z)/18:3(6Z,9Z,12Z))	C44H80NO7P	788.556458 [765.567261]	0.473572	M+Na [1+]
HMDB11279	PC(P-18:1(11Z)/18:3(9Z,12Z,15Z))	C44H80NO7P	788.556458 [765.567261]	0.473572	M+Na [1+]
HMDB11278	PC(P-18:1(11Z)/18:3(6Z,9Z,12Z))	C44H80NO7P	788.556458 [765.567261]	0.473572	M+Na [1+]
HMDB11247	PC(P-18:0/18:4(6Z,9Z,12Z,15Z))	C44H80NO7P	788.556458 [765.567261]	0.473572	M+Na [1+]
HMDB13415	PC(o-16:1(9Z)/20:4(8Z,11Z,14Z,17Z))	C44H80NO7P	788.556458 [765.567261]	0.473572	M+Na [1+]
HMDB11221	PC(P-16:0/20:4(8Z,11Z,14Z,17Z))	C44H80NO7P	788.556458 [765.567261]	0.473572	M+Na [1+]
HMDB11220	PC(P-16:0/20:4(5Z,8Z,11Z,14Z))	C44H80NO7P	788.556458 [765.567261]	0.473572	M+Na [1+]
HMDB08488	PC(20:4(8Z,11Z,14Z,17Z)/P-16:0)	C44H80NO7P	788.556458 [765.567261]	0.473572	M+Na [1+]
HMDB08455	PC(20:4(5Z,8Z,11Z,14Z)/P-16:0)	C44H80NO7P	788.556458 [765.567261]	0.473572	M+Na [1+]
HMDB11154	LPA(P-16:0e/0:0)	C19H39O6P	789.504089 [394.248413]	0.47406	2M+H [1+]
HMDB10572	PG(16:0/18:0)	C40H79O10P	789.504211 [750.541077]	0.474182	M+K [1+]
HMDB10600	PG(18:0/16:0)	C40H79O10P	789.504211 [750.541077]	0.474182	M+K [1+]
HMDB08126	PC(18:1(9Z)/P-16:0)	C42H82NO7P	788.554077 [743.582886]	0.475952	M+2Na-H [1+]
HMDB08093	PC(18:1(11Z)/P-16:0)	C42H82NO7P	788.554077 [743.582886]	0.475952	M+2Na-H [1+]
HMDB08028	PC(16:1(9Z)/P-18:0)	C42H82NO7P	788.554077 [743.582886]	0.475952	M+2Na-H [1+]
HMDB11305	PC(P-18:1(9Z)/16:0)	C42H82NO7P	788.554077 [743.582886]	0.475952	M+2Na-H [1+]
HMDB11272	PC(P-18:1(11Z)/16:0)	C42H82NO7P	788.554077 [743.582886]	0.475952	M+2Na-H [1+]
HMDB11240	PC(P-18:0/16:1(9Z))	C42H82NO7P	788.554077 [743.582886]	0.475952	M+2Na-H [1+]
HMDB11210	PC(P-16:0/18:1(9Z))	C42H82NO7P	788.554077 [743.582886]	0.475952	M+2Na-H [1+]
HMDB11209	PC(P-16:0/18:1(11Z))	C42H82NO7P	788.554077 [743.582886]	0.475952	M+2Na-H [1+]
HMDB07997	PC(16:0/P-18:1(9Z))	C42H82NO7P	788.554077 [743.582886]	0.475952	M+2Na-H [1+]
HMDB07996	PC(16:0/P-18:1(11Z))	C42H82NO7P	788.554077 [743.582886]	0.475952	M+2Na-H [1+]
HMDB11151	PC(O-16:0/18:2(9Z,12Z))	C42H82NO7P	788.554077 [743.582886]	0.475952	M+2Na-H [1+]
HMDB11908	Ganglioside GM2 (d18:0/26:1(17Z))	C76H138N2O26	789.510681 [1494.953735]	0.480652	M+2ACN+2H [2+]
HMDB12363	PS(16:1(9Z)/14:0)	C36H68NO10P	789.513184 [705.458069]	0.483154	M+IsoProp+Na+H [1+]
HMDB12353	PS(16:0/14:1(9Z))	C36H68NO10P	789.513184 [705.458069]	0.483154	M+IsoProp+Na+H [1+]
HMDB12343	PS(14:1(9Z)/16:0)	C36H68NO10P	789.513184 [705.458069]	0.483154	M+IsoProp+Na+H [1+]
HMDB12333	PS(14:0/16:1(9Z))	C36H68NO10P	789.513184 [705.458069]	0.483154	M+IsoProp+Na+H [1+]
HMDB08229	PC(18:4(6Z,9Z,12Z,15Z)/14:0)	C40H72NO8P	789.515320 [725.499573]	0.485291	M+ACN+Na [1+]
HMDB08197	PC(18:3(9Z,12Z,15Z)/14:1(9Z))	C40H72NO8P	789.515320 [725.499573]	0.485291	M+ACN+Na [1+]

HMDB08164	PC(18:3(6Z,9Z,12Z)/14:1(9Z))	C40H72NO8P	789.515320 [725.499573]	0.485291	M+ACN+Na [1+]
HMDB09417	PE(20:4(8Z,11Z,14Z,17Z)/15:0)	C40H72NO8P	789.515320 [725.499573]	0.485291	M+ACN+Na [1+]
HMDB08905	PE(15:0/20:4(8Z,11Z,14Z,17Z))	C40H72NO8P	789.515320 [725.499573]	0.485291	M+ACN+Na [1+]
HMDB08904	PE(15:0/20:4(5Z,8Z,11Z,14Z))	C40H72NO8P	789.515320 [725.499573]	0.485291	M+ACN+Na [1+]
HMDB09384	PE(20:4(5Z,8Z,11Z,14Z)/15:0)	C40H72NO8P	789.515320 [725.499573]	0.485291	M+ACN+Na [1+]
HMDB07909	PC(14:1(9Z)/18:3(9Z,12Z,15Z))	C40H72NO8P	789.515320 [725.499573]	0.485291	M+ACN+Na [1+]
HMDB07908	PC(14:1(9Z)/18:3(6Z,9Z,12Z))	C40H72NO8P	789.515320 [725.499573]	0.485291	M+ACN+Na [1+]
HMDB07877	PC(14:0/18:4(6Z,9Z,12Z,15Z))	C40H72NO8P	789.515320 [725.499573]	0.485291	M+ACN+Na [1+]
HMDB10580	PG(16:0/20:4(5Z,8Z,11Z,14Z))	C42H75O10P	788.543579 [770.509766]	0.48645	M+NH4 [1+]
HMDB10575	PG(16:0/18:2(9Z,12Z))	C40H75O10P	788.543579 [746.509766]	0.48645	M+ACN+H [1+]
HMDB10679	PG(18:3(9Z,12Z,15Z)/18:1(9Z))	C42H75O10P	788.543579 [770.509766]	0.48645	M+NH4 [1+]
HMDB10678	PG(18:3(9Z,12Z,15Z)/18:1(11Z))	C42H75O10P	788.543579 [770.509766]	0.48645	M+NH4 [1+]
HMDB10664	PG(18:3(6Z,9Z,12Z)/18:1(9Z))	C42H75O10P	788.543579 [770.509766]	0.48645	M+NH4 [1+]
HMDB10663	PG(18:3(6Z,9Z,12Z)/18:1(11Z))	C42H75O10P	788.543579 [770.509766]	0.48645	M+NH4 [1+]
HMDB10650	PG(18:2(9Z,12Z)/18:2(9Z,12Z))	C42H75O10P	788.543579 [770.509766]	0.48645	M+NH4 [1+]
HMDB10645	PG(18:2(9Z,12Z)/16:0)	C40H75O10P	788.543579 [746.509766]	0.48645	M+ACN+H [1+]
HMDB10637	PG(18:1(9Z)/18:3(9Z,12Z,15Z))	C42H75O10P	788.543579 [770.509766]	0.48645	M+NH4 [1+]
HMDB10636	PG(18:1(9Z)/18:3(6Z,9Z,12Z))	C42H75O10P	788.543579 [770.509766]	0.48645	M+NH4 [1+]
HMDB10631	PG(18:1(9Z)/16:1(9Z))	C40H75O10P	788.543579 [746.509766]	0.48645	M+ACN+H [1+]
HMDB10622	PG(18:1(11Z)/18:3(9Z,12Z,15Z))	C42H75O10P	788.543579 [770.509766]	0.48645	M+NH4 [1+]
HMDB10621	PG(18:1(11Z)/18:3(6Z,9Z,12Z))	C42H75O10P	788.543579 [770.509766]	0.48645	M+NH4 [1+]
HMDB10616	PG(18:1(11Z)/16:1(9Z))	C40H75O10P	788.543579 [746.509766]	0.48645	M+ACN+H [1+]
HMDB10594	PG(16:1(9Z)/20:3(8Z,11Z,14Z))	C42H75O10P	788.543579 [770.509766]	0.48645	M+NH4 [1+]
HMDB10593	PG(16:1(9Z)/20:3(5Z,8Z,11Z))	C42H75O10P	788.543579 [770.509766]	0.48645	M+NH4 [1+]
HMDB10589	PG(16:1(9Z)/18:1(9Z))	C40H75O10P	788.543579 [746.509766]	0.48645	M+ACN+H [1+]
HMDB10588	PG(16:1(9Z)/18:1(11Z))	C40H75O10P	788.543579 [746.509766]	0.48645	M+ACN+H [1+]
HMDB13332	3-Hydroxy-5, 8-tetradecadiencarnitine	C21H37NO5	789.523560 [383.267181]	0.49353	2M+Na [1+]
HMDB02082	Bisnorcholic acid	C22H36O5	788.535706 [380.256287]	0.494324	2M+3H2O+2H [2+]

* Glycerophospholipids are highlighted *yellow*. Diglycerides are highlighted *green*.

Abbreviations: PC = Phosphatidylcholine, PG = Phosphatidylglycine, PS = Phosphatidylserine, DG = Diacylglycerol (Diglyceride)

4.3 Discussion:

The specificity of all cell types within the palatine tonsil niche is not yet fully understood, functionally or anatomically, as recent studies regularly describe new information on the substructure of the lymphoepithelium (Clark 2000), the possible existence of M cells (Park 2003), and the production of surface anti-microbial peptides (Ball 2007, Schwaab 2010). The need for reliable *in vitro* models to model niche-specific disease remains an important impetus to explore the utility of primary organ sources and tumor-derived lines. Lange and colleagues concluded that their own preliminary characterization of UT-SCC-60A and UT-SCC-60B cell lines with respect to Toll-Like receptor expression "justify the use of the [UT-SCC-60A and UT-SCC-60B] cell lines as a model system to examine…tonsillar epithelial cells" (Lange 2009).

As was recently shown by Pegtal *et al* using a similar primary cell cultivation scheme, we established a reasonably clean population of HPTE using commercially available serum-containing and serum-free media supplemented with growth factors (Pegtal 2004). In our current study, Detroit 562, UT-SCC-60A, UT-SCC-60B, and HPTE cells on visual inspection all stained positive for keratins k8, k18, k19 and pankeratin markers but were negative for the fibroblast marker, ant-vimentin. These data suggest that the cultures were principally of epithelial lineage (Clark 2000).

Most epithelial tissues are complex, and therefore simple keratin protein expression may be useful in probing the origin of epithelial cells. While Clark *et al* described pan-tonsillar markers in their *in situ* analysis of tonsil biopsies, their ascribed specificity for simple keratins to identify crypt cells are likely most significant with the support of anatomical orientation and within context of an intact tissue. Notably, the same three keratins identified within the tonsil to designate crypt cells are also typical of adenocarcinomas, and are present in certain other carcinomas (Omary 2009). Non-specificity was seen in our study with epithelial monolayers since all keratins tested were present in all of our cell types with similar staining intensities as determined solely by visual inspection. Detroit 562 cells derived from a nasopharyngeal squamous cell carcinoma do not likely contain crypt cell epithelia, so simple keratin distribution may not be the most effective means for distinguishing our cell types. Our findings are consistent with Weber *et al,* who in 1984 also verified that Detroit 562 cells expressed keratin K8, K18, and K19 in their analysis of the relationship between these proteins and a human tumor marker, tissue polypeptide antigen (TPA). Keratin distribution differences may, however, provide a crude visual assessment of heterogeneity in tonsil-derived epithelial monolayers that thus far remain poorly characterized in the literature. A more rigorous analysis of our primary epithelial cells versus the Detroit 562 line may be able to better resolve this difference than the techniques described above.

Challenges and benefits to culturing primary epithelial cells

Several intrinsic challenges exist when relying on human samples, such as tissue availability, incomplete medical history, and inter-sample variability. Our IRB-approved protocol did not provide us the ability to further acquire patient records to confirm patient history of culture-positive (rather than "suspected") GrAS infection. As the first step of our culturing procedure, tonsil samples were immediately placed in an antibiotic / anti-mycotic solution. This solution greatly mitigated inappropriate bacterial growth, but fungal contamination continued as a significant problem that sporadically confounded our primary culture. Multiple anti-fungals across differing concentrations were used with similar apparent inefficiency in completely eliminating this fungal threat. The extended length of time our cells were in culture surely served as a contributor to this propensity for eventual fungal contamination.

In her *Methods in Molecular Medicine* protocol entry on culturing primary cells, Louise Donnelly underscored the importance of recognizing that cell lines are only models of human primary epithelial cells. To her point, she compares responses of A549 cells, BEAS-2B and passaged human primary epithelium to stimulation with "cytomix" (interleukin-1β, tumor necrosis factor-α, and interferon-γ). A significantly higher level of granulocyte macrophage-colony stimulation factor (GM-CSF) was produced by the primary cells relative to the immortalized cell lines by up to a 4-fold differential (Donelly 2001). In our present study, the

use of LC-MS in ESI positive mode detected 3 potential metabolite biomarkers found uniquely in primary tonsil epithelial cell spent media versus our three tumor cell lines. Further investigation suggested that one of these markers is likely a phospholipid or diglyceride.

Due to the constraints of primary culturing, Donnelly concluded that cell lines remain of critical importance and contends that they be used to interrogate mechanistic pathways, requiring the use of many expendable cells. She warns that data should not necessarily be extrapolated to *in vivo* conditions, or even to the activity of *in vitro* primary cells. Indeed, it is undetermined the effect that our findings from our metabolome investigation might have on experiments remains undetermined but it represents an important reminder about the limitations of assertions made solely based on immortalized cell date. She concludes that more definitive conformational experiments may be performed using primary cells as the presumably more relevant model (Donnelly 2001). It is with this latter premise in mid that we have moved forward with performing many of our larger experiments with our UT-SCC-60B and UT-SCC-60B cell to follow up with primary cells, when available. We report in our subsequent studies, whenever possible, the results from both the immortalized and HPTE cells to demonstrate confirmatory or disparate findings

§5.0 M1 STREPTOCOCCUS ADHERENCE AND INVASION PHENOTYPES SUGGESTIVE OF TISSUE-SPECIFIC TROPISM FOR TONSIL EPITHELIUM

5.1 Introduction:

Our understanding of how *S. pyogenes* can asymptomatically colonize its human host and/or cause disease has revealed a cadre of virulence factors that are M type and strain-specific conferring the pattern specificity between the so classified specialists and generalists. Transmission of the "throat tropic" M types is largely mediated through respiratory droplets or secretions and direct contact with host mucus surfaces. Onset of a group A streptococcal infection requires that this immotile pathogen not only avoid clearance by opposing mucociliary flow by the upper respiratory tract, but while so doing, traverse over much of the oropharyngeal mucosal surface before finally adhering to- and then colonizing its target epithelium (Beachey 1987). Clinical observations convincingly indicate that group A streptococci have a pronounced predilection for colonizing tonsillar epithelium *in vivo* (Ellen 1974, Hokonohara 1988, Lija 1999, Roberts 2012). The number of *in vitro* studies described in the literature demonstrative of human pharyngeal tissue adherence tropism is surprisingly few (Ellen 1974).

Park and colleagues' murine intranasal infection model confirmed that GrAS has a tropism towards an ascribed tonsil-homolog of paired lymphoid lobes along the animal's lateral nasopharyngeal wall (nasal-associated lymphoid tissue, NALT) (Park 2003). The mechanism of the latter model rests greatly on M cell-specific

adherence properties, which has subsequently not been reliably extended to human or primate tonsillitis models. This example reveals a major shortcoming of experimental animal models to accurately represent diseases caused by this human-specific pathogen and the challenge to studying GrAS tissue tropisms. Bessen *et al* also notes that extensive genetic diversity among strains often give rise to strain-dependent phenotypes in various *in vitro* and *in vivo* models (Bessen, Lizano 2010)

The Detroit 562 human nasopharyngeal cell line is a well-characterized epithelial line that has been used extensively by many groups to model streptococcal infection and to specifically explore GrAS pharyngeal adherence properties (Duncan 1978, Fluckiger 1998, Ryan 2001, Pancholi 2003, Hong 2005, Ryan 2007, Manetti 2007). Our laboratory in particular has used this as an important tool for understanding characteristics of the early host-pathogen colonization process, which may help explain the clinically observed tropism exhibited by this pathogen. Our studies with this cell type have recently revealed novel receptors for M protein - sialic acid- mediated host-pathogen interactions as well as important global transcriptional data on GrAS gene expression upon adhering to Detroit 562 cells (Ryan 2001, 2007).

Morphologic heterogeneity of our human primary tonsil epithelial (HPTE) monolayer has demonstrated characteristics in shape and keratin staining suggestive of a subpopulation of cultured crypt – like lymphoepithelia cells. While

we continue to characterize this subtype, the effect the tonsil has already shown to have on its local microenvironment, as evidenced by the monolayer's distinct metabolite production, may prove significant in our ability to more reliably recreate an *in vitro* system more closely resembling the *in vivo* microenvironment. The palatine tonsil tumor-derived UT-SCC-60A and UT-SCC-60B epithelial cell lines may contribute an additional model to study tonsil-specific disease pathogenesis. The reliability of these tumor lines to mimic primary tonsil epithelial cells and, by extension intact tonsil, during streptococcal infection has yet to be explored.

In this chapter, we revisit the widely used Detroit 562 nasopharyngeal cell based *in vitro* co-culture assay to observe streptococcal colonization and infection phenotype of a clinically isolated M type 1 strain of Group A streptococcus, SF370. We then explore the relative differences in streptococcal adherence predilection during co-culture with Detroit 562, UT-SCC-60A, UT-SCC-60B, and human primary tonsil epithelial cells. Following a brief update on a modification to the classically described standard internalization assay, we immediately employ this method to compare GrAS internalization across respective epithelia.

5.2 Results

5.2.1 Streptococci are heterogeneously distributed along monolayers

Early observations of the interaction between *S. pyogenes* and our pharyngeal cell monolayers revealed a non-homogeneous distribution of the bacterium following co-culture with Detroit-562. When monolayers with adherent bacteria were examined under the microscope, it appeared that not all Detroit 562 cells were alike in their ability to allow streptococcal adherence. While some cells had many bacteria adhering to them, no bacteria were associated with other epithelial cells in the same area (Figure 5.1). Viewed under lower magnification (wider view), it becomes apparent that the bacteria consistently attach as clumps occupying patches along the monolayer (Figure 5.1). Sonication did not appear to affect this tendency towards irregular distribution (unpublished observation). UT-SCC-60A, UT-SCC-60B, and HPTE cell monolayers infected with *S. pyogenes* demonstrated a less pronounced heterogeneity between bound and unbound epithelia as compared to Detroit-562 cells (not show). In summary, there was some degree of aggregation exhibited by GrAS during association with the surface of all epithelial monolayers examined. Notably, our observation on cell surface streptococcal aggregation is consistent with previously reported accounts of this phenomenon by other investigators co-culturing streptococci with Detroit 562 cells. (Bartelt 1978, Manetti 2007). The implications from the numerous speculative mechanisms proposed by different groups will be discussed later in this section.

Figure 5.1. Distribution of *S. pyogenes* along epithelial monolayer

S. pyogenes strain SF370SM^{R} was transformed with pCM18 (see Methods) to constitutively express GFP (*green*). SF370-pCM18 in serum-free DMEM (~5 x 10^{7} cfu / ml) was co-cultured with Detroit 562 (*A-C*) and UT-SCC-60B (*D*) epithelial cell monolayers on glass coverslips for 30 minutes at 37ºC, supplemented with 5% CO_2. Associated bacteria were removed by vigorous washing with PBS and monolayers were briefly fixed with 4% paraformaldehyde. Fluorescence micrographs of representative monolayers are presented, visualized with phase contrast and / or FITC filter (480nm).

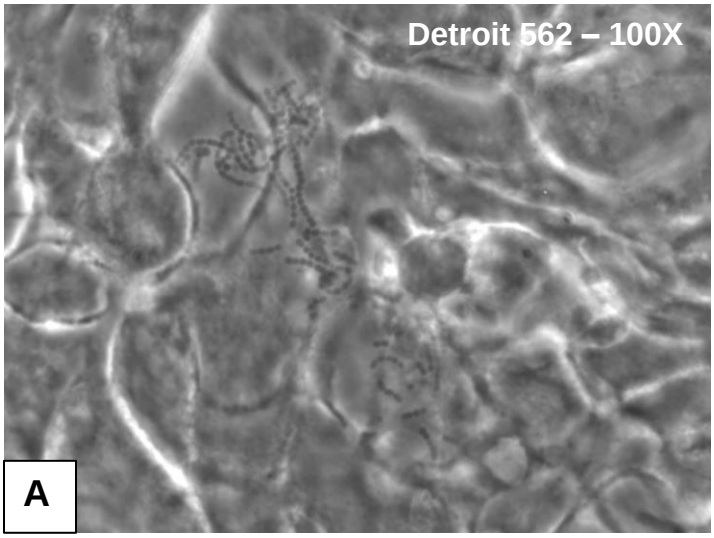
Detroit 562 – 100X
A

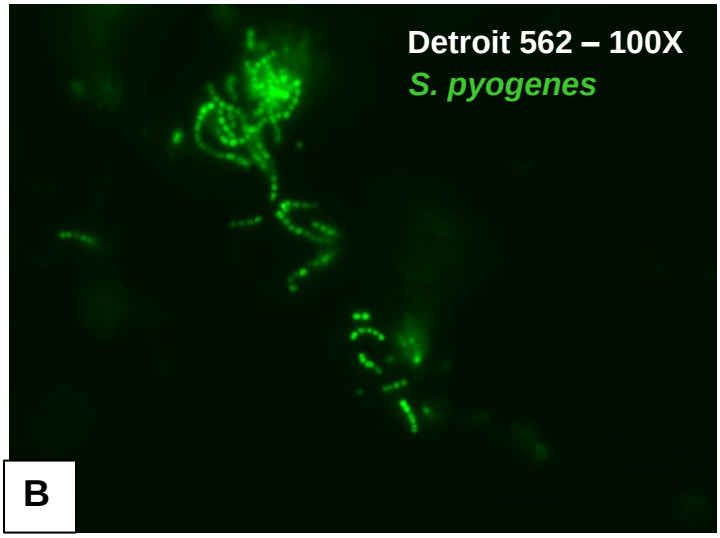
Detroit 562 – 100X
S. pyogenes
B

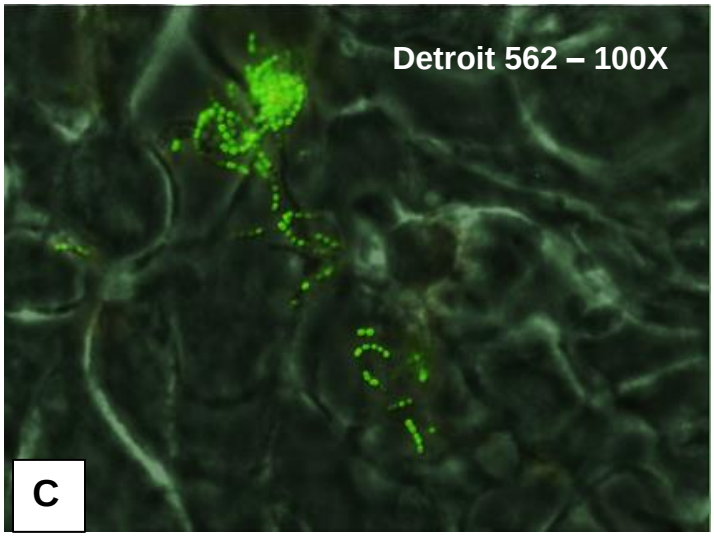
Detroit 562 – 100X
C

5.2.2 Persistent adherent GrAS exhibit biofilm-like growth possibly refractory to treatement with antibiotics

Mannetti and colleagues recently described a link between the streptococcal aggregation phenotype, GrAS pili and biofilm formation on Detroit 562 nasopharyngeal cells. Employing a similar experimental set up, their team showed *S. pyogenes* strain SF370 adhered to Detroit 562 monolayers following15 minutes of being co-cultured and formed extensive clumps of cells typical of biofilm microcolonies by 2hrs. The clumped microcolonies extended into 3D space, a characteristic arguably pathognomonic of biofilms, as was confirmed by three-dimensional immunofluorescence imaging. It is well established that biofilm formation, via matrixes of secreted proteins, polysaccharides, and nucleic acids, offer a means of protection for member bacteria against host antimicrobial peptides and antibiotic therapies. Recently, Ogawa et al showed a hyper-biofilm forming M type 1 GrAS strain produced fully matured biofilms, where penicillin, erythromycin, and clindamycin, either individually or in combination, could not inhibit growth / viability even when the concentration of each antibiotic was greater than the 10-fold minimum inhibitory concentration (MIC) for planktonic bacteria (Ogawa2011).

Consistent with these finding, we have verified that a subpopulation of adherent SF370 remain visible microscopically on the surface of Detroit 562 cells following 1h of antibiotic treatment with Penicillin and Gentamycin, as indicated by the

standard invasion assay (Figure 5.2A,B). Given this observation, we first sought to determine the effectiveness of using the amidase lytic enzyme, PlyC (Fischetti, 1971, Nelson 2001) at a modest concentration of 0.05U per well, to more effectively eliminate persistent adherent bacteria. Our study consistently demonstrated a marked decrease in visibly attached bacteria following PlyC treatement, although monolayer surface sterilization was infrequently achieved. We decided against increasing the concentration of PlyC or the increasing the length of incubations since Nelson *et a*l have recently shown that PlyC may become internalized by epithelial cells when applied at high concentrations (Nelson DC, *unpublished*). Incubating the monolayers with antibiotics for 1h followed by PlyC treatment proved to consistently sterilize the monolayer surface as was confirmed microscopically (Figure 5.2), which suggests a synergistic effect between the two therapies on our *in vitro* assay.

Significantly, the viability of the persisting adherent streptococci was never confirmed. Invasion viability and invaded-streptococci re-emergence experiments rely on accurate removal of extracellular bacteria. We performed experiments where aliquots of antibiotics from infected-wells during invasion assays were plated on blood agar plates. Our results from these tests were usually negative but they notably do not account for adherent bacteria that are alive but dormant within a biofilm.

Figure 5.2. Efficacy of using amidase lysin, PlyC, on persisting adherent *S. pyogenes* versus antibiotics alone during *in vitro* assay

SF370-pCM18 (*green*) in serum-free DMEM (~5 x 10^7 cfu / ml) was co-cultured with Detroit 562 (ATCC, CCL-138) epithelial cell monolayers on glass coverslips for 120 min at 37ºC, supplemented with 5% CO_2. Associated bacteria were removed by vigorous washing with PBS and subsequently treated with Antibiotics cocktail (Penicillin 100ng / µL+ Gentamicin 100ng / µL) and /or PlyC (0.05U / well) for 60min. Monolayers were washed with PBS and briefly fixed with 4% paraformaldehyde. Fluorescence micrographs of representative monolayers are presented, visualized under phase contrast and / or FITC filter (480nm).

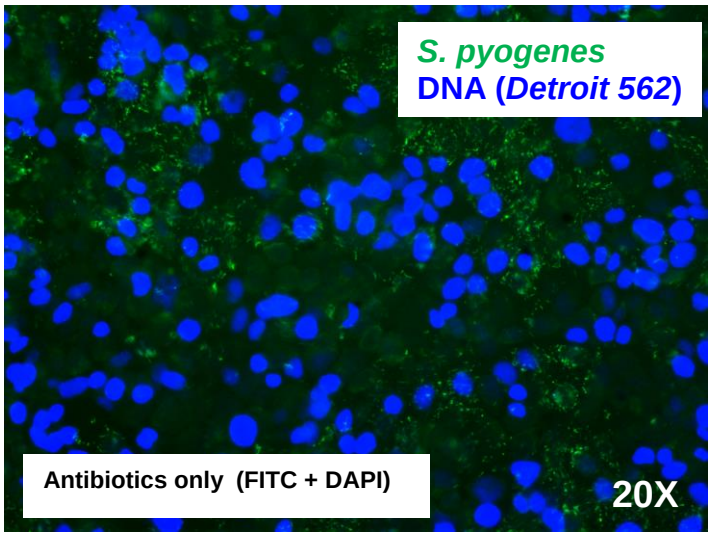
S. pyogenes
DNA (Detroit 562)
Antibiotics only (FITC + DAPI)
20X

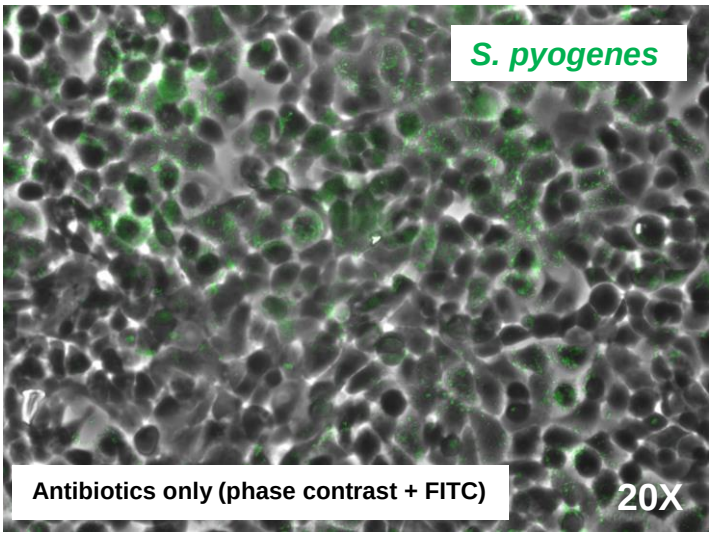
S. pyogenes
Antibiotics only (phase contrast + FITC)
20X

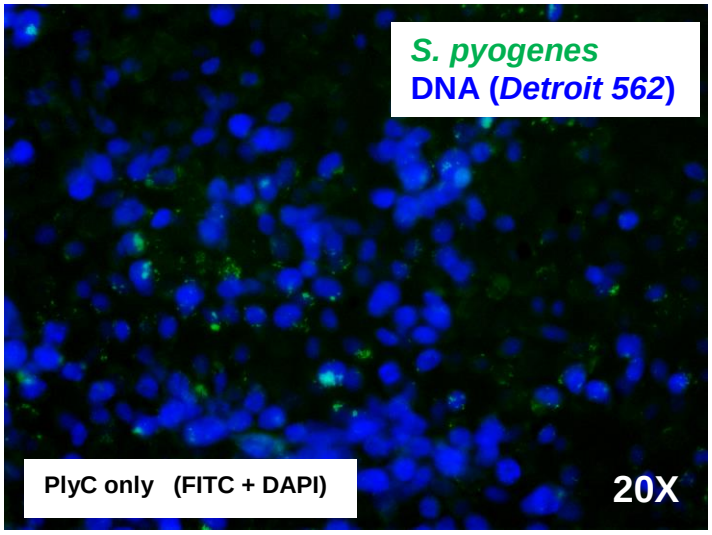
S. pyogenes
DNA (Detroit 562)
PlyC only (FITC + DAPI)
20X

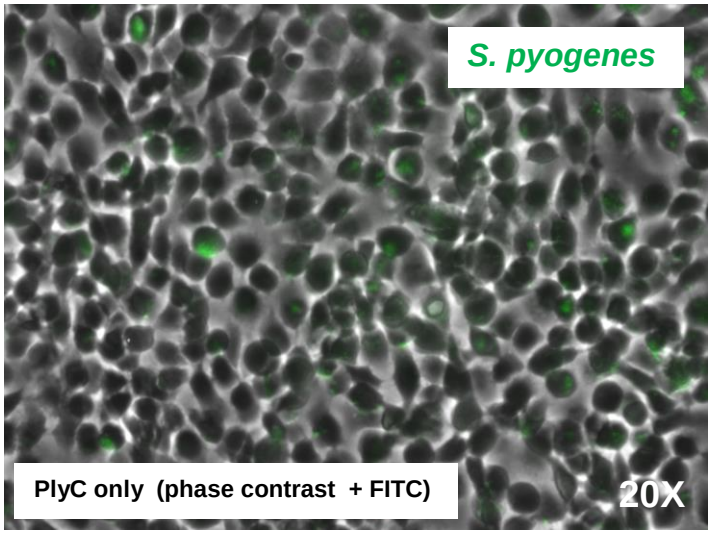
S. pyogenes
PlyC only (phase contrast + FITC)
20X

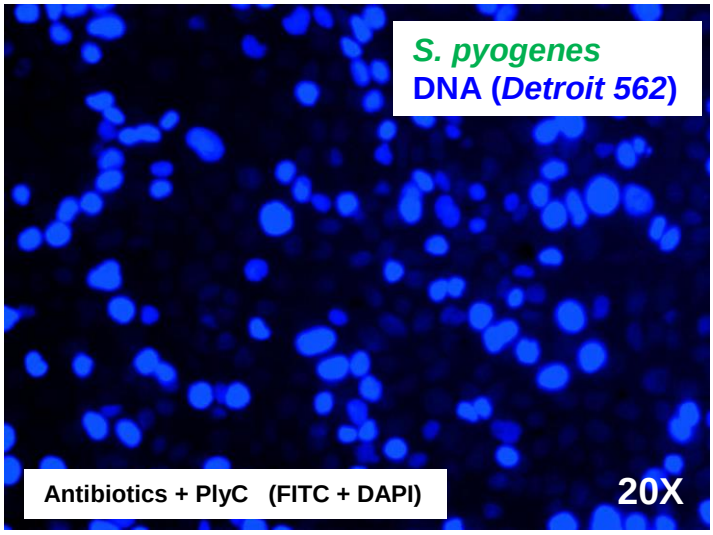
S. pyogenes
DNA (Detroit 562)
Antibiotics + PlyC (FITC + DAPI)
20X

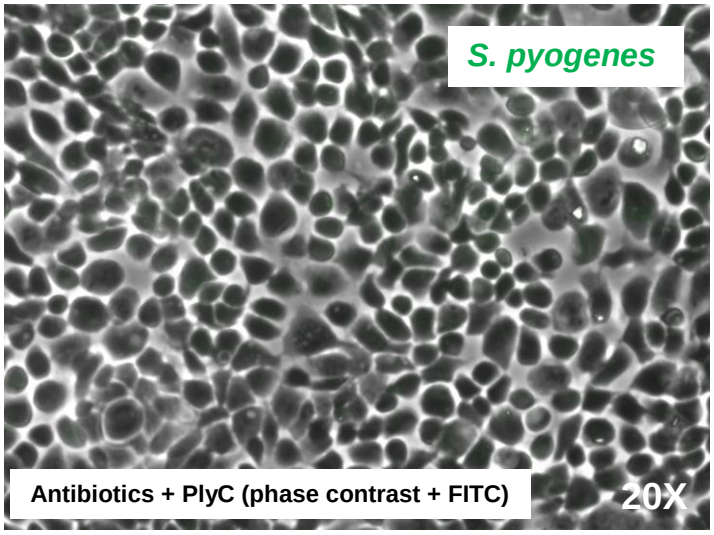
S. pyogenes
Antibiotics + PlyC (phase contrast + FITC)
20X

5.2.3 Streptococcal tonsil-specific phenotype suggests apparent tissue tropism

Clinical observations demonstrate a generally confined presentation during Group A Streptococcal induced pharyngo-tonsillitis, or “Strep Throat”. One of the major symptoms distinguishing this from non-streptococcal infection is a localized inflammation and erythema at the palatine tonsil with or without exudate (Dajani 1995). Extended pharyngeal membrane discoloration involving the soft palate is not seen in GrAS disease, but rather is indicative of other etiologies of pharyngitis such as gonococcus *spp* (Vincent 2004).

Ellen et al established almost 40 years ago tonsil tissue specificity in a virulent strain of streptococci. In their study, tonsil epithelial cells scraped from a healthy male patient, along with a panel of epithelia from other sites, were cultured with GrAS and *Escherichia coli* (Ellen 1974). They demonstrated greater adherence of GrAs to tonsillar cells as compared to the other cell types, a finding incongruent with observed *E. coli* adherence predilections. The disparate locations from which they tested the streptococcal tropism limits the implications of their finding between other neighboring oral mucosa, normally spared during streptococcal disease. While numerous investigators have identified streptococci’s ability to adhere to oral tissues including tongue and buccal surfaces, comparisons between these surfaces have not convincingly demonstrated tropism towards the tonsil in man, either *in vivo* or *in vitro*.

In order to preliminarily explore whether streptococci exhibit higher affinity to palatine tonsil-derived epithelial cells compared with anatomically proximate nasopharyngeal-derived cells, a representative cell lines and a throat-tropic (emm pattern A-C) strain, M type 1 SF370, were chosen for our model system. We conducted a mixed cell infection experiment in which Detroit 562, UT-SCC-60A, UT-SCC-60B, and Human Primary Tonsil Epithelial cells were infected simultaneously in the same well (Amelung 2011).

Consistent with the apparent clinical presentation, our M1 strain exhibited a strong preference for all three palatine tonsil cell lines over the Detroit 562 (nasopharyngeal) cells as assessed by visual comparison of infected cells (Figure5.3. We quantitatively verified this observation by conducting an adherence assay comparing all four (4) cell types using established standard techniques as previously described (Romero 2003, Ryan 2001, Manetti 2007, Ryan 2007). Our assays demonstrated that adherence was greater than 5-times more efficient in tonsil cell lines, consistent with our observations by microscopy (Figure 5.4). This enhanced adherence efficiency was reproducible and calculated to be very significant ($p < 0.001$) demonstrating a clear difference between tonsil versus non-tonsil monolayers when simultaneously infected with the same inoculum. A similar epithelial cell type-specific response was observable when measuring invasion efficiency (Figure 5.5).

Figure 5.3 Visualization of apparent streptococcal tissue-specific tropism toward tonsil epithelial cell types. Cultured epithelial cells were seeded to ~90% confluency*, respectively, on glass coverslips. Coverslips were placed adjacent to one another in the same well of a Falcon® 6-well tissue culture plate and simultaneously inoculated with M type 1 *S. pyogenes* (~5 x 10^7). (*A*) Diagram of experimental set up for a single well containing coverslips with the four epithelial cell types. Fluorescence micrographs of infected (*B*) Detroit 562, (*C*) UT-SCC-60A, (*D*) UT-SCC-60B, and (*E*) Human Primary Tonsil Epithelial [HPTE] cells are presented. GrAS was labeled with PlyCB conjugated with Alexa 554 (red). Epithelial nuclei were stained with DAPI (blue). All images captured at 20X magnification.

**Note: Size and morphology differences between epithelial cell types influence cell density of confluent monolayers. At 95% confluence: Detroit 562 = 1.2 x 10^6, UT-SCC-60A = 5.0 x 10^5, UT-SCC-60B = 1.3 x 10^6, and HPTE = 4.5 x 10^5 (see Section §4.0 for additional description)*

S. pyogenes
(5 x 10^7 cfu / mL)
in DMEM

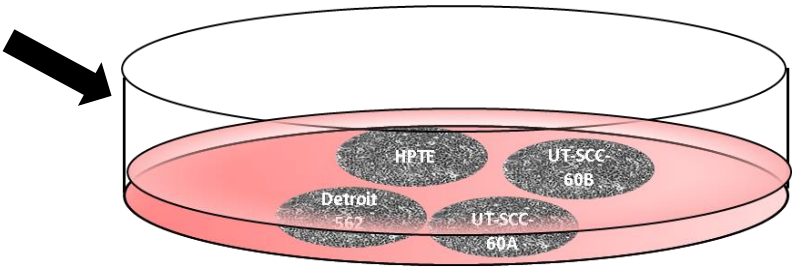

A

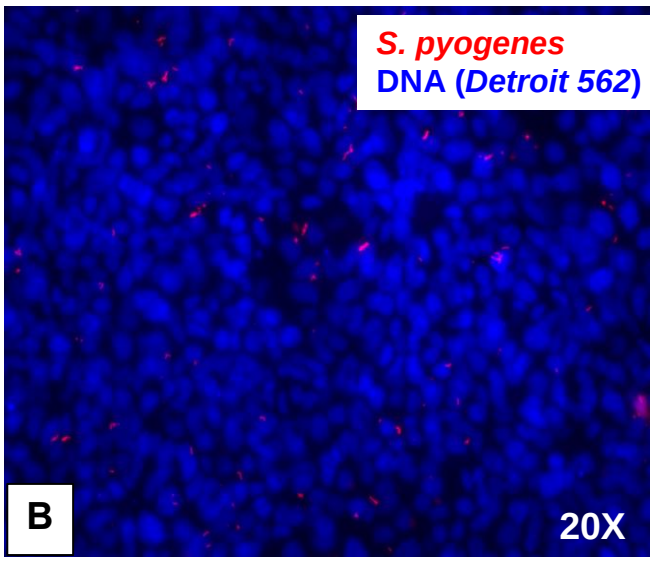

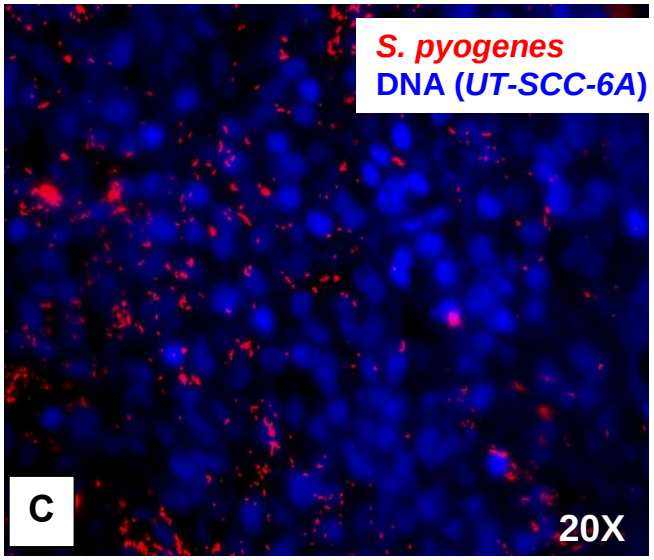

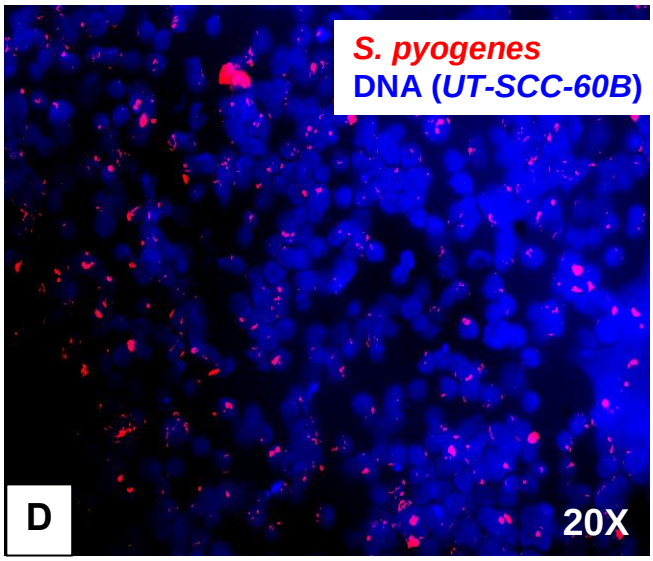

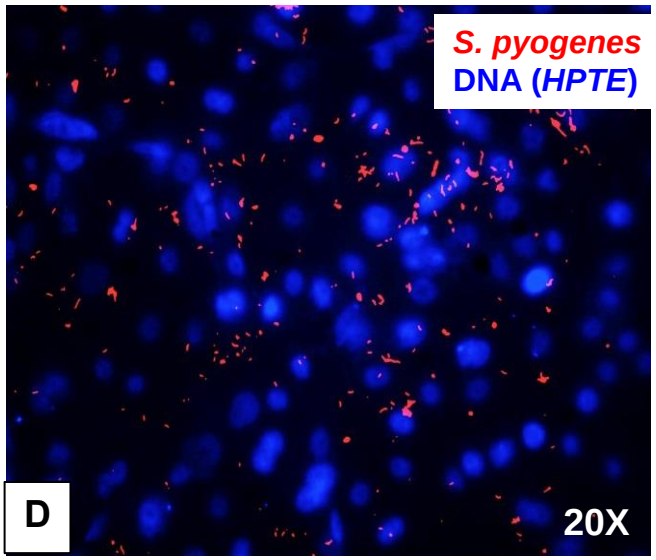

Figure 5.4 M type 1 streptococci exhibit greater adherence efficiency towards tonsil-derived epithelium.

S. pyogenes strain SF370SM^{R} was co-cultured with nasopharyngeal-derived (Detroit 562- grey bar) and tonsil-derived (UT-SCC-60A, and HPTE – black bars) epithelial monolayers, respectively at multiplicity of infection (MOI) ~100:1. Associated bacteria were removed with PBS and cfu's were counted on blood agar as described in the methods. Results are the mean ± standard deviation of at least three independent experiments performed on separate days in triplicate. Statistical significance (reported as *p* value) was determined by Student's t-test.

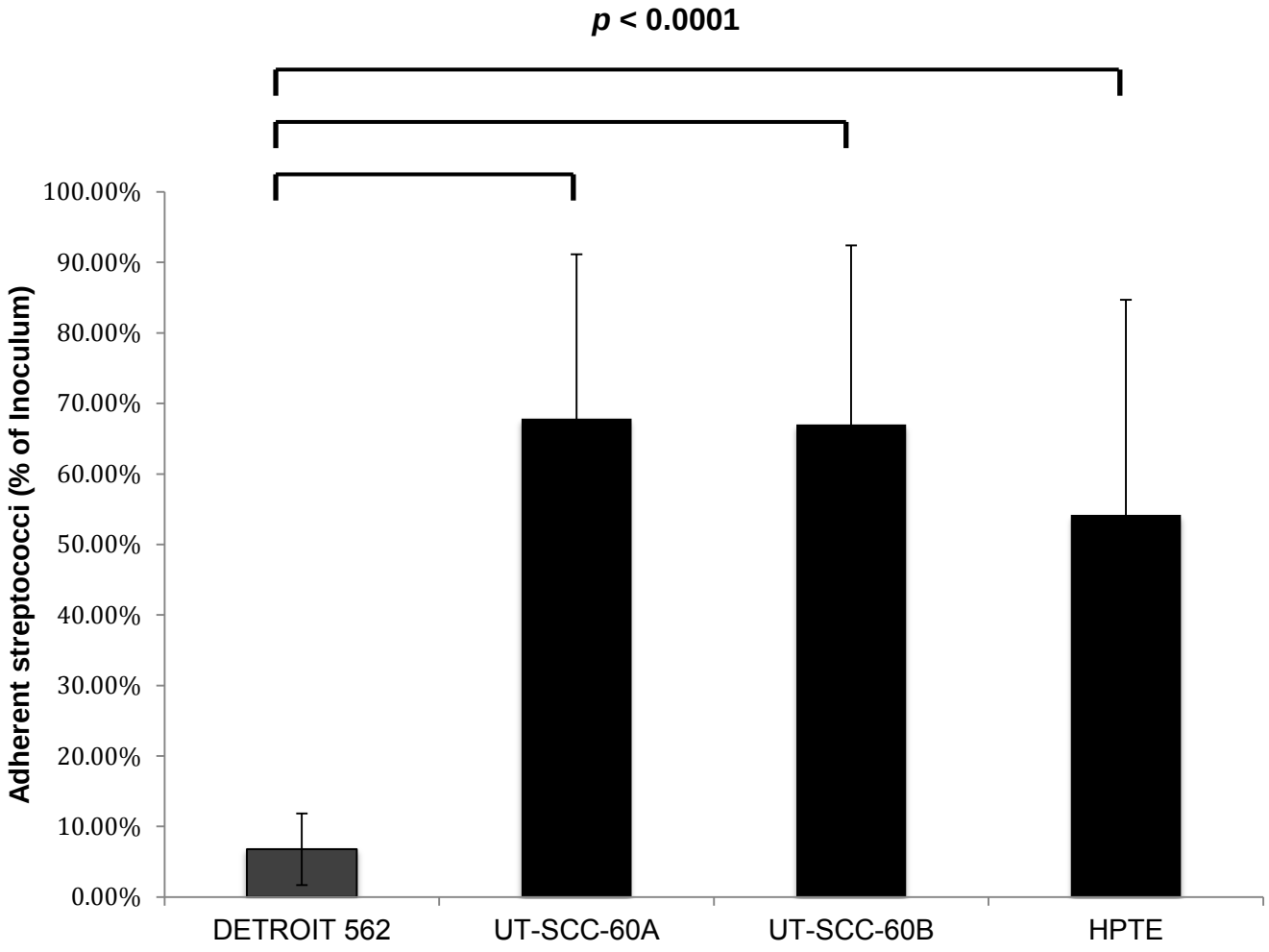
p < 0.0001
Adherent streptococci (% of Inoculum)
100.00%
90.00%
80.00%
70.00%
60.00%
50.00%
40.00%
30.00%
20.00%
10.00%
0.00%
DETROIT 562
UT-SCC-60A
UT-SCC-60B
HPTE

Figure 5.5. M type 1 streptococci are internalized more efficiently by tonsil-derived epithelium

S. pyogenes strain SF370SM^{R} was co-cultured with nasopharyngeal-derived (Detroit 562- grey bar) and tonsil-derived (UT-SCC-60A, and HPTE – black bars) epithelial monolayers, respectively at multiplicity of infection (MOI) ~100:1. Adherent bacteria were killed with antibiotics and treatment with amidase lysin, PlyC, as described in the methods. Results are the mean ± standard deviation of two to four independent experiments performed on separate days in triplicate. Statistical significance (reported as p value) was determined by Student's t-test.

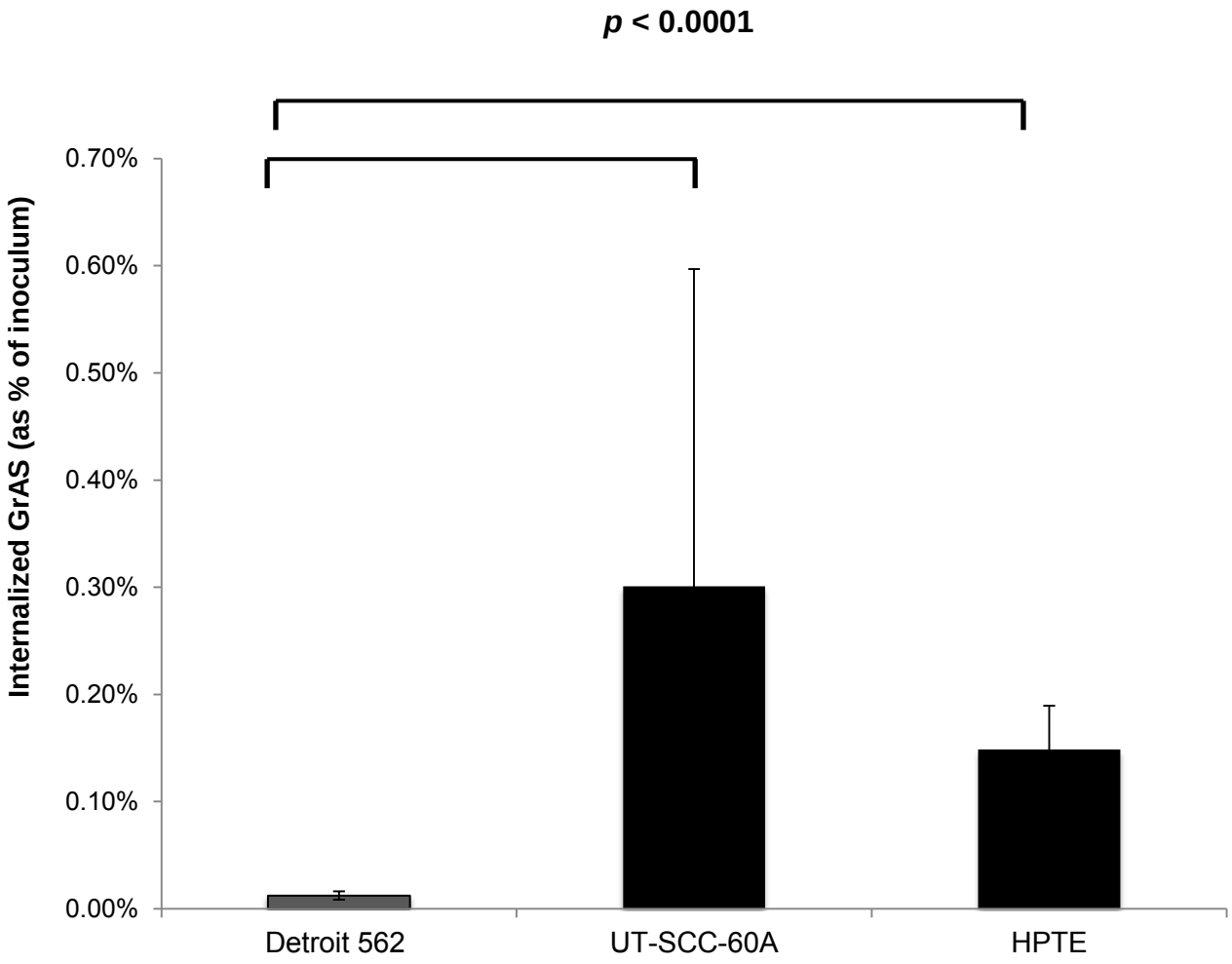
p < 0.0001
Internalized GrAS (as % of inoculum)
0.70%
0.60%
0.50%
0.40%
0.30%
0.20%
0.10%
0.00%
Detroit 562
UT-SCC-60A
HPTE

5.3 Discussion:

In vitro assays were used to investigate a key early event in streptococcal infections, initial adherence to mucosal surfaces of the human oropharynx. This approach may mimic a child inhaling aerosolized droplets of *S. pyogenes* and effectively inoculating their upper airway. Our *in vitro* investigations demonstrate clear differences in adherence phenotypes between streptococcal strain-matched assays and epithelial monolayers derived from two neighboring sites in the human oropharynx. These findings are consistent with the clinical observation that group A streptococcal infection appears to occur preferentially at the palatine tonsil.

Our monolayer model system revealed thought provoking findings that have been previously noted by other researchers, but remain unclear or otherwise poorly explained. Among these observations is the non-homogeneous distribution of GrAS, especially across our Detroit 562 monolayer. Bartelt *et al* were the first to document the heterogeneity of streptococcal distribution on a Detroit 562 monolayer nearly 30 yrs ago. Furthermore, they also reported that the percentage of the bacterial inoculum followed an inverse relationship with concentration as adherence percentage decreased as more bacteria was applied. In cell cultures “saturated” with GrAS, they observed using microscopy that only about 50% of the Detroit epithelial cells contained adherent streptococci.

In our current study, we used a multiplicity of infection of ~100:1 as an inoculumdose that has been published in numerous streptococcal adherence assays with Detroit 562 cells (Pancholi, 2003, Edwards 2008) as we sought to identify streptococcal binding preferences between these and tonsil derived cell types. We also regularly performed repeat experiments at 10 times our reported MOI (1000:1) and also noted a decrease in the percentage of inoculum that adhered (unpublished observations). Interestingly, we see an apparent maximum to the number of absolute number of bacteria that can bind a monolayer. Based on hemocytometer counts of confluent monolayers and CFU calculations on blood agar, we found a maximum streptococcal saturation that was cell type-specific, ranging from 100:1 CFU (per Detroit 562 cell) to >350:1 CFU (per UT-SCC-60B cell). Numbers no longer increased in our assays repeated in duplicate on consecutive independent days at MOI's 1000 - 3000:1 (data not shown). Higher MOI's were not attempted based on visual inspection of compromised monolayer integrity.

The heterogeneous distribution observed in our study as well as by others may be indicative of the well-established phenomena of oral streptococcal aggregation. Numerous investigators have purported that GrAS bind human salivary components, which in turns induces bacterial aggregation (Edwards 2008, Courtney 1991). While some of the described binding ligands responsible for this process are unique to saliva (ie. gp340), other components such as albumin and fibronectin can be readily found in standard growth media and along

the surface of our epithelial cells. These components are known to provide a “bridge” that facilitates enhanced epithelial adherence by the bacterium. Though unlikely, it is possible that serum or epithelial surface matrix components not evenly removed during washing steps might account for areas of localized aggregation. Since this is a recurring observation seen specifically during Detroit 562 cell adherence assays, however, we reject the plausibility that this is the case.

Another more intriguing explanation might be that there is heterogeneity within the epithelial cell cultures. It may be that "receptor sites" on the epithelial cells are present only during certain stages of the cell division cycle or that the epithelial cells consist of subpopulations that differ in their ability to allow streptococcal adherence. Since our in vitro assay uses epithelial monolayers at nearly complete confluence (~90-95%), we make an assumption that the respective cell types being compared (nasopharyngeal versus tonsil-derived), are at similar stages of senescence with minimal proliferate subpopulations. This may indeed be a more likely difference between Detroit 562 cells and other types if their surface topography is exceptionally more affected by cell cycle stage. Further analysis of the Detroit 562 cell surface *in vitro* is needed to continuously revisit the implications for how this reflects the *in vivo* pharyngeal surface whether this serves as a reliable model *in vitro* for streptococcal pharyngotonsillitis.

In summary, using epithelia from an anatomically relevant, clinically – derived source, the palatine tonsil, has allowed us to reproduce an appreciable “tropism” *in vitro*. These observations, however, have many caveats that require further investigation regarding the precarious difference in distribution patterns across these anatomically related cell types, possibly alluding to tissue-specific differences. The novel tonsil tumor lines UT-SCC-60A and UT-SCC-60B may provide a powerful tool as a reliable system to investigate mechanisms for these phenotypes and establish a basis for eventual confirmation by primary cells and *in vivo* screens.

§6.0 STREPTOCOCCAL TRANSCRIPTIONAL CHANGES UPON ASSOCIATION WITH EPITHELIAL CELLS FROM HUMAN NASOPHARYNX VERSUS PALATINE TONSIL

6.1 Introduction:

The arsenal of extracellular proteins and secreted virulence factors wielded by Group A Streptococci GrAS have been extensively studied for the past 70 years, which is a testament to the impact this bacterium has had on human disease. While the extracellular presentation of these proteins is well studied, their regulation and connectedness with other bacterial responses has only recently become better understood. Advances in genome wide analysis over the last 15-20 years has ushered in an enhanced appreciation of GrAS virulence by studying the underlying molecular causes of disease pathogenesis. Since the first complete sequence of the *Streptococcus pyogenes* genome was reported in 2001 by Ferretti *et al*, numerous laboratories have developed *in vitro* systems using microarrays to capture snapshots of transcriptome –level shifts within the pathogen in response to specific environmental stresses and conditions (Ferretti 2000, Shelburne, Sumby 2005) Sitkiewicz & Musser 2006). Studies have also been performed *in vivo* using sample isolates from infected primates (Virtaneva 2005, Shea 2010) and humans (Livezey 2011). These studies have offered new insights while bringing forth new questions. Previously described virulence factors have been elaborated in a more genome-wide context while no fewer than 13 new proteins involved in pathogenesis were found within the first ten years of the advent of genome wide microarray (Musser 2009). Insight provided

from studies using these molecular tools has already aided the design of potential therapeutic and vaccine approaches to combatting streptococcal disease (Ferretti 2001).

There are now 14 completed GrAS genome sequences (Table 6.1). Each genome is approximately 1.9 Mb in size, with approximately 10% of the overall gene content encoded on variably present exogenous genetic elements such as prophages and integrated conjugative elements (ICE). It has been shown that even among GrAS of the same M type, there is considerable variation in prophage content and overall prophage-associated virulence factor profile (Musser 2009). While phage represent only a minor fraction of the total GrAS genome, they may account for up to 74% of the variation between strains (Banks, Beres 2002).

Towards the effort of exploiting this new sequenced information and molecular tools, our lab has recently developed novel oligonucleotide microarrays, which represent every identified unique open reading frame from published group A streptococcal serotypes. Moreover we have designed a suite of statistical algorithms to extract biologically meaningful data generated from microarray experiments that explore various streptococcal-host interactions. Uniquely, this novel software suite provides analysis that incorporates the physical position of genes on the bacterial chromosome to identify groupings of potentially related genes and speculative operons. This powerful tool named GenomeCrawler (www.rockefeller.edu/vaf/streparray.php) has been applied to investigate

transcriptional changes in streptococci during various environmental conditions and stages of infection (Ryan 2007, Aziz 2010, Juncosa 2012).

Table6.1. Sequenced *S. pyogenes* genomes

***S. pyogenes* strain**	**M-type**	**Genome Size (bp)**	**CDS Count**	**% of CDS with no assigned funtion**	**No. of prophages**	**Reference**
SF370	1	1,852,441	1,697	37.1	4	Ferretti, et al. 2001
MGAS5005	1	1,838,554	1,865	16.6	3	Sumby, et al. 2005
MGAS10270	2	1,928,252	1,987	17.2	5	Beres, et al. 2006
MGAS315	3	1,900,521	1,865	35.5	6	Beres, et al. 2002
SSI-1	3	1,894,275	1,861	37.17	6	Nakagawa, et al. 2003
MGAS10750	4	1,937,111	1,979	17.2	4	Beres, et al. 2006
Manfredo	5	1,841,271	1,803	28.4	5	Holden, et al. 2007
MGAS10394	6	1,899,877	1,886	22.7	8	Banks, et al. 2004
MGAS2096	12	1,860,355	1,898	17.3	2	Beres, et al. 2006
MGAS9429	12	1,836,467	1,878	16.7	3	Beres, et al. 2006
MGAS8232	18	1,895,017	1,845	38.6	5	Smoot, et al. 2002
MGAS6180	28	1,897,573	1,894	18	4	Green, et al. 2005
NZ131	49	1,815,724	1,699	25.7	3	Mcshan, et al. 2008
Alab49	53	1,827,308	1,773		4	Bessen, et al. 2011

The pathogen adapts transcriptionally to the host environment

While much of the earlier work on pathogen response to the host were focused on changes in pH, temperature, carbohydrate sources, and superoxide availability, our laboratory recently reported that streptococci actively responded to a host cell small molecule, named SPIF, leading to phage induction and phage encoded virulence expression (Broudy 2001, Broudy 2002). In order to cause infection, the bacteria must first enter the oral cavity, generally via a low-glucose

saliva aerosol, or by hand contact with nasal discharge from an infected individual. This early inoculum then mixes with the oral milieu of the new host eliciting adaptive transcriptional modifications appropriate to their new environment.

An attempt to contextualize streptococcal adaptation to its host with respect to its global effect transcriptionally has been recently undertaken by numerous groups. Our lab has investigated the adaptive dynamics of the initial infection sequence in an *in vitro* epithelial model measuring streptococcal transcriptome shifts during co-culture with epithelial cell-free conditioned media (prepared from Detroit 562 cells). In comparison to bacteria cultured in freshly MEM as a control, GrAS elaborated a global transcriptional response where over 430 individual genes were differentially expressed. Similarly, after transient contact or “association” with pharyngeal monolayers + conditioned media, streptococci differentially expressed over 490 genes in comparison again to bacteria only cultured in fresh MEM. Significantly, there was found to be a great deal of overlap in the genes affected (337 genes) by the two experimental conditions (Juncosa 2012). The bacterial transcriptome was sampled at various times post-exposure to host cells, which revealed that streptococcal gene expression is dramatically remodeled following initial exposure to the host environment but generally maintains its directional change (up- or downregulated) through loose association with the host cell surface (Juncosa 2012).

Following the continuum of stages that lead to infection and disease, our lab identified 79 genes differentially expressed by *S. pyogenes* upon adherence with Detroit 562 monolayers in comparison to those bacteria only loosely associated with this epithelium (Ryan 2007). The relatively few genes that were differentially expressed in Ryan's analysis points to a noteworthy distinction between this and Juncosa *et al*'s experimental design. The bacterial group being compared for relative "differences" in expression (adherent versus associated bacteria) has presumably undergone the same large-scale transcriptome shifts upon initial adaption to the host-modified environment. Differences in expression for streptococci that have tightly bound to host cells (versus those only loosely associated) may represent additional fine-tuning of the transcriptional program necessary to initiate and maintain close contact with target epithelial cells (Ryan 2007, Juncosa 2012). These sets of experiments represent the first reported account of transcriptional changes following *S. pyogenes* adaptive responses from initial infection to adherence on the pharyngeal epithelial cell surface.

While we have shown that a single streptococcal strain may alter its adaptation and colonization mechanisms based on host environment and stage of infection, it has yet to be demonstrated whether this pathogen elicits a unique and transcriptionally discernable response to different mucosal epithelial cells types associated with the human pharynx following mere transient contact as might naturally occur *in vivo* during infection. Due to anatomical proximity, comparing the bacteria's response to the related epithelia of the nasopharynx and palatine

tonsil may offer a unique appreciation for the extent to which a “throat selective” GrAS M type strain might distinguish between two host cells within their only natural reservoir. Developing an *in vivo* system would likely prove irreconcilably challenging to sufficiently control for the expected dispersal of the inoculum throughout the pharyngeal mucosa by the action of host mucocilliary secretions. Furthermore, bacterial sampling post-inoculation would be limited to only adherent bacteria, which misses the important transcriptional status following introduction to the oropharynx likely important for determining tropism. As reported earlier, we have observed significant phenotypic differences in adhesion and invasion of host cells by streptococci following co-culture with tonsil-derived epithelial cells versus nasopharyngeal cells. Informed by these observations, we hypothesize that there are dynamic transcriptional shifts elaborated by the bacteria during co-culture, which may differ significantly between the respective epithelial cell types.

In the following chapter, we describe our study capturing the relative changes in *S. pyogenes* transcriptional responses to co-culture with a newly described human palatine tonsil tumor cell line, UT-SCC-60B, as compared to the Detroit 562 nasopharyngeal epithelial cell line. Using a custom microarray platform and novel clustering algorithms, our results revealed the upregulated operons that we then test to further confirm our novel cell line’s ability to model a previously described response to human primary tonsil epithelial cells

§6.2 Results

§6.2.1 Differential expression of individual genes during association with human tonsil epithelial cell monolayers

Streptococcus pyogenes M type 1 strain SF370 was co-cultured *in vitro* with epithelial tumor lines derived from two anatomically proximate locations often regarded indistinguishably as parts of the human "throat": the nasopharynx (Detroit 562) and palatine tonsil (UT-SCC-60B), respectively. We employed an established association assay (Ryan 2007) (Juncosa 2012), as previously described. Associated bacteria were recovered and RNA was immediately extracted for analysis of transcript expression, capturing a snapshot of the streptococcal transcriptional profiles following 2.5h co-culture with their respective monolayers. We performed 8 independent experimental replicates on separate days to incorporate biological variation into our experimental design.

Our control for this experiment was the cDNA isolated from bacteria co-cultured with Detroit 562 cells. Accordingly, our "standard" color configuration incorporated Cy3 (green) to control Detroit 562 cDNA, while Cy5 (red) was incorporated into UT-SCC-60B cDNA. Dye swap experiments were included to account for technical variability in dye incorporation. (Appendix 6.1)

Using robust summary statistics and permutation algorithms, our analysis of the replicate arrays identified 78 individual genes (4.4% of the total SF370 genome) differentially expressed when streptococci are exposed to palatine tonsil epithelial cells as compared to Detroit 562 cells. Only genes expressing $\log_2$-fold changes with *p*-values <0.05, as determined by the Westfall-Young step down permutation algorithm, were considered significant and included in Tables 6.1 and 6.2. To further understand the relative transcriptional shifts taking place in the bacteria co-cultured with palatine tonsil epithelia, we classified these differentially expressed genes according to the COGs (Clusters of Orthologous Groups of proteins) database. This classification system predicts function based upon phylogenetic relationships and assigns genes to the broad categories of basic cellular processes (Tatusov 2000). While nearly 40% of our gene list belonged to uncharacterized phage or had otherwise unknown / predicted functions, the remaining COGs list includes a range of functions from regulation of virulence, to lipid transport and metabolism, to control of the cell cycle. We found that the majority of the significantly affected genes in our study were up regulated (58%, 45/78) as compared to control (Tables 6.2 and 6.3). Interestingly, while most COGs contained genes that were either up- or down-regulated, fourCOGs included genes that were only up-regulatedted: (1) lipid transport and metabolism; (2) post translational modifications, protein turnover, and chaperones; (3) cell well / membrane / envelope biogenesis; and (4) nucleotide transport and metabolism. We note thatof the down-regulated genes across all COGs, approximately 64% were of unknown function and/ or were

phage-associated, leaving the consequence of these shifts in expression difficult to speculate until more information is collected on the putative roles of these genes.

Phage-associated genes

33 of the genes significantly down-regulated during co-culture with the tonsil-derived line, 12 (36%) were phage-related. In fact, we found that all of the phage genes which underwent significant fold changes were downregulated. Although SF370 contains one inducible (Φ370.1) and three defective (Φ370.2, Φ370.3 and Φ370.4) integrated prophages, we noted the differential expression of genes from both inducible and non-inducible phage and the prophage integrated conjugative elements (ICE)-like region of difference, designated Φ370.RD1, which putatively encodes a streptin lantibiotic product (Musser 2007).
Among the known phage genes that were differentially expressed, 6 (50%) encoded structural proteins necessary for bacteriophage assembly. Of note, the head morphogenesis gene (Spy0681) for inducible SF370 prophage, Φ370.1 was down-regulated, and both the head morphogenesis (Spy1464) and tail fiber (Spy1441) genes for a non-inducible prophage, Φ370.3, were downregulated.

Virulence-associated genes

We did identify four differentially expressed genes that are known to be associated with streptococcal virulence: *SagA* (Spy0738), *vrf* (Spy0887), pilus minor subunit (*spy0130*,) and *amrA* (Spy0797). Three of these virulence genes

were observed to be upregulated while the Streptolysin S associated gene A, *SagA*, was down-regulated. Interestingly, the largest log_2-fold change observed in our analysis in either the positive or negative directions occurred by virulence genes. *SagA* experienced the most highly negative Log_2-fold change of -2.20 while the average fold decrease among downregulated genes was only about -1.13 Log_2-fold change. Pilus minor subunit *spy0130* (also regarded as ancillary protein 2), however, had an increased relative expression by Log_2-fold of 3.2 while the average increase in up regulated genes was 1.46. In addition, the most significant (lowest *p*-value) of all differentially expressed genes meeting our algorithm's criteria was also *Spy0130*. The remaining upregulated virulence genes will be discussed following our further analysis of this data with the additional context of neighbor gene clustering and its implications.

Based on the known relationship between subgroups of genes being differentially expressed, preliminary speculation can be made regarding the bacteria's adaptive differences between co-culture in UT-SCC-60B versus Detroit 562 cells. For example, there may be differences in metabolism, indicated by the increase in gene expression for lipid transport and metabolism mechanisms, concomitant with the down regulation of two carbohydrate metabolism genes. Alternatively, it is possible that the bacteria are dividing more in the presence of the tonsil-derived monolayer as indicated by the increased expression of cell wall biogenesis and post-translational modification genes, both of which would require lipid metabolism and transport.

As this information is only a snapshot of the bacteria's transcriptional state a single moment in time, greater context regarding the prior transcriptional status would provide a more comprehensive picture of individual genes. Additional context however may be achievable by incorporating information based on the expected contribution additional related genes and pathways may play not represented under our initial analysis

Table 6.2. Differential expression of genes following SF370 co-culture with human tonsil epithelium versus control

Streptococcal genes exhibiting significant changes in expression during association with palatine tonsil-derived cells compared with bacteria associated with Detroit 562 (nasopharyngeal) cells. Genes are organized by Clusters of Orthologous Groups of proteins (COG) classification* as described in the annotated *S. pyogenes* SF370 genome.

*Note – "Virulence" designation assigned to known transcriptional regulators of virulence and any gene encoding established virulent factors / products

COG Classification	Total	Up-regulated genes	Down-regulated genes
Function Unknown	17	8	9
Phage	12	0	12
Translation, ribosomal structure and biogenesis	9	7	2
Lipid transport and metabolism	7	7	0
Post-translational modification, protein turnover, chaperones	6	6	0
Nucleotide transport and metabolism	4	4	0
Virulence*	4	3	1
Carbohydrate transport and metabolism	3	1	2
Inorganic ion transport and metabolism	3	2	1
cell wall / membrane / envelope biogenesis	3	3	0
Amino acid transport and metabolism	2	1	1
Replication, recombination, and repair	2	0	2
Cell cycle control, cell division	2	1	1
Energy production and conversion	1	0	1
General function prediction only	1	1	0
Total	**78**	**45**	**33**

Table 6.3 Streptococcal genes exhibiting significant changes during association with UT-SCC-60B monolayers compared to association with Detroit 562.

[a]Genes rank is ordered by highest significance (lowest *p*-value calculated using Westfall-Young permutations).

[b]Locus tag, COG designation, and gene function / product designations from the annotated SF370 genome. Phage-associated genes have been highlighted in purple.

Rank[a]	Locus Tag[b]	Gene Name[b]	COG Designation[b]	Known or proposed function / product	*p*-Value (Westfall-Young)	Log_2-Fold Change	
1	M1_Spy_0130		virulence	Minor Pilin subunit; Links pilus to cell wall (AP2)	0.00E+00	3.62	↑
5	M1_Spy_0887	*vfr*	virulence	Stand-alone regulator. Repression of speB via RopB	0.00E+00	1.49	↑
34	M1_Spy_0797	*amrA*	virulence	Stand-alone regulator. Activation of Mga regulon	5.20E-03	1.05	↑
66	M1_Spy_0738	*sagA*	virulence	(sagA) streptolysin S associated protein	3.06E-02	**-2.20**	↓
8	M1_Spy_0047	*rpsJ*	Translation, ribosomal structure and biogenesis	30 S ribosomal protein S10	2.00E-04	2.62	↑
31	M1_Spy_0461	*rplA*	Translation, ribosomal structure and biogenesis	50S ribosomal protein L1	3.40E-03	1.90	↑
43	M1_Spy_0886	*engB*	Translation, ribosomal structure and biogenesis	ribosome biogenesis GTP-binding protein YsxC	1.07E-02	1.05	↑
49	M1_Spy_1770	*gatB*	Translation, ribosomal structure and biogenesis	aspartyl/glutamyl-tRNA amidotransferase subunit B	1.63E-02	1.31	↑
55	M1_Spy_1888	*rpmB*	Translation, ribosomal structure and biogenesis	50S ribosomal protein L28	2.02E-02	1.54	↑
74	M1_Spy_0913	*rpsA*	Translation, ribosomal structure and biogenesis	30S ribosomal protein S1	3.87E-02	1.24	↑
26	M1_Spy_0504	*smpB*	Translation, ribosomal structure and biogenesis	tmRNA-binding protein	1.90E-03	**-0.88**	↓
64	M1_Spy_1161	*rgbA*	Translation, ribosomal structure and biogenesis	ribosomal biogenesis GTPase	2.82E-02	**-1.01**	↓
65	M1_Spy_0849	*trmD*	Translation, ribosomal structure and biogenesis	tRNA (guanine-N(1)-)-methyltransferase	2.95E-02	1.14	↑
33	M1_Spy_1755		Transcription	MarR family [REGULATOR]	4.40E-03	1.25	↑
41	M1_Spy_0503		Transcription	exoribonuclease R	8.50E-03	**-0.81**	↓
27	M1_Spy_1163	*smf*	Replication, recombination, and repair	Smf family DNA processing protein	2.90E-03	**-1.19**	↓
76	M1_Spy_1510	*mutT*	Replication, recombination, and repair	mutator protein / Oxidative damage repair enzymes	4.25E-02	**-1.18**	↓
3	M1_Spy_0288	*csdA*	Post-Translational modifications, protein turnover, chaperones	aminotransferase	0.00E+00	1.37	↑
39	M1_Spy_1173	*gid*	Post-Translational modifications, protein turnover, chaperones	tRNA (uracil-5-)-methyltransferase	8.00E-03	1.05	↑

56	M1_Spy_0885	*clpX*	Post-Translational modifications, protein turnover, chaperones	ATP-dependent protease ATP-binding subunit	2.04E-02	0.90	↑
61	M1_Spy_1374	*nrdH*	Post-Translational modifications, protein turnover, chaperones	glutaredoxin	2.52E-02	1.86	↑
69	M1_Spy_0287	*sufD*	Post-Translational modifications, protein turnover, chaperones	ABC-type transport system involved in Fe-S cluster assembly	3.32E-02	1.01	↑
7	M1_Spy_0850		Post-Translational modification, protein turnover, chaperones	thioredoxin reductase	2.00E-04	1.89	↑
11	M1_Spy_1464		Phage - structural	(Φ370.3) Head morphogenesis	2.00E-04	**-1.34**	↓
14	M1_Spy_1465		Phage - structural	(Φ370.3) putative structural protein	2.00E-04	**-1.35**	↓
38	M1_Spy_0945		Phage - UNKNOWN	(Φ370.2) hypothetical protein	7.20E-03	**-1.05**	↓
50	M1_Spy_1487		Phage - UNKNOWN	(Φ370.3) hypothetical protein	1.65E-02	**-0.92**	↓
67	M1_Spy_1442		Phage - UNKNOWN	(Φ370.3) hypothetical protein	3.09E-02	**-1.05**	↓
71	M1_Spy_1075		Phage - UNKNOWN	(Φ370-RD.1) hypothetical protein	3.50E-02	**-1.11**	↓
18	M1_Spy_1441		Phage - structural	(Φ370.3) Tail fiber gene	5.00E-04	**-1.06**	↓
30	M1_Spy_0681		Phage - structural	(Φ370.1) Head morphogenesis	3.30E-03	**-0.98**	↓
53	M1_Spy_1457		Phage - structural	(Φ370.3) putative structural protein	1.78E-02	**-1.01**	↓
57	M1_Spy_0661		Phage - structural	(Φ370.1) putative structural protein	2.09E-02	**-0.72**	↓
29	M1_Spy_1438		Phage - pathogenesis	(Φ370.3) Muramidase	3.00E-03	**-1.10**	↓
21	M1_Spy_0943		Phage - Lysogeny	(Φ370.2) Lysogeny	6.00E-04	**-1.15**	↓
6	M1_Spy_2206	*guaB*	Nucleotide transport and metabolism	inosine 5\'-monophosphate dehydrogenase	2.00E-04	1.20	↑
9	M1_Spy_1378	*nrdF.2*	Nucleotide transport and metabolism	ribonucleotide-diphosphate reductase subunit beta	2.00E-04	1.65	↑
24	M1_Spy_1375	*nrdE.2*	Nucleotide transport and metabolism	ribonucleotide-diphosphate reductase subunit alpha	1.40E-03	1.40	↑
72	M1_Spy_0894	*deoD2*	Nucleotide transport and metabolism	purine nucleoside phosphorylase	3.69E-02	0.78	↑
13	M1_Spy_1751	*fabK*	Lipid transport and metabolism	trans-2-enoyl-ACP reductase II	2.00E-04	1.66	↑

16	M1_Spy_1749	*fabG*	Lipid transport and metabolism	3-ketoacyl-ACP reductase	4.00E-04	1.45	↑
19	M1_Spy_0880	*mvaS.1*	Lipid transport and metabolism	3-hydroxy-3-methylglutaryl-coenzyme A	5.00E-04	1.23	↑
28	M1_Spy_1747	*accB*	Lipid transport and metabolism	acetyl-CoA carboxylase biotin carboxyl carrier protein subunit	3.00E-03	1.57	↑
44	M1_Spy_0881	*mvaS.2*	Lipid transport and metabolism	3-hydroxy-3-methylglutaryl-CoA synthase	1.11E-02	1.17	↑
48	M1_Spy_1745	*accC*	Lipid transport and metabolism	acetyl-CoA carboxylase biotin	1.56E-02	1.77	↑
60	M1_Spy_1746	*fabZ*	Lipid transport and metabolism	(3R)-hydroxymyristoyl-ACP dehydratase	2.35E-02	1.37	↑
23	M1_Spy_1240	*phoU*	Inorganic ion transport and metabolism	phosphate uptake regulatory protein	1.20E-03	1.09	↑
52	M1_Spy_0319		Inorganic ion transport and metabolism	ABC transporter substrate binding protein	1.74E-02	**-1.57**	↓
75	M1_Spy_1242	*pstB2*	Inorganic ion transport and metabolism	phosphate transporter ATP-binding protein	4.09E-02	1.00	↑
62	M1_Spy_0867		General function prediction only	ABC transporter ATP-binding protein	2.60E-02	0.87	↑
10	M1_Spy_1193		Function unknown	hypothetical protein	2.00E-04	**-1.08**	↓
12	M1_Spy_2153		Function unknown	hypothetical protein	2.00E-04	1.71	↑
15	M1_Spy_1591		Function unknown	hypothetical protein	3.00E-04	**-1.44**	↓
17	M1_Spy_1736		Function unknown	hypothetical protein	5.00E-04	1.64	↑
20	M1_Spy_1460		Function unknown	hypothetical protein	5.00E-04	**-1.64**	↓
32	M1_Spy_1731		Function unknown	hypothetical protein	4.20E-03	**-1.02**	↓
36	M1_Spy_0796		Function unknown	hypothetical protein	6.20E-03	1.34	↑
37	M1_Spy_0439		Function unknown	hypothetical protein	6.70E-03	1.01	↑
40	M1_Spy_1940		Function unknown	hypothetical protein	8.00E-03	2.23	↑
42	M1_Spy_1290		Function unknown	hypothetical protein (signal peptide)	1.01E-02	1.39	↑
46	M1_Spy_1482		Function unknown	hypothetical protein	1.31E-02	**-1.24**	↓
51	M1_Spy_0382		Function unknown	hypothetical protein	1.74E-02	**-0.70**	↓

54	M1_Spy_1263		Function unknown	small membrane integral protein	1.86E-02	**-0.94**	↓
59	M1_Spy_0604		Function unknown	hypothetical protein	2.30E-02	0.67	↑
68	M1_Spy_1945		Function unknown	hypothetical protein	3.14E-02	1.90	↑
70	M1_Spy_1530		Function unknown	hypothetical protein	3.36E-02	**-0.78**	↓
73	M1_Spy_1405		Function unknown	hypothetical protein	3.75E-02	**-1.71**	↓
78	M1_Spy_1192	*citC*	Energy production and conversion	citrate lyase synthetase	4.77E-02	**-0.60**	↓
22	M1_Spy_1897		cell wall / membrane / envelope biogenesis	Small conductance mechanosensitive channel	8.00E-04	1.23	↑
25	M1_Spy_0794		cell wall / membrane / envelope biogenesis	glycosyl transferase	1.80E-03	0.87	↑
47	M1_Spy_1358	*murZ*	cell wall / membrane / envelope biogenesis	UDP-N-acetylglucosamine 1-carboxyvinyltransferase	1.52E-02	1.50	↑
2	M1_Spy_2185	*gidA*	Cell cycle control, cell division	tRNA uridine 5-carboxymethylaminomethyl modification enzyme	0.00E+00	2.42	↑
77	M1_Spy_1730	*hit*	Cell cycle control, cell division	Diadenosine tetraphosphate hydrolase	4.35E-02	**-0.79**	↓
35	M1_Spy_1854	*glpF.2*	Carbohydrate transport and metabolism	glycerol uptake facilitator protein	5.80E-03	1.23	↑
58	M1_Spy_1711		Carbohydrate transport and metabolism	PTS system galactose-specific transporter subunit IIA	2.22E-02	**-1.66**	↓
63	M1_Spy_1399	*nagB*	Carbohydrate transport and metabolism	N-acetylglucosamine-6-phosphate isomerase	2.75E-02	**-1.02**	↓
4	M1_Spy_1506		Amino acid transport and metabolism	amino acid ABC transporter ATP-binding protein	0.00E+00	2.26	↑
45	M1_Spy_1542		Amino acid transport and metabolism	Dipeptidase (glutathione-mediated detox)	1.20E-02	**-1.21**	↓

6.2.2 Applying neighbor clustering algorithms reveal additional insights on S. pyogenes gene expression profiles

"GenomeCrawler is a dynamic windowing ("GenomeCrawler") algorithm that sequentially steps through the microarray data and identifies clusters of adjacent genes exhibiting similar fold changes in expression. Neighbor clustering was designed to identify expanded groupings of potentially related genes from our array data by incorporating two reliable predictors of genes that share common function or regulation, namely physical proximity and similar expression profiles GenomeCrawler applies a separate permutation algorithm, using the sum of each gene's *t*-statistics to calculate adjusted *P* values for each cluster." We applied the algorithms to our microarray data set and then visually inspect the resulting clusters, omitting those incongruent with the neighbor cluster definition as described in the Methods section.

A number of different sized clusters containing the same gene(s) remained following initial visual curating. To avoid overlapping cluster groups, we curate clusters and chose the most significant grouping containing the largest number of members A total of 55 clusters containing 216 genes were identified by this. Clusters ranged in grouping sizes from including 2 to 32 genes. (Table 6.4)

In some cases, resulting clusters identified previously described or predicted operons (i.e. *Spy0127 – Spy 130*). In others, our analysis identified novel groupings of genes, which may indicate functional relationships not previously

known. Of the 78 individual genes we identified in our initial analysis as undergoing significant differential expression, 62 (78%) were components of significant clusters whereas 16 remained un-grouped. In approximately 25% of the resulting groupings (n = 14), we identified significance gene clusters, even though none of the cluster members had initially identified as undergoing significant $\log_2$-fold changes in expression. In such clusters, our algorithm revealed that the combined contributions of the non-significant gene fold changes resulted in a significant cluster. Ryan *et al* initially coined this concept of "significance by combined gene contributions" in their published work employing the Genome Crawler algorithm (Ryan 2007).

A nearly equivalent number of clusters were up regulated (29) as were down regulated (26). We identified eight significantly down-regulated phage gene clusters, which accounting for 30% of all gene clusters with noted decreases in expression.

Using a previously described scheme for organizing neighbor clustering analysis data (Ryan 2007), we qualitatively subdivided our clusters into three categories based on the availability of functional information on their gene content. Twenty-three (42%) of our 55 neighbor clusters were designated as Type I clusters, composed of genes that have been functionally defined either in the annotated genome or in subsequent published reports. Twenty-seven (49%) were designated Type II clusters containing both known and unknown genes. Finally, 5

(.09%) were categorized as Type III, which contained only unknown genes. (Table 6.4)

Table 6.4 Qualifying neighbor clusters identified in the *S. pyogenes* SF370 genome by GenomeCrawler analysis of palatine tonsil epithelia – associated bacteria versus nasopharyngeal – associated microarray data. Type I gene clusters – contain only genes of known function (highlighted in shades of *yellow*). Type II gene clusters – combination of both genes of known and unknown function (highlighted in shades of *green*). Type III gene clusters – contain only genes of unknown function (highlighted in shades of *blue*)

[a]Locus (Spy) numbers and common gene names are as designated in the annotated SF370 genome. Genome function designations are also from annotated genome. Fold change P values calculated by Cyber-T and Westfall-Young permutations as previously described. Bold Log_2Fold indicate downregulation (-) change in expression ratios between palatine tonsil epithelia – associated streptococci versus control nasopharyngeal –associated streptococci. Astericks indicates individual gene not scored as significant as $p<0.05$.

Start	Stop	Function / COG[a]	*p*-value[b] (Cluster)	Cluster Member[a]	Gene Name[a]	Description / Gene Product	*p*-value[c] (Indiv. genes)	Δ Log_2 Fold
Spy0047	**Spy0078**	**Translation, ribosomal structure, and biogenesis**	**1.00E-04**	Spy0047	*rpsJ*	30S ribosomal protein S10	2.00E-04	2.62
				Spy0049	*rplC*	50S ribosomal protein L3	0.1109*	2.28
				Spy0050	*rplD*	50S ribosomal protein L4	0.3993*	2.34
				Spy0051	*rplW*	50S ribosomal protein L23	0.4364*	1.22
				Spy0052	*rplB*	50S ribosomal protein L2	0.2411*	1.54
				Spy0053	*rpsS*	30S ribosomal protein S19	0.7039*	1.30
				Spy0054			0.1009*	1.12
				Spy0055	*rplV*	50S ribosomal protein L22	0.1605*	1.28
				Spy0056	*rpsC*	30S ribosomal protein S3	0.3367*	1.79
				Spy0057	*rplP*	50S ribosomal protein L16	0.1226*	0.94
				Spy0058			0.1373*	1.12
				Spy0059	*rpmC*	50S ribosomal protein L29	0.6973*	1.35
				Spy0060	*rpsQ*	30S ribosomal protein S17	0.2557*	1.17
				Spy0061		50S ribosomal protein L14	0.2004*	1.35
				Spy0062	*rplX*	50S ribosomal protein L24	0.7391*	1.57
				Spy0063	*rplE*	50S ribosomal protein L5	0.4231*	1.12
				Spy0064	*rpsN*	30S ribosomal protein S14	0.0945*	1.43
				Spy0065	*rpsH*	30S ribosomal protein S8	0.7465*	1.48
				Spy0066	*rplF*	50S ribosomal protein L6	0.2186*	1.36
				Spy0067	*rplR*	50S ribosomal protein L6	0.3756*	1.37
				Spy0068			0.3446*	1.81
				Spy0069	*rpsE*	30S ribosomal protein S5	0.56*	1.51
				Spy0070			0.5687*	1.72
				Spy0071	*rpmD*	50S ribosomal protein L30	0.8102*	0.49
				Spy0072	*rplO*	50S ribosomal protein L15	1*	0.01
		Intracellular trafficking and scretion		Spy0073	*secY*	putative preprotein translocase	1*	0.06

		Nucleotide transport and metabolism		Spy0074	*adk*	adenylate kinase	0.9893*	0.35
				Spy0075	*infA*	putative translation initiation factor IF-1	0.8102*	0.49
				Spy0076	*rpmJ*	50S ribosomal protein B	1*	0.01
				Spy0077	*rpsM*	30S ribosomal protein S13	1*	0.06
				Spy0078	*rpsK*	30S ribosomal protein S11	0.9893*	0.35
Spy0127 -	**Spy0130**	**virulence**	**7.00E-04**	Spy0127	*SipA1*	putative signal peptidase I	0.7331*	1.38
				Spy0128		major pilus (shaft) subunit	0.553*	2.46
				Spy0129	*SrtC1*	pilus associated sortase C1	0.9934*	0.93
				Spy0130		pilin minor subunit / cell wall linker	0	3.62
Spy0285 -	**Spy0290**	**Post-Translational modification, protein turnover, chaperones**		Spy0285	*sufC*	putative ABC transporter (ATP-binding protein)	0.2725*	0.83
				Spy0287	*sufD*	ABC-type transport system involved in Fe-S cluster assembly	0.0332	1.01
		Amino acid transport & metabolism		Spy0288	*csdA*	putative aminotransferase	0	1.37
		Energy production and conversion		Spy0289		similar to NifU protein	0.2108*	1.22
				Spy0290		conserved hypothetical protein	0.445*	1.34
Spy0319 -	**Spy0321**	**Inorganic ion transport and metabolism**	**0.0134**	Spy0319		ABC transporter substrate binding protein	0.0174	**-1.57**
				Spy0320		putative ABC transporter (ATP-binding protein)h	0.3305*	**-1.50**
				Spy0321		putative ABC transporter (permease protein)	0.367*	**-1.14**
Spy0326 -	**Spy0327**	**Inorganic ion transport**	**0.0329**	Spy0326		K+ transport systems, NAD-binding component	0.0655*	0.76
				Spy0327	*ntpJ*	V-type Na+ -ATPase subunit J	0.3148*	0.94
Spy0460 -	**Spy0461**	**Translation, ribosomal structure, and biogenesis**	**0.0155**	Spy0460	*rplK*	50S ribosomal protein L11	0.4118*	1.98
				Spy0461	*rplA*	50S ribosomal protein L1	0.0034	1.90
Spy0503 -	**Spy0505**	*Transcription*	**0.0042**	Spy0503		putative exoribonuclease R / RNAse	0.0085	**-0.81**

		Translation, ribosomal structure, and biogenesis		Spy0504	*smpB*	tmRNA-binding protein	0.0019	**-0.88**
		Post-Translational modification, protein turnover, chaperones		Spy0505		putative glutamine cyclotransferase	0.128*	**-0.78**
Spy0511 -	**Spy0513**	**Amino acid transport and metabolism**	**0.0407**	Spy0511	*gloA*	putative lactoylglutathione lyase	0.7264*	**-0.73**
		Energy production and conversion		Spy0512		putative NAD(P)H-flavin oxidoreductase	0.1863*	**-0.84**
				Spy0513	*pepQ*	putative XAA-PRO dipeptidase; X-PRO dipeptidase	0.2885*	**-0.75**
Spy0755 -	**Spy0761**	**Energy production / conversion**	**0.0088**	Spy0755	*atpB*	putative proton-translocating ATPase a subunit	0.8932*	0.39
				Spy0756	*atpF*	putative proton-translocating ATPase, subunit b	0.6166*	0.52
				Spy0757	*atpH*	putative proton-translocating ATPase, delta subunit	0.348*	0.70
				Spy0758	*atpA*	putative proton-translocating ATPase, alpha subunit	0.593*	0.86
				Spy0759	*atpG*	putative proton-translocating ATPase, gamma subunit	0.1905*	0.78
				Spy0760	*atpD*	putative proton-translocating ATPase, beta subunit	0.3601*	0.79
				Spy0761	*atpC*	putative proton-translocating ATPase, epsilon subunit	0.0874*	0.73
Spy0849 -	**Spy0852**	*Translation, ribosomal structure, and biogenesis*	**0.0016**	Spy0849	*trmD*	putative tRNA (guanine-N1)-methyltransferase	0.0295	1.14
		Posttranslational modification, protein turnover, chaperones		Spy0850		putative thioredoxin reductase	0.0002	1.89
		General function prediction only		Spy0851		probable regulatory protein	0.8808*	1.26
		Coenzyme transport and metabolism		Spy0852	*apbA*	putative 2-dehydropantoate 2-reductase	0.05	1.16
Spy0880 -	**Spy0881**	**Lipid transport and metabolism**	**0.005**	Spy0880	*mvaS.1*	putative 3-hydroxy-3-methylglutaryl-coenzyme A	0.0005	1.23
				Spy0881	*mvaS.2*	putative 3-hydroxy-3-methylglutaryl-coenzyme A synthase (HMG-CoA synthase)	0.0111	1.17
Spy1097 -	**Spy1100**	**Coenzyme transport and metabolism**	**0.021**	Spy1097	*folE*	GTP cyclohydrolase	0.7809*	**-0.36**

				Spy1098	*folP*	dihydropteroate synthase	0.4987*	**-0.52**
				Spy1099	*folQ*	dihydroneopterin aldolase	0.1257*	**-0.58**
				Spy1100	*folK*	hydroxymethylpterin pyrophosphokinase	0.1925*	**-0.57**
Spy116		*Translation, ribosomal structure,*						
1 -	**Spy1163**	*and biogenesis*	**0.0066**	Spy1161		Predicted GTPases	0.0282	**-1.01**
		Replication, recombination and repair		Spy1162	*rnh*	putative ribonuclease HII	0.4548*	**-0.59**
				Spy1163	*smf*	putative DNA processing protein (Smf family)	0.0029	**-1.19**
Spy124		**Inorganic ion tansport and**				putative phosphate uptake regulatory		
0 -	**Spy1243**	**metabolism**	**0.0055**	Spy1240	*phoU*	protein	0.0012	1.09
				Spy1241	*pstB*	phosphate ABC transporter (ATP-binding protein)	0.8424*	0.48
				Spy1242	*pstB2*	putative phosphate ABC transporter (ATP-binding protein	0.0409	1.00
				Spy1243	*pstC*	putative phosphate ABC transporter	0.2706*	0.89
Spy125		**Defense**						
4 -	**Spy1257**	**mechanisms**	**0.0333**	Spy1254			0.473*	**-0.65**
				Spy1255	*SalY?*	COG577: ABC-type antimicrobial peptide transport system, permease component	0.1656	**-0.84**
				Spy1257	*SalX?*	COG1136: ABC-type antimicrobial peptide transport system,ATPase component	0.4026	**-0.96**
Spy135		*Cell wall/membrane*				putative UDP-N-		
8 -	**Spy1359**	*biogenesis*	**0.0332**	Spy1358	*murZ*	acetylglucosamine 1-	0.0152	
		Coenzyme transport and metabolism		Spy1359	*metK*	S-adenosylmethionine synthetase	0.7516*	**-0.07**
Spy137		*Post-Translational modification, protein*						
4 -	**Spy1375**	*turnover, chaperones*	**0.0055**	Spy1374	*nrdH*	putative glutaredoxin	0.0252	1.86
		Nucleotide transport and metabolism		Spy1375	*nrdE.2*	putative ribonucleotide reductase alpha-chain	0.0014	1.40
Spy137						ribonucleotide diphosphate reductase		
8 -	**Spy1379**	*Nucleotide transport and metabolism*	**0.0159**	Spy1378	*nrdF.2*	small subunit	0.0002	1.65
		Inorganic ion tansport and metabolism		Spy1379		putative chloride channel protein	0.9943*	0.49
Spy174		**Lipid Transport and**				acetyl-CoA carboxylase		
5 -	**Spy1749**	**metabolism**	**0.0019**	Spy1745	*accC*	biotin	0.0156	1.77

				Spy1746	*fabZ*	(3R)-hydroxymyristoyl-ACP dehydratase	0.0235	1.37
				Spy1747	*accB*	acetyl-CoA carboxylase biotin carboxyl carrier protein subunit	0.003	1.57
				Spy1749	*fabG*	3-ketoacyl-ACP reductase	0.0004	1.45
Spy1751 -	**Spy1758**	**Lipid Transport and metabolism**	**1.40E-03**	Spy1751	*fabK*	putative trans-2-enoyl-ACP reductase II	0.0002	1.66
				Spy1753	*acpP*	putative acyl carrier protein	0.5995*	0.58
				Spy1754	*fabH*	fabH putative beta-ketoacyl-[ACP] synthase III	0.3849*	0.96
				Spy1755		[REGULATOR] MarR family	0.0044	1.25
				Spy1758	*phaB*	putative enoyl CoA hydratase	0.1324*	0.93
Spy1770 -	**Spy1772**	*Lipid Transport and metabolism*	**0.0101**	Spy1770	*gatB*	aspartyl/glutamyl-tRNA amidotransferase subunit B	0.0163	1.31
		Post-Translational modification, protein turnover, chaperones		Spy1771	*gatA*	Glutamyl-tRNA Gln amidotransferase subunit A	0.1124*	1.07
		Translation, ribosomal structure, and biogenesis		Spy1772	*gatC*	Glu-tRNA Gln amidotransferase subunit C	0.3028*	0.90
Spy1940 -	**Spy1941**	**Translation, ribosomal structure, and biogenesis**	**0.0424**	Spy1940		hypothetical protein	0.008	2.23
				Spy1941	*cysS*	cysteinyl-tRNA synthetase	0.9493*	0.85
Spy2092 -	**Spy2093**	**Translation, ribosomal structure, and biogenesis**	**0.0312**	Spy2092	*rpsB*	30S ribosomal protein S2	0.1349*	1.85
				Spy2093	*tsf*	putative elongation factor TS	0.1684*	2.05
Spy0281 -	**Spy0282**	*General function prediction only*	**2.00E-04**	Spy0281	*mecA*	putative negative regulator of genetic competence	0.8124*	0.68
		Cell wall/membrane biogenesis		Spy0282	*rgpG*	possibly involved in regulation of genetic competence	0.4895*	0.71
Spy0358 -	**Spy0367**	*General function prediction only*	**0.014**	Spy0358		putative membrane spanning protein	0.1413*	0.53
		Function unknown		Spy0359		Uncharacterized protein conserved in bacteria	0.9308*	0.36
		Cell wall/ membrane/ envelope biogenesis		Spy0361	*glr*	glutamate racemase	0.9301*	0.47

		Nucleotide transport and metabolism		Spy0362		Xanthosine triphosphate pyrophosphatase	0.5768*	0.53
		General function prediction only		Spy0363		phosphoesterase	0.6548*	0.48
		Multifunctional		Spy0364		CBS domain	0.5062*	0.61
		Replication, recombination and repair		Spy0365	*XerD*	site-specific tyrosine recombinase XerD-like protein	0.5139*	0.67
		Function unknown		Spy0366	*scpA*	segregation and condensation protein A	0.5124*	0.47
		Transcription		Spy0367	*scpB*	segregation and condensation protein B	0.6457*	0.53
Spy037 9 -	**Spy0382**	*Posttranslational modification, protein turnover, chaperones*	**0.0129**	Spy0379	*pflC*	pyruvate-formate lyase activating enzyme	0.2173*	**-1.27**
		Energy production and conversion		Spy0380		Exopolyphosphatase; **Possible adhesin** (intrageneric coaggregation-relevant adhesin)	0.4667*	**-0.70**
		function unknown		Spy0382		conserved streptococcal hypothetical protein	0.0174	**-0.70**
Spy043 9 -	**Spy0441**	*function unknown*	**0.0052**	Spy0439		hypothetical protein	0.0067	1.01
		Lipid transport and metabolism		Spy0440	*fabG*	3-ketoacyl-ACP reductase	0.0645*	1.18
		General function prediction only		Spy0441		NAD-dependent oxidoreductase	0.1238*	1.10
Spy056 7 -	**Spy0569**	*General function prediction only*	**0.0493**	Spy0567		Predicted hydrolases of the HAD superfamily	0.2834*	0.90
		General function prediction only		Spy0568		Predicted hydrolases of the HAD superfamily	0.7443*	0.63
		Intracellular trafficking and secretion		Spy0569	*ftsY*	putative signal recognition particle (docking protein)	0.3685*	0.49
Spy065 8 -	**Spy0667**	**Phage**	**0.0022**	Spy0658		(Φ370.1) putative Cro-like protein, phage associated	0.3003*	**-0.67**
				Spy0659		(Φ370.1) hypothetical protein, phage associated	0.6513*	**-0.67**
				Spy0660		(Φ370.1) hypothetical protein, phage associated	0.3359*	**-0.73**
				Spy0661		(Φ370.1) hypothetical protein, phage associated	0.0209	**-0.72**
				Spy0663		(Φ370.1) hypothetical protein, phage associated	0.9237*	**-0.51**
				Spy0664		(Φ370.1) hypothetical protein, phage	0.6749*	**-0.61**

					associated		
			Spy0665		(Φ370.1) hypothetical protein, phage associated	0.1435*	**-0.63**
			Spy0666		(Φ370.1) replication, phage associated	0.2469*	**-0.59**
			Spy0667		(Φ370.1) hypothetical protein, phage associated	0.3414*	**-0.63**
Spy0680 -	**Spy0681**	**Phage**	**0.0073**	Spy0680		(Φ370.1) Head morphogenesis, phage associated	0.0575*	**-0.91**
			Spy0681		(Φ370.1) Head morphogenesis (Portal protein), phage associated	0.0033	**-0.98**
Spy0791 -	**Spy0798**	**Cell wall/membrane biogenesis**	**1.00E-04**	Spy0791	*rgpEc*	putative glycosyltransferase - possibly involved in cell wall localization and side chain formation of rhamnose-glucose polysaccharide	0.6189*	0.46
			Spy0792	*rgpFc*	conserved hypothetical protein - possibly involved in cell wall localization and side chain formation of rhamnose-glucose polysaccharide	0.1973*	0.65
			Spy0793		phosphoglycerol transferase related; alkaline phosphatase superfamily	0.1907*	0.85
			Spy0794		putative glycosyl transferase	0.0018	0.87
		Function unknown		Spy0796		hypothetical protein	0.0062	1.34
		virulence regulator		Spy0797	*amrA*	[REGULATOR] Activation of Mga regulon	0.0052	1.05
		Function unknown		Spy0798		predicted membrane protein	0.0598*	1.29
Spy0873 -	**Spy0875**	Function unknown	**0.0179**	Spy0873		conserved hypothetical protein	0.1163*	**-0.57**
		two component system		Spy0874	*sptR*	(sptR-sptS) Important for persistence in human saliva; Activation of spd, speB, sic, has, and complex	0.5299*	**-0.37**
		two component system		Spy0875	*sptS*	carbohydrate utilization pathways	0.0749*	**-0.54**
Spy0883 -	**Spy0887**	*Coenzyme transport and metabolism*	**1.00E-04**	Spy0883	*dyr*	putative dihydrofolate reductase	0.8166*	0.40
		Function unknown		Spy0884		hypothetical protein	0.0767*	0.88

		Posttranslational modification / prottein turnover		Spy0885	*clpX*	ATP-dependent Clp protease subunit X	0.0204	0.90
		General function prediction only		Spy0886	*engB*	conserved hypothetical GTP-binding protein	0.0107	1.05
		virulence regulator		Spy0887	*vfr*	[REGULATOR] Repression of speB via RopB; No DNA binding activity	0	1.49
Spy0894 -	**Spy0895**	**Nucleotide transport and metabolism**	**0.0191**	Spy0894	*deoD2*	putative purine nucleoside phosphorylase	0.0369	0.78
		General function prediction only		Spy0895		histidine protein kinase	0.1079*	0.95
Spy0916 -	**Spy0917**	*Function unknown*	**0.0461**	Spy0916		hypothetical protein	0.623*	**-0.88**
		Posttranslational modification, protein turnover, chaperones		Spy0917		Glutathione S-transferase	0.0746*	**-1.00**
Spy1192 -	**Spy1193**	**Energy production / conversion**	**0.0035**	Spy1192	*citC*	putative citrate lyase synthetase (citrate (pro-3S)-lyase ligase)	0.0477	**-0.60**
		Function unknown		Spy1193		hypothetical	0.0002	**-1.08**
Spy1402 -	**Spy1405**	**Cell wall/membrane biogenesis**	**0.008**	Spy1402		hypothetical protein	0.1363*	**-1.58**
		Function Unknown		Spy1404		hypothetical protein	0.0678*	**-1.54**
				Spy1405		hypothetical protein	0.0375	**-1.71**
Spy1425 -	**Spy1429**	*Function Unknown*	**0.0279**	Spy1425		hypothetical protein	0.232*	**-1.84**
		General function prediction only		Spy1427		putative transcriptional regulator ?	0.1341*	**-2.07**
		Carbohydrate transport and metabolism		Spy1429	*gpmA*	putative phosphoglycerate mutase	0.6725*	**-0.48**
Spy1438 -	**Spy1442**	**Phage**	**0.0053**	Spy01438		(Φ370.3) Muramidase (flagellum-specific)	0.003	**-1.10**
				Spy01440		(Φ370.3) putative holin		
				Spy01441		(Φ370.3) Tail fiber gene	0.0005	**-1.06**
				Spy01442		(Φ370.3) - phage associated	0.0309	**-1.05**
Spy1457 -	**Spy1465**	**Phage**	**2.00E-04**	Spy01457		(Φ370.3) putative structural protein	0.0178	**-1.01**
				Spy01460		(Φ370.3) - phage associated	0.0005	**-1.64**
				Spy01462		(Φ370.3) - phage associated	0.3555*	**-1.17**
				Spy01463		(Φ370.3) - phage associated	0.1166*	**-1.26**
				Spy01464		(Φ370.3) Head morphogenesis	0.0002	**-1.34**

				Spy0146 5		(Φ370.3) putative structural protein	0.0002	**-1.35**
Spy148 6 -	**Spy1487**	**Phage**	**0.0161**	Spy0148 6		(Φ370.3) putative repressor - phage associated	0.1819*	**-1.04**
				Spy0148 7		(Φ370.3) Lysogeny	0.0165	**-0.92**
Spy151 0 -	**Spy1511**	**Replication, recombination and repair**	**0.0479**	Spy0151 0	*mutT*	putative mutator protein	0.0425	**-1.18**
				Spy0151 1		hypothetical protein	0.7238*	**-0.68**
Spy152 9 -	**Spy1530**	**Carbohydrate transport and metabolism**	**0.0203**	Spy0152 9	*glcK*	glucose kinase	0.1806*	**-0.56**
		Function unknown		Spy0153 0		conserved hypothetical protein	0.0336	**-0.78**
Spy154 1 -	**Spy1547**	**Amino acid transport & metabolism**	**0.0022**	Spy1541	*arcC*	putative carbamate kinase	0.1302*	**-1.00**
				Spy1542		Dipeptidase (glutathione-mediated detox)	0.012	**-1.21**
				Spy1543		predicted membrane protein	0.3614*	**-1.45**
				Spy1544	*arcB*	putative ornithine transcarbamylase	0.1573*	**-1.72**
				Spy1546		hypothetical protein	0.1856*	**-1.93**
				Spy1547	*sagP / (arcA)*	arginine deiminase / [VIRULENCE] **Activator of SpeB**	0.0584*	**-1.90**
Spy173 0 -	**Spy1731**	**Cell cycle control, cell division**	**0.0068**	Spy1730	*hit*	putative cell-cycle regulation histidine triad	0.0435	**-0.79**
		Function unknown		Spy1731			0.0042	**-1.02**
Spy173 3 -	**Spy1736**	Transcription	**0.0088**	Spy1733		[REGULATOR] Cell envelope-related repressor	0.2927*	0.62
		Lipid metabolism		Spy1734		Acetyltransferase, including N-acetylases of ribsomal proteins	0.9782*	0.54
		General function prediction only		Spy1735		hypthetical / COG802: Predicted ATPase or kinase	0.2225*	1.13
		General function prediction only		Spy1736			0.0005	1.64
Spy194 4 -	**Spy1946**	*Function unknown*	**0.0083**	Spy1944	*cysE*	serine acetyltransferase	0.0553*	1.29
		Translation, ribosomal structure, and biogenesis		Spy1945		hypothetical protein	0.0314	1.90
				Spy1946	*pnpA*	putative polynucleotide phosphorylase, alpha chain	0.1783*	1.45

Spy2112 -	**Spy2114**	**Translation, ribosomal structure, and biogenesis**	**0.0199**	Spy2112		conserved hypothetical protein	0.3502*	**-0.57**
		Replication, recombination and repair		Spy2113		Predicted endonuclease involved in recombination	0.1506*	**-0.63**
		Function unknown		Spy2114		hypothetical protein	0.1451*	**-0.63**
Spy2185 -	**Spy2186**	**Cell cycle control, cell division**	**9.00E-04**	Spy2185	*gidA*	tRNA uridine 5-carboxymethylaminomethyl modification enzyme	0	2.42
		Function unknown		Spy2186		hypothetical protein	0.3646*	1.68
Spy2209 -	**Spy2211**	*Function unknown*	**0.0486**	Spy2209		conserved hypothetical protein	0.1952*	1.05
		Nucleotide transport and metabolism		Spy2210		ABC transporter, ATP-binding protein	0.9766*	0.23
		Function unkown		Spy2211		predicted membrane protein	0.1319*	1.07
Spy0603 -	**Spy0604**	**Function unknown**	**0.033**	Spy0603		Hypothetical protein (signal peptide)	0.5017*	1.08
				Spy0604		hypothetical protein	0.023	0.67
Spy0945 -	**Spy0947**	**Phage**	**0.0054**	Spy0945		(Φ370.**2**) hypothetical protein, phage associated	0.0072	**-1.05**
				Spy0946		(Φ370.2) putative P1-type antirepressor, phage associated	0.0799*	**-0.99**
				Spy0947		(Φ370.2) hypothetical protein, phage associated	0.0692*	**-0.98**
Spy0956 -	**Spy0963**	**Phage**	**0.0122**	Spy0956		(Φ370.2) hypothetical protein, phage associated	0.9042*	**-0.79**
				Spy0957		(Φ370.2) hypothetical protein, phage associated	0.2373*	**-0.95**
				Spy0958		(Φ370.2) hypothetical protein, phage associated	0.5753*	**-0.80**
				Spy0959		(Φ370.2) hypothetical protein, phage associated	0.2934*	**-1.00**
				Spy0960		(Φ370.2) hypothetical protein, phage associated	0.0994*	**-0.98**
				Spy0961		(Φ370.2) hypothetical protein, phage associated	0.8586*	**-0.54**
				Spy0962		(Φ370.2) hypothetical protein, phage associated	0.9604*	**-0.60**
				Spy0963		(Φ370.2) hypothetical protein, phage associated	0.4782*	**-0.66**

Spy1075 - Spy1077		**Phage**	**0.0447**	Spy1075		(Φ370-RD.1) hypothetical protein, phage associated	0.035	**-1.11**
				Spy1077		(Φ370-RD.1) putative methyl transferase, phage associated	0.7174*	**-0.97**
Spy2153 - Spy2154		*Function unknown*	**0.0045**	Spy2153		conserved hypothetical protein	0.0002	1.71
		Function unknown		Spy2154		Hypothetical protein [transmembrane]	0.2017*	1.09

6.2.3 SF370 pili play a significant role during adherence and invasion during co-culture with HPTE and tonsil tumor-derived cell lines

Among the notable Type I clusters identified, neighbor cluster *Spy0127* – *Spy0130* encoding the pilus forming operon within the GrAS FCT-2 (Fibronectin and Collage binding and T antigen) pathogenicity region was significantly up regulated in comparison with our control bacteria associated with Detroit cells. Previously, our lab determined this cluster was indeed an operon through *in silico* analysis and reverse transcription of deletion mutants (Ryan 2007). These findings were concurrently examined and verified by others. (Abbot 2007, Manetti 2007). Ryan *et al* observed in their microarray studies that this cluster was upregulated during adherence to Detroit 562 monolayers as compared to control bacteria that were associated but not yet adhered. In our work presented here, we see a significant upregulation of the pilus operon, which indicates a role for the pili in preparation for, or subsequent adherence to, the tonsillar cells. Our finding that there is a significant increase in transcription of this operon as compared to the control (Detroit 562 cells) suggests that the pili, or transcription of one or all genes may be even more important to adherence to the bacterium's target tissue (the tonsil) as compared to a proximal cell type (Detroit cell), We tested this hypothesis in studies with the pili knock-out mutant presented later in this work.

Our finding that the pili operon genes are significantly upregulated at the association stage with tonsillar epithelial cells as compared to Detroit cells

suggests that pili may contribute to the tropism for tonsillar cells, if we assume that the mechanisms for adherence to the two cell types are the same. Increased expression during association may simply indicate earlier gene activation in the tonsil environment than in the Detroit 562 environment, or it might indicate the expression of more total number of pili being synthesized and organized at the bacterial cell surface. Since the mechanism for adherence to the tonsillar cell types has yet to be explored, this leads to a new avenue for research into the question of tropism.

To confirm the effect of pili on interactions with our tonsil epithelial cells, we used a previously characterized deletion mutant of the pilus-associated sortase C1 gene, Δ *Spy0129*, (Ryan 2007) in our standard adherence and invasion assay. This SF370 mutant is deficient in proper pili production and cell-surface presentation. As was demonstrated with Detroit 562 cells (Abbot 2007, Ryan 2007), we found that the adherence of the pili-mutant to both primary and tumor-derived tonsil epithelial cells was significantly decreased, (Figure. 6.1) Of note, adherence was not completely abolished by the absence of pili, indicating that other adhesins likely contribute to adherence, albeit to a lesser degree than the pili.

We also assayed strain SF370 in invasion assays using both tonsillar cell lines. We report here that invasion capacity by strain SF370 is significantly decreased as compared to Detroit 562 cells. (Figure. 6.2)

Figure 6.1. Δ*Spy0129* deletion decreases Streptococcal adherence across all epithelial monolayers

Δ *Spy0129* mutant was created and verified as apiliated as previously described (Ryan 2007). Detroit 562, UT-SCC-60A, UT-SCC-60B, and HPTE cell monolayers were grown to ~95% confluence on Falcon® 24-well tissue culture plates. Wells were inoculated with either Δ *Spy0129* or parental strain SF370SM^{R} (Wild Type, SF370 SMR) at Multiplicity of Infection 100:1 in DMEM without serum. Associated bacteria were removed with PBS and colony forming units (cfu) were counted on blood agar as described in the methods. Results are the mean ± standard deviation of at least three independent experiments performed on separate days in triplicate. Statistical significance (reported as *p* value) was determined by Student's t-test. Asterisks indicates $p < 0.0001$

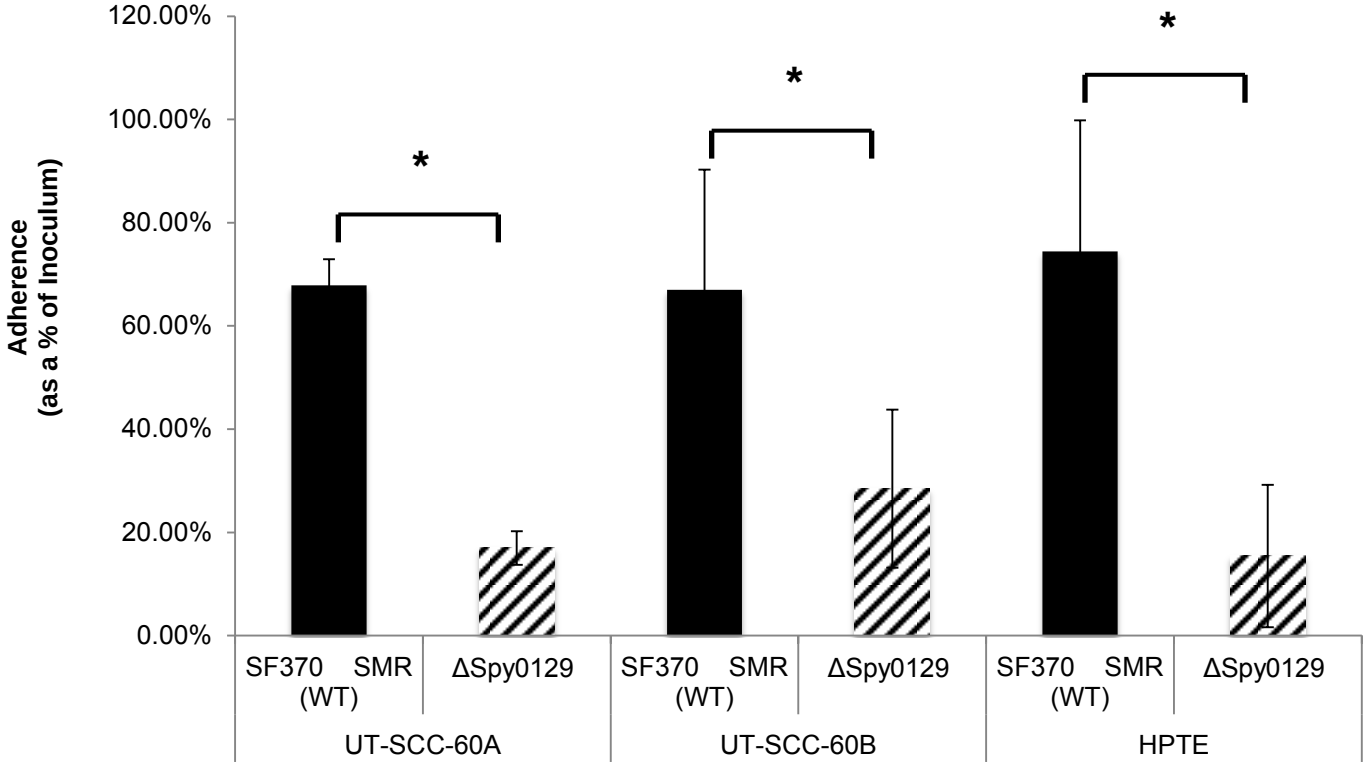
Adherence
(as a % of Inoculum)
120.00%
100.00%
80.00%
60.00%
40.00%
20.00%
0.00%
*
*
*
SF370 SMR (WT)
ΔSpy0129
SF370 SMR (WT)
ΔSpy0129
SF370 SMR (WT)
ΔSpy0129
UT-SCC-60A
UT-SCC-60B
HPTE

Figure 6.2. Internalization of M type 1 Δ*Spy0129* mutant is greatly decreased

Δ Spy0129 mutant was created and verified as apiliated as previously described (Ryan 2007). Detroit 562, UT-SCC-60A, UT-SCC-60B, and HPTE cell monolayers were grown to ~95% confluence on Falcon® 24-well tissue culture plates. Wells were inoculated with either Δ*Spy0129* or parental strain SF370SM^R (Wild Type, SF370 SMR) at Multiplicity of Infection 100:1 in DMEM without serum. Associated bacteria were removed by vigorous washing with PBS and subsequently treated with Antibiotics cocktail (Penicillin 100ng / µL+ Gentamicin 100ng / µL) and PlyC (0.05U / well). Monolayers were washed with PBS and cfu's were counted on blood agar as described in the methods. Results are the mean ± standard deviation of at least three independent experiments performed on separate days in triplicate. Statistical significance (reported as *p* value) was determined by Student's t-test. Asterisks indicates *p* < 0 .0001

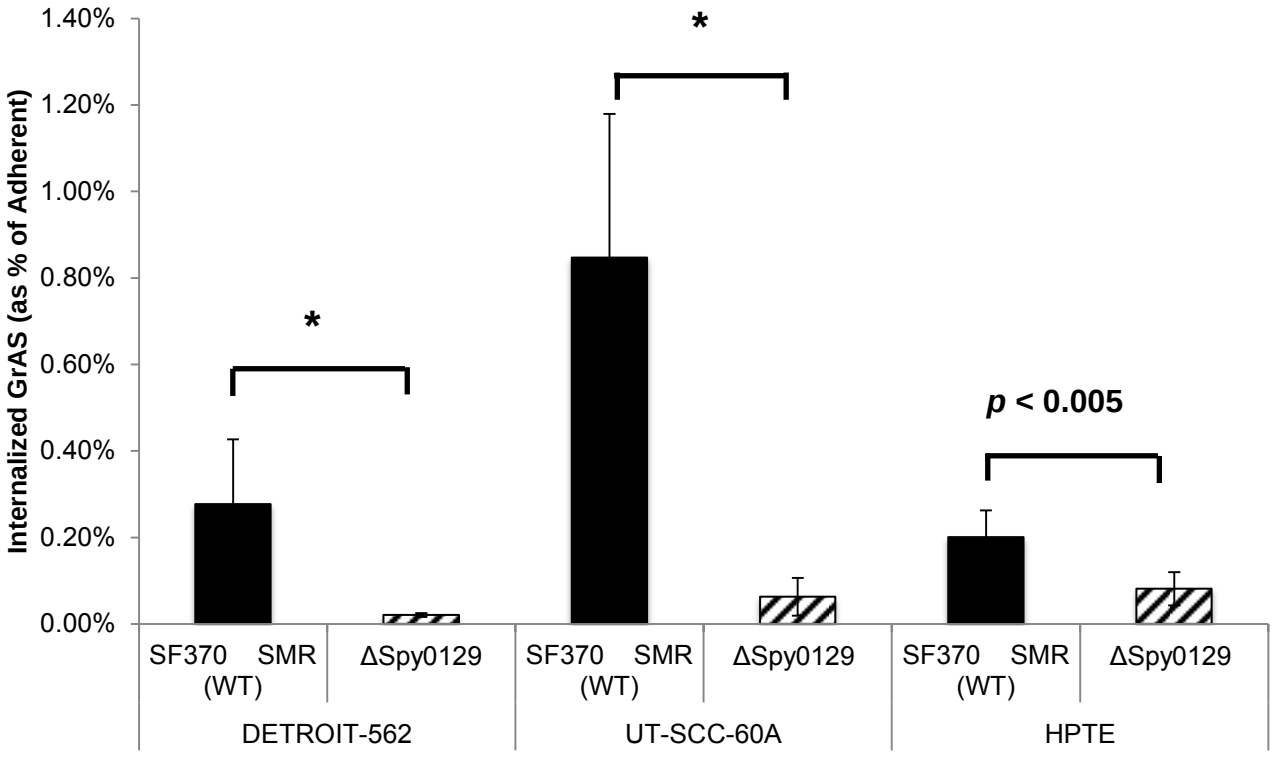
Internalized GrAS (as % of Adherent)
1.40%
1.20%
1.00%
0.80%
0.60%
0.40%
0.20%
0.00%
*
*
p < 0.005
SF370 (WT)
SMR
ΔSpy0129
SF370 (WT)
SMR
ΔSpy0129
SF370 (WT)
SMR
ΔSpy0129
DETROIT-562
UT-SCC-60A
HPTE

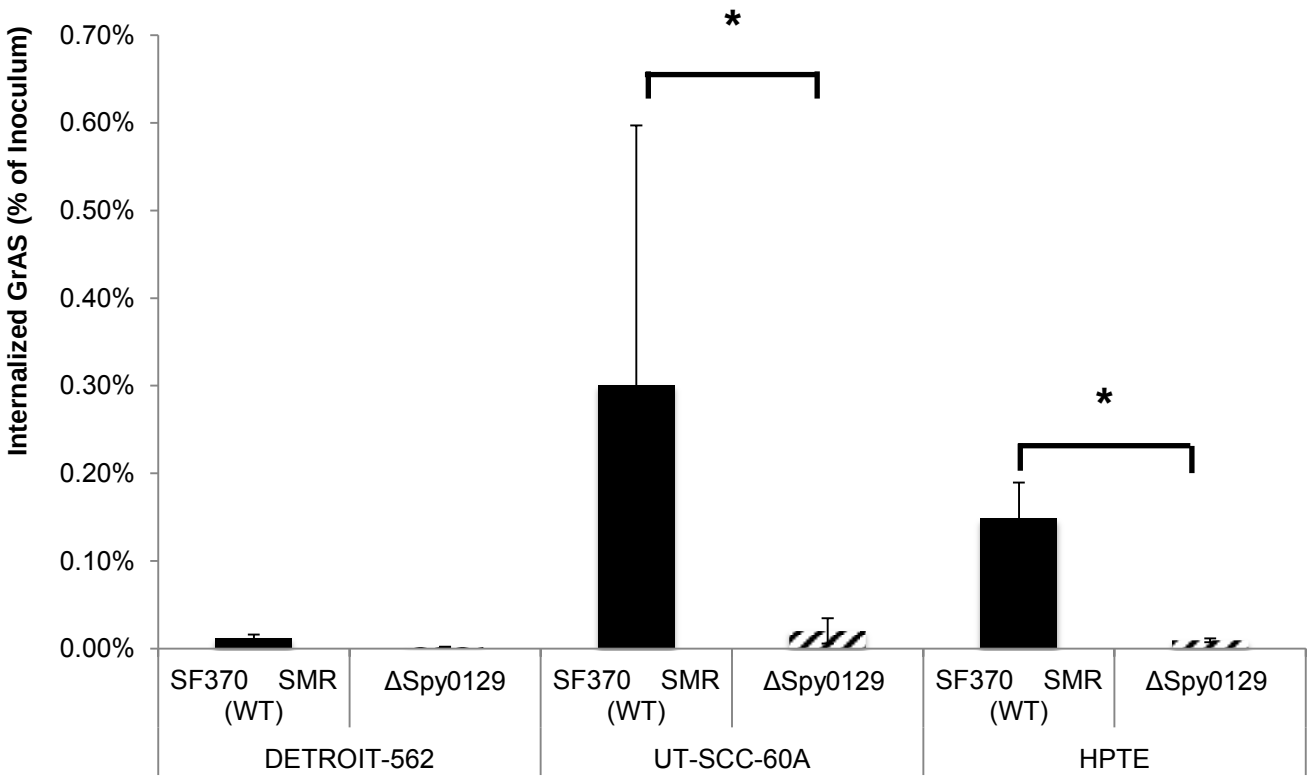
Internalized GrAS (% of Inoculum)
0.70%
0.60%
0.50%
0.40%
0.30%
0.20%
0.10%
0.00%
*
*
SF370 (WT)
SMR
ΔSpy0129
SF370 (WT)
SMR
ΔSpy0129
SF370 (WT)
SMR
ΔSpy0129
DETROIT-562
UT-SCC-60A
HPTE

6.3 Discussion

6.3.1 Regulatory systems

GrAS transcription is regulated through the concerted action of 13 conserved 'two-component' signal transduction systems (TCS, containing a sensor kinase and a response regulator) and >60 'stand-alone' transcription factors (named due to their ability to independently regulate transcription). Between our individual gene and cluster analyses, we identified one two-component system, *sptR-sptS* (Spy0874-Spy0875), which has been shown to be important for persistence in adult whole saliva. The role of this TCS during persistence in human saliva involves linking central metabolic processes with the production of a broad range of putative and known virulence factors (Shelburne 2005).

We were also able to identify five putative and known regulators. The first, *amrA (*Spy0797) is so named for "activation of *mga* regulon" expression locus A. It was found to be directly involved with regulating this locus during knockout experiments, but the mechanism of this regulator remains unknown. Based on sequence homology, Ribardo *et al* also predicted that *amrA* may be a membrane protein involved in the transport of a polysaccharide component during bacterial cell wall production in addition to its modulatory role of *mga*. We additionally identified the regulator, *vfr (*Spy088) named for virulence factor regulator. The function ascribed has been to serve as a repressor of SpeB via *RopB*. The

putative cell wall envelope regulator, *Spy1733* and the MarR Family regulators *Spy1755*, were identified in our analysis although their functions are currently unknown. All of the stand-alone regulators were up regulated in our analysis. The upregulation of *vfr* is consistent with our assumed mechanisms for adherence, as the bacteria would want to suppress SpeB from cleaving surface adhesins. The expression of *amrA* is consistent with its COG designation for cell wall biogenesis, as many other genes associated with this function were similarly upregulated. The *mga* locus, and associated virulence factors, showed no effect in our analysis so it is possible this regulator may plays dual functions when being expressed. As the mechanism for it's regulation of *mga* continues to be explored, it will be interesting to consider if our finding reflects such a dual role.

While virulence potential may not be fully described for all the identified TCS and regulatory systems, the direction of their expression change generally appears to be decreasing expression of enzymes that would disarm the bacterial surface proteins necessary for adhesion (*vrf* and *sptR-sptS*) as well as affecting metabolic strategies based on sensing environmental sources of nutrients (*Spy1755* and *sptR-sptS)*.

6.3.2 Complex carbohydrate vs lipid and secondary metabolic pathways for energy

As was apparent from our initial analysis of individual genes (Table 6.1), the neighbor cluster data identified additional significantly regulated genes that were associated with COG designations Lipid Transport and Metabolism (14 out of 14 genes with this COG), cell wall, membrane biogenesis (7/8), and post translational modification and protein turnover (7/10) were up regulated. This is in contrast to complex carbohydrate utilization pathways, which were mostly downregulated, an observation that is consistent with the downregulation of the *SptR-SptS* TCS.

While it is clear the microenvironment of the tonsillar monolayer would not necessarily be rich in available carbohydrate sources, the increased expression of lipid transport and metabolism genes may be a unique feature induced by the tonsil epithelium monolayer. Juncosa *et al* reported no significant change in SF370 expression of the *SptR-SptS* TCS either during co-culture with pharyngeal conditioned media or following 2.5h associated with Detroit 562 monolayers (Juncosa 2012). Inversely, this TCS was reported as upregulated in SF370, which were adhered to Detroit 562 cells (Ryan 2007).

To try to understand these observations in the broader context, we were drawn to the previously described mevalonic acid pathway, which has been linked to lipid

transport, and has recently been proposed as part of a model for bacterial persistence within the tonsil niche *in* vivo (Shea 2010). This pathway converts acetyl-CoA to isopentenyl-pyrophosphate (IPP), a short-chain phospholipid produced by GrAS that is identical to IPP produced by host epithelial cells and γ / δ T cells. . A potential role relating the mevalonic acid biosynthesis pathway and the host T cell anergy / proliferation axis was proposed by Shea et al 2010 during their longitudinal microarray-based study in macaques. This group was interested in the "interactome" between GrAS transcripts and their influence on concomitant host gene expression or vice versa. Throughout the stages of macaque infection, they found significant activation of mevalonic pathway enzymes correlating with host cell stress response and T cell regulation. In our analysis, we saw an upregulation of mevalonic pathway genes *mvaS.1* (Spy0880) and *mvaS.*2 (Spy0881) as well as the differential regulation of a number of other lipid metabolic pathways during association with tonsillar cells. We plan to continue these studies to determine if any such gene clusters play a role in persistence within the tonsillar environment.

The mevalonic acid operon (*Spy0880-Spy0881*) is positioned directly downstream of the *sptR-sptS* TCS. Although Shea and colleagues hypothesized that expression of the melavonic acid genes, the activity of the sptR/sptS two-component system, and consequent production of IPP, promoted enhanced GrAS survival in the oropharynx, they concede that additional information is needed on the exact role of the IPP stimulated γ / δ T cells (Shea 2010).

Recently, a *sptR* deletion mutant was created in the SF370 background (Shelburne 2005). This knockout resulted in an increase in gene expression within the FCT operon. In particular, the major shaft subunit (Spy0128) responsible for GrAS pilus length and stability was up regulated (Shea 2010). Pili expression was accompanied by downregulation of the *sptR-sptS* regulon. We observed a similar expression profile in our data: namely, the downregulation of the *sptR-sptS* TCS and the concomitant upregulation of pili genes with downregulation of nearly all differentially expressed carbohydrate metabolism associated genes (Tables 6.2 and 6.3). The similarities between our system and the *SptR* knockout simply reconfirm the proposed role of this TCS on regulating the expression of particular genes.

6.3.3 Phage-related genes

A survey of the known phage genes that were down-regulated (in both gene cluster and individual gene analyses) are consistent with previous reports from our lab on streptococcal association and adherence to Detroit 562 cells at a 2.5 hour incubation time point. The specific downregulation of Φ370.3 -encoded muramidase and holin may indicate a decreased release of the phage, which would lyse the bacteria and prevent adherence to the target cell. The experiments reported by Juncosa *et a*l mirror our Detroit cell control conditions, demonstrated a relative down-regulation of all prophage genes in these cells as well compared to bacteria in fresh media. Taken together, the data presented here indicate that in the tonsil environment, streptococci are further repressing

expression of these phage genes beyond the downregulation already described for the Detroit cell environment. It will be interesting to study why and how phage genes are so actively repressed in the tonsillar environment.

The high number of phage-associated genes that have unknown or hypothetical functions indicates how little is known about the role of phages in GrAS pathogenesis. This is despite the fact that phage ORFs have been shown to account for up to 74% of the variability in a GrAS genome (Banks 2004) and undoubtedly play a large role in all forms of infection.

6.3.4 Final Comment

In this chapter, we investigated the relative global transcriptional differences exhibited by a single representative “throat specialist” *emm* pattern strain of streptococci when exposed to nasopharyngeal versus palatine tonsil-derived epithelium. It is clear that *in vivo*, this non-motile bacterium successfully infects the human palatine tonsil, entering either a carrier state or initiating a focal disease. Our previous studies have demonstrated that streptococci undergo adaptive transcriptional responses to the changing environment. Our current study, however, is the first demonstration of streptococcal tissue-specific responses between two anatomically relevant locations that would naturally be in contact with the pathogen. We have shown that the bacteria produces a unique response with features such as increased early activity of the GrAS pili encoded operon and a unique metabolism shift. These observations, though limited in

scope with what may be interpreted, surely offers the foundation for asking more precise questions about streptococcal pathogenesis and its mechanisms underlying this apparent tissue predilection.

§7.0 STREPTOCOCAL EPITHELIAL INTERNALIZATION

7.1 Introduction

S. pyogenes causes invasive disease, finding access to deep tissues of its host, to cause necrotizing fasciitis, abscesses, and disseminated sepsis. Although historically regarded as an extracellular mucosal pathogen, recent laboratory and clinical observations made over the past 20 years have challenged the earlier assumption of this pathogen's obligate extracellular status. Noting similarities between group A streptococci and the gram positive *Listeria monocytogenes*, including internalin, which shares structural similarities to streptococcal surface proteins, LaPenta and colleagues sought to explore streptococcal internalization properties through *in vitro* modeling of upper airway streptococcal infection. In 1994, they reported that group A streptococci are internalized by cultured human epithelial cells, which are a non-phagocytic cell type, at frequencies as high as Listeria in certain strains (LaPenta 1994). With these findings, they were among the first to propose that entry into epithelial cells might serve as an initial step towards tissue invasion. Since this report, models of GrAS invasion and subsequent dissemination have been expanded to include paracellular and transcellular mechanisms.

7.1.1 Paracellular Invasive Dissemination

In the paracellular model, *S. pyogenes* interact with epithelial cell surface receptors, inducing changes in either epithelial or endothelial morphology to form gaps between an otherwise continuous tissue layer. Cywes *et al* demonstrated a CD44-dependent mechanism for GrAS binding that induced appreciable cytoskeletal rearrangements in human keratinocytes leading to membrane ruffling and disruption of intercellular junctions. In their model, extracellularly bound CD44 transduces an intracellular signal for Rac1-mediated actin polymerization. This event in turn results in local movement of the cell membrane to form lamellipodia and open intercellular junctions with neighboring cells permitting a paracellular entry point for invasive GrAS (Cywes 2001). Pancholi *et al* has additionally proposed a mechanism where the fibrinolytic digestion of intercellular junctions by proteolytically active plasminogen may enhance GrAS pericellular penetration through pharyngeal cell monolayers, as mediated by streptococcal enolase, SEN (Pancholi 2003).

7.1.2 Transcellular Invasion

In a transcellular model, the GrAS is internalized by epithelial cells and subsequently reemerges from the cells, presumably via the basolateral surface. Most transcellular models require a eukaryotic extracellular matrix “bridging molecule”, either fibronectin or collagen. One such model depends on binding of M protein to fibronectin which bridges the bacteria to alpha5beta1 integrin (Cleary, 2000) leading to a phosphatidylinositol 3-kinase (PI3K) (Purushothaman

et al., 2003)-dependent signaling cascade for cytoskeletal rearrangement and subsequent ingestion of streptococci (Dombek 1999). Similarly, in another model Sfbl is the main factor required for attachment and invasion using fibronectin as its bridging molecule and the alpha5beta1 integrin as cellular receptor. The mechanism of uptake in this model is characterized by the generation of large membrane invaginations at the bacteria-cell interface without evidence of actin recruitment or cellular injury (Molinari 2000).

The virulence factor Sfb1is not present in all invasive strains, like in the well characterized clinical isolate A8 strain (Molinari 2000). Alternatively, during transcellular invasion by A8, a proteinaceous moiety was described, which does not interact with alpha5beta1 or need any known bridging molecule. Bacterial attachment stimulates elongation and massive recruitment of neighboring microvilli, fusing to surround streptococcal chains, eventually engulfing the bacteria (Molinari 2000). Furthermore, not all integrin-mediated transcellular invasion necessarily requires a bridging molecule as shown by Caswell *et al*. in 2007 in their Scl1-dependent internalization model utilizing a M41 strain with HEp-2 epithelial cells. They were able to demonstrate direct interactions between the surface expressed Scl1 and the alpha2beta1 integrin that facilitated internalization (Caswell 2007).

With the evolution of presumably many routes to the interior of human epithelial cells, many question the limit to the transiency this otherwise extracellular

bacterium necessarily must exhibit in transcellular models. *Osterlund et al.* were able to move beyond *in vitro* observations of potentially a laboratory artifact by providing clinical evidence of streptococcal internalization. In their study, they reported the presence of viable intra- and extracellular streptococci on excised tonsil tissues using electron microscopy and immunohistochemistry. Convincingly, they found intracellular *S. pyogenes* in pharyngeal epithelial cells in 13 of 14 patients with tonsillitis (93%). Furthermore, intracellular *S. pyogenes* were found in macrophage-like cells in eight (73%) and in epithelial cells in four (36%) tonsils from 11 asymptomatic *S. pyogenes* carriers. This observation led to the expanding of the suggestion that the tonsil may contain an intracellular reservoir of *S. pyogenes* that mediates recurrent infection by evading non-penetrating antibiotics (Osterlund 1997, Cue 2000). Multiple groups have since contributed additional evidence towards a potential intracellular niche for the pathogen by demonstrating *S. pyogenes* intracellular survival for up to 7 days, *in vitro* across numerous immortalized human epithelial lines grown in an antibiotic supplemented medium. In some cases, the ability of viable *S. pyogenes* to be externalized and establish an extracellular infection has been assessed upon the removal of the extracellular antibiotic (Osterlund 1997).

As different GrAS strains may utillize differing mechanisms for epithelial internalization, different host cells also engage a range of intracellular pathways when infected by streptococci. Among the numerous factors suggested that may influence these pathways are the serotype(s) of the invading streptococci,

environmental stresses, input signals, and the mounted bacterial transcriptional response. To better understand the disparate mechanisms at play, several groups have investigated the intracellular pathways required for the uptake (or active invasion) process, from phenotypic (Pancholi 1997) (Wang 2006) (Nakagawa 2006) and global transcriptional perspectives (Argawal 2012) (Klenk 2007) of both the host and pathogen.

7.1.3 Potential Role of Autophagy

Nakagawa *et al* reported that intracellular *S. pyogenes* are initially visualized in HeLa cell endocytes and then readily escape via Streptolysin O (SLO) to gain a replicative niche in the cytoplasm. The process for bacteria escape from these endocytes subsequently stimulates autophagy, a fundamental cellular homeostatsis pathway in the intracellular degredation and recycling pathways. Nearly 80% of cytomplasmic streptococci eventually become trapped in autophagosome-like compartments as determined by fluorescence microscopy. These compartments then become degraded upon fusion with lysosomes lending the investigators to conclude that autophagy plays a protective role during streptococcal infection (Nakagawa 2004).

7.1.4 Host Cell Response to Invasion

On the epithelial side, Klenk and colleagues noted in HEp-2 cells 86 genes that were differentially transcribed following being co-cultured with a M49 GrAS strain including genes for cytoskeleton proteins, transcription factors and apoptosis-related factors (Klenk 2005). In addition, apoptosis was phenotypically observed in his and other studies following streptococcal invasion, albeit by different apoptosis mechanisms in an often serotype-dependent manner (Tsai 1999, Klenk 2005, Klenk 2007, Argawal 2012). If the epithelium has been transiently damaged by previous or ongoing microbial infection, then Streptococcal infectivity may gain direct access to tonsillar interior. Because of the close proximity of non-epithelial cell types to the tonsil surface and crypt epithelium (ie. lymphocyte follicles, fibroblasts, PMNs, and monocytes), apoptosis may assure the dissemination of released streptococci to interact in these associated invasive niches. Wang *et al* demonstrated that GrAS interactions with human primary tonsil fibroblasts stimulated an increase in TGF-Beta, which in turn was able to signal pharyngeal epithelium to upregulate the expression of alpha5-beta1 integrins at its surface *in vitro*. They then provided evidence for a proposed mechanism where increased alpha5-beta1 integrins on the epithelial monolayer leads to increased bacterial invasion when inoculated with GrAS through intracellular signaling (Wang 2006).

As presented in sections 5 and 6, we show that our representative throat specialist M type 1 *S. pyogenes* strain demonstrates a significantly divergent invasiveness phenotypes based on anatomic origin of epithelial cell. As has been established in the literature, internalization and intracellular fate depends on serotype and potentially tissue-type distinctions. In order to better understand the implications of the intracellular GrAS phenotype, in the context of our study, strain SF370 was co-cultured with three of our human epithelial cell lines (Detroit 562, UT-SCC-60A, and UT-SCC-60B). After permitting the pathogen to adhere and become internalized by the host cells we employ novel methods to prohibit bacteria re-emergence. Additionally, immunofluorescence microscopy provides us with preliminary data as the ground work for future studies investigating intracellular mechanisms underlying intracellular GrAS survival.

7.2 Results

7.2.1 Streptococcal viability following internalization may be epithelial cell type-dependent

We employed a novel strategy for maintaining an intracellular bacterial population following co-culture with human oral epithelial monolayers as described in the Methods. Two anti-reemergence PlyC solutions (with- or without Tannic Acid [T.A.]) were applied to monolayers and viability of intracellular bacteria was assessed at times points over the course of 24 hrs. Our initial time point (T_0), represented the baseline number of internalized bacteria for each monolayer, based on the number of bacteria internalized following the start of the 2.5h co-culture. Consistent with what has been demonstrated in earlier chapters, our representative M type 1 strain of GrAS was preferentially internalized by the UT-SCC-60B epithelial monolayer ($p < 0.0001$). Following 2 h of selective anti-reemergence pressure, the enumeration of total recovered intracellular GrAS from the tonsil-derived epithelial monolayers revealed an increase by nearly 6X that of the baseline recovered amount, irrespective of T.A. treatment. The number of bacteria recovered from the Detroit 562 monolayers only increased an insignificant amount in the T.A treated wells and decreased in the PlyC-only treated wells (Figure7.1). The number of viable bacteria declined significantly by the 16h post-infection time point (T_{16}). At this time, the number of bacteria recovered from the UT-SCC-60B monolayer had returned to near its baseline, maintaining this level of intracellular viability up to 24 h post infection. During this

same time, our ability to recover viable bacteria was just barely above undetectable.

Figure 7.1. *S. pyogenes* intracellular viability is cell type dependent

M type 1 strain SF370 in serum-free DMEM (~1x 10^8 CFU) was co-cultured with UT-SCC-60B and *B*) Detroit 562 epithelial cell monolayers for 120 min at 37ºC. Associated bacteria were removed by vigorous washing with PBS and subsequently treated with antiamidase lysin PlyC (0.05U / well) only *(solid* bars) -or- PlyC with the exocytosis inhibiting agent, Tannic Acid (*striped* bars) as described in Methods. T_x= Xhrs post initiation of PlyC selective pressure against bacterial reemergence. Data presented is from a representative experiment of duplicate wells plated in triplicate. Difference between Detroit 562 and UT-SCC-60B cell types at every (condition-matched) time point is highly significant ($p < 0.000$) as determined by student t-test.

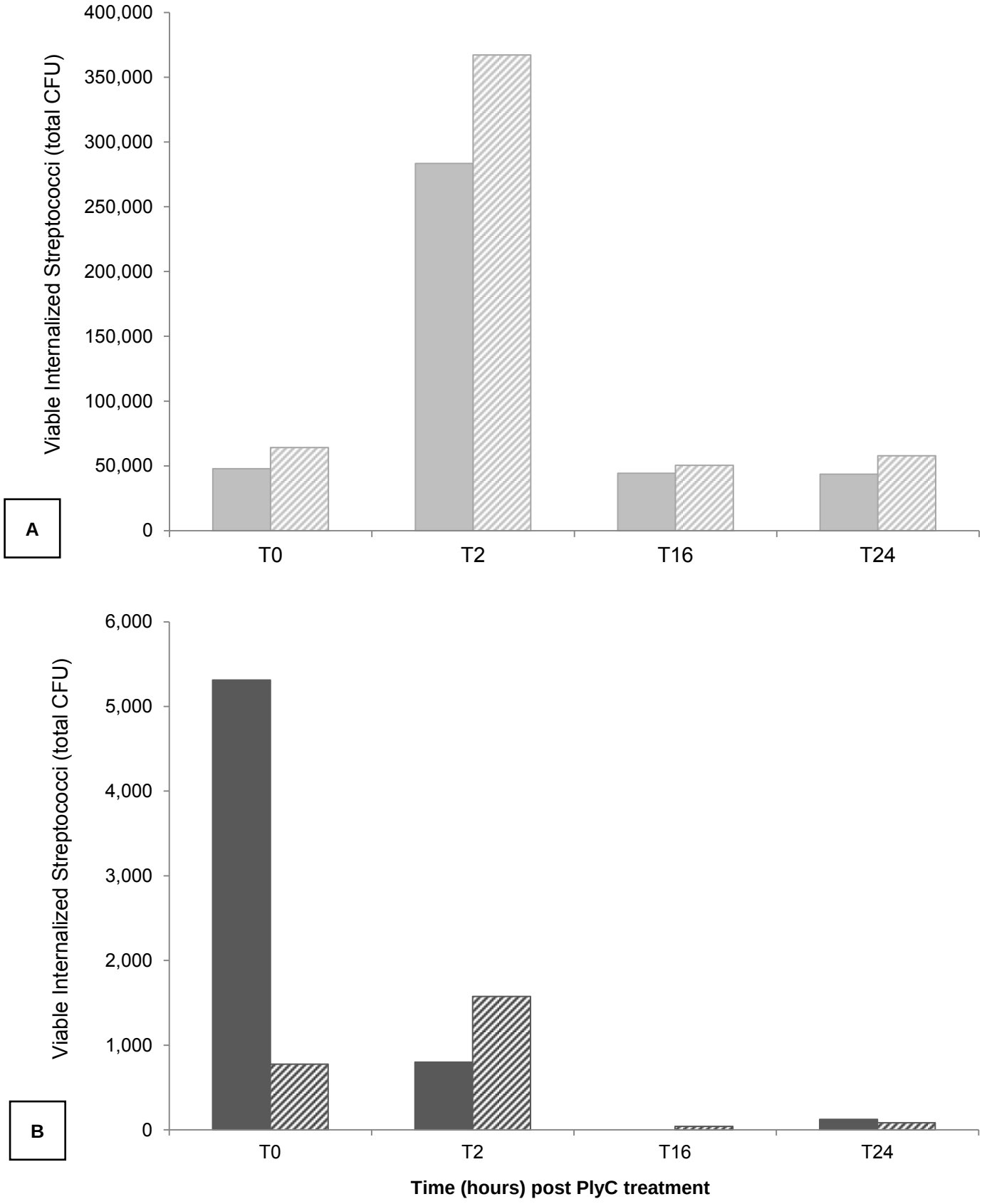
A
Viable Internalized Streptococci (total CFU)
400,000
350,000
300,000
250,000
200,000
150,000
100,000
50,000
0
T0
T2
T16
T24
B
Viable Internalized Streptococci (total CFU)
6,000
5,000
4,000
3,000
2,000
1,000
0
T0
T2
T16
T24
Time (hours) post PlyC treatment

7.2.2 *Intracellular Compartment of internalized Streptococci*

Increased internalization is likely of no benefit to the pathogen if they are immediately destined to be cleared by the activities of lysosome-mediated degradation or similarly deleterious intracellular pathways. Our experiments demonstrate GrAS increased adherence and internalization capacity during co-culture with tonsil-derived epithelium. To gain an appreciation for the fate of internalized streptococci in our tonsil tumor epithelial cell system, we performed microscopy-based co-localization studies using markers from known pathways implicated in streptococcal intracellular persistence in non-phagocytic cells. We focused principally on the UT-SCC-60 A and UT-SCC-60B epithelial cells in light of the pronounced sustained intracellular viability as compared to Detroit 562 cells (Figure 7.1).

As many of the integrin-mediated mechanisms proposed as routes for GrAS intracellular entry, ultimately enter bring the bacterium into the cell's endocytic pathway, we first sought to identify whether the bacteria was found along vesicles associated with this process. Early endosomes are the first location within the endocytic pathway and is likely to reflect recently endocytosed debris and microorganisms. Consistent with this mode of transcellular entry, we consistently observed *S. pyogenes* in association with clustered groups of vesicles staining positively for the Early Endosome Antigen 1 (EEA1) (Figure

7.2A). We were also able to find GrAS co-localized within these vacuoles providing evidence suggestive that intracellular *S. pyogenes* within the UT-SCC-60A and UT-SCC-60B epithelium at least in part are engaged with this process.

Nakagawa *et al* have proposed that GrAS escape from endosomes into the epithelial cell cytoplasm, which stimulates autophagy. They've gone on to show that intracellular *S. pyogenes* is captured by LC3-positive autophagosome-like vacuoles and degraded upon fusion of these compartments with lysosomes in HeLa cells (Nakagawa 2004). Using LC3 as an important marker for autophagy, we observed apparent co-localization of SF370 with LC3-positive vesicles with relatively similar frequency of distribution across the cell as was seen with the early endosomes (Figure 7.3).

Figure 7.2 *S. pyogenes* co-localizes with Early Endosomes at 2.5h post infection. Fluorescence micrographs of GrAS-associated Early Endosomes in UT-SCC-60A epithelial monolayers following co-culture with strain SF370. Extracellular bacteria were removed by antibiotic and lysin treatment. Monolayers were fixed, permeabolized and stained as described in Methods. DNA was labeled with DAPI unless otherwise noted. A*)* Early Endosome are visualized by anti-Early Endosome Antigen-1 (EEA1)-FITC mAb (green). *B) S. pyogenes* was labeled with PlyCB-Alexa 554. *C-D)* White arrow indicates *S. pyogenes* co-localizes with EEA1-positive compartment. Images taken originally at 40X. White box demarcates the area digitally magnified x10 in *D*)

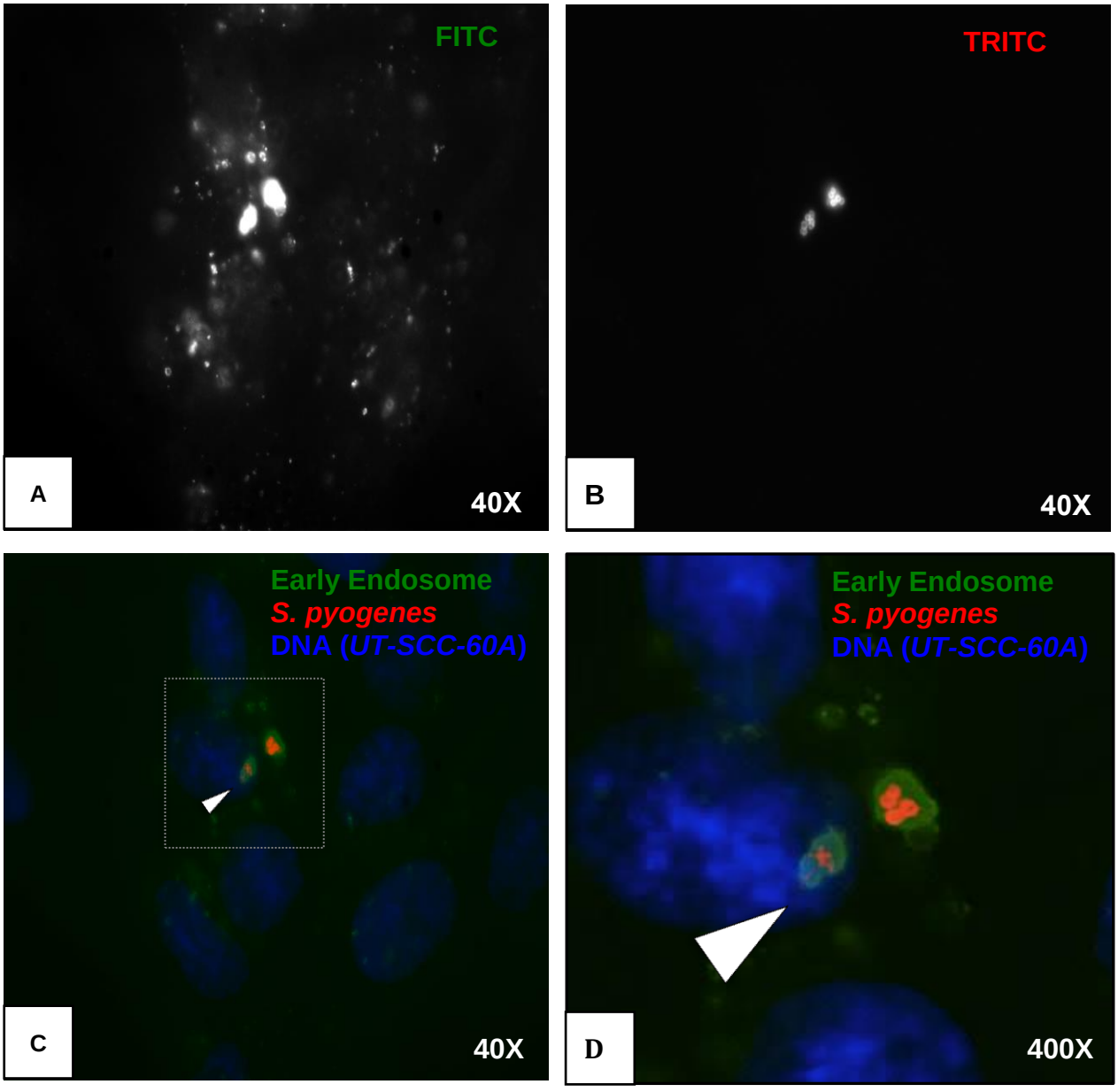
FITC
A
40X
TRITC
B
40X
Early Endosome
S. pyogenes
DNA (UT-SCC-60A)
C
40X
Early Endosome
S. pyogenes
DNA (UT-SCC-60A)
D
400X

Figure 7.3 *S. pyogenes* also co-localizes with Autophagosome marker at 2.5h post infection.

Fluorescence micrographs of LC3 distribution (green) in UT-SCC-60B epithelial monolayers following co-cultured with strain SF370. Extracellular bacteria were removed by antibiotic and lysin treatment. Monolayers were fixed, permeabolized and stained as described in Methods. DNA was labeled with DAPI unless otherwise noted. *A).* LC3-positive vacuoles were visualized using α-LC3-FITC mAb (green). *B.) S. pyogenes* was labeled with PlyCB-Alexa 554(red). *C-D.)* White arrow indicates *S. pyogenes* colocalizes with LC3-positive compartment. *E.* Early Endosomes were visualized by anti-Early Endosome Antigen-1 (EEA-1)-FITC mAb (green). Images taken originally at 40X. White box demarcates the area digitally magnified x7 in *D*).

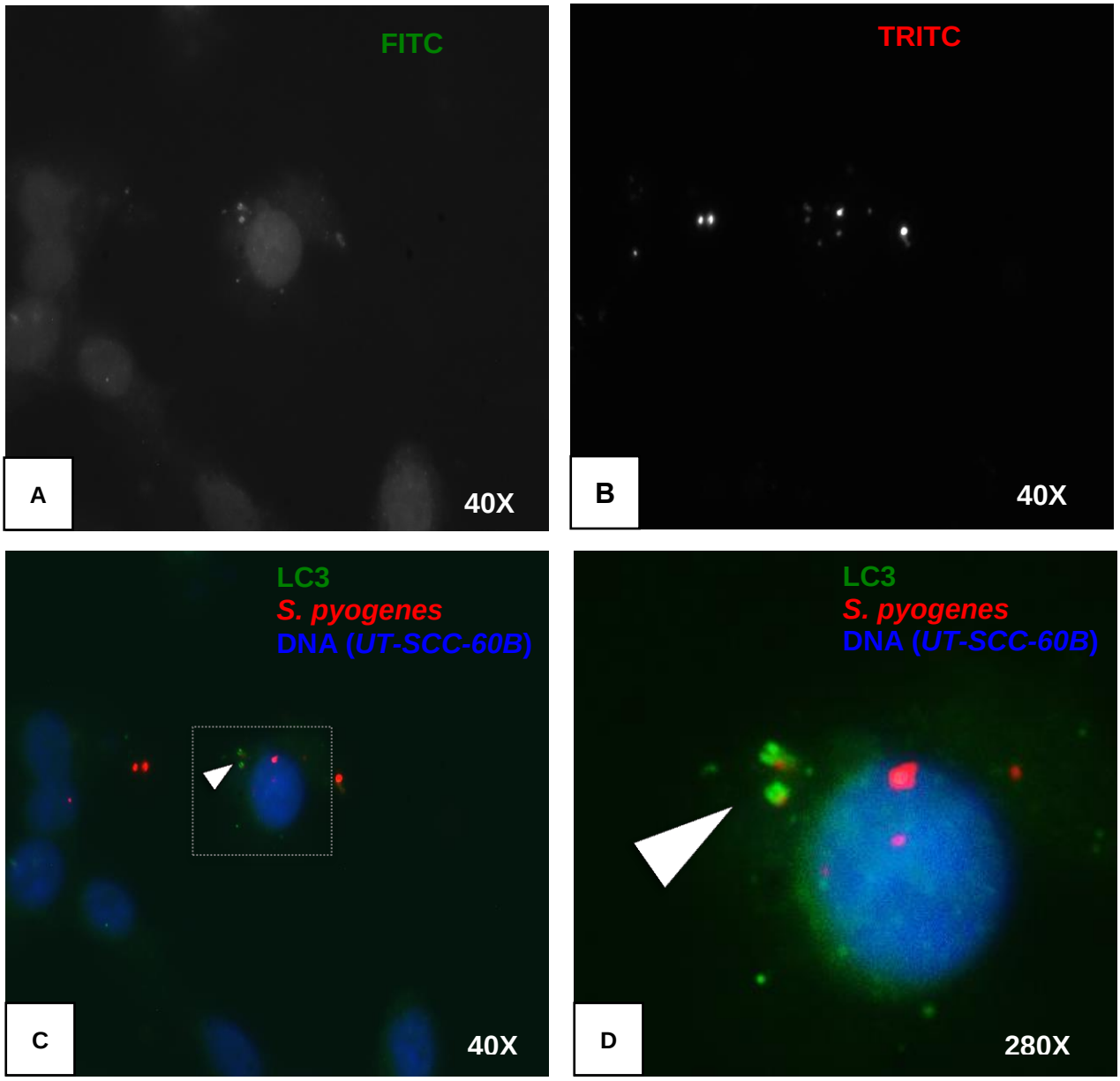
FITC
A
40X
TRITC
B
40X
LC3
S. pyogenes
DNA (UT-SCC-60B)
C
40X
LC3
S. pyogenes
DNA (UT-SCC-60B)
D
280X

7.3 Discussion:

Depending on the *S. pyogenes* strain, the bacteria are killed within the vacuole, survive in a resting or even multiplying state, or leave the early phagocytic vacuole towards the cytosol, where they again either rest or multiply (Kreikemeyer 2004). In our study, once the *S. pyogenes* are internalized, they often remained viable and continued multiplying during the initial hours following invasion, possibly indicative of an amenable intracellular replicative niche. While GrAS that were internalized by UT-SCC-60B cells continued growing most markedly, we later saw an equally marked drop, likely demonstrative of some intracellular killing process. Importantly, however, we note sustained viability of internalized bacteria was evident in our tonsil-derived epithelial system for at least 24hrs.

The intracellular status of GrAS could protect the bacteria from antibiotics and host defense mechanisms. It appears to be a prerequisite for GrAS persistence in host tissues, which in the case of tonsillar epithelium leads to recurrent infections or an asymptomatic carrier status. As patients with persistent GrAS are the only source for GrAS transmission in non-epidemic settings continued exploration of the underlying mechanisms of GrAS adherence and internalization processes may inform our strategies to address moving forward to effectively interfere with these processes.

We also report here our use of PlyC in suspension with minimal media to provide the selective pressure against streptococcal reemerge from an otherwise

transient intracellular niche. This transiency is a necessary final requirement of the proposed theory for an intracellular sanctuary, or reservoir, as a cause for recurring infection. The classic experimental set up for measuring intracellular viability continuously exposes the epithelial monolayer with antibiotic solutions (Osterlund 1995, Marouni 2004). These experiments, however, may not account for bacterial recalcitrance due to microcolony and / or biofilm formation (Marnetti 2007). We have shown in earlier studies the ability for PlyC to effectively sterilize the monolayer surface as confirmed by microscopy (*see* section 5). Numerous studies have supported the sterilizing capacity of PlyC against streptococcus spp providing significant support for the effectiveness of this narrow spectrum agent for a broad range of uses. To our knowledge, this is the first reported use of the phage lysin, PlyC (Fischetti 1971), for the purpose of applying a selective pressure against reemerging pathogens to investigate intracellular viability.

§8.0 CONCLUSIONS

This study has extended our lab's continued work on the transcription shifts observable in *S. pyogenes* from initial contact with host factors in suspension (conditioned media), to transient contact / association with neighboring epithelial cells (Detroit 562), to transient contact / association with palatine tonsil epithelium (UT-SCC-60B), to adherence with nasopharyngeal (Detroit 562) surface. It is clear that *in vivo*, the GrAS must experience adaptive transcriptional changes at every step of infection as shown convinsingly by our model. The bacteria may also adhere to non-tonsil tissues in the pharynx, particularly during asymptomatic carriage of the pathogen in the nasopharynx. While we have discovered numerous unique qualities that may be unique to the stage of infection modeled, improvements in models and annotation will only provide us the opportunity to ask even more precise questions. As there currently doesn't exist a deposited tonsil cell line availbale through AT-CCL, our new UT-SCC-60A and UT-SCC-60B tonsil epithelial model has been shown to be an affective surrogate for the more precious HPTE cells, mirroring effects during our *in vitro* experiments performed in parallel. We believe these tools will prove helpful to study this uniquely human disease process that is otherwise difficult to study in unnatural host animal models or otherwise poorly representative tissue lines.

APPENDIX

APPENDIX4.1. Immunofluorescence (IF) staining for epithelial and fibroblast markers

Confocal microscopy images of cultured Detroit 562, UT-SCC-60A, UT-SCC-60B and Human Primary Tonsil Epithelial Cell (HPTEC) monolayers labeled with a mouse or rabbit antibody against keratins k8/18 (A, B), k19 (not shown), pankeratin (C,D), and vimentin (not shown). Secondary Alexa558-labeled goat antibody against either mouse or rabbit was applied for visualization by fluorescence.

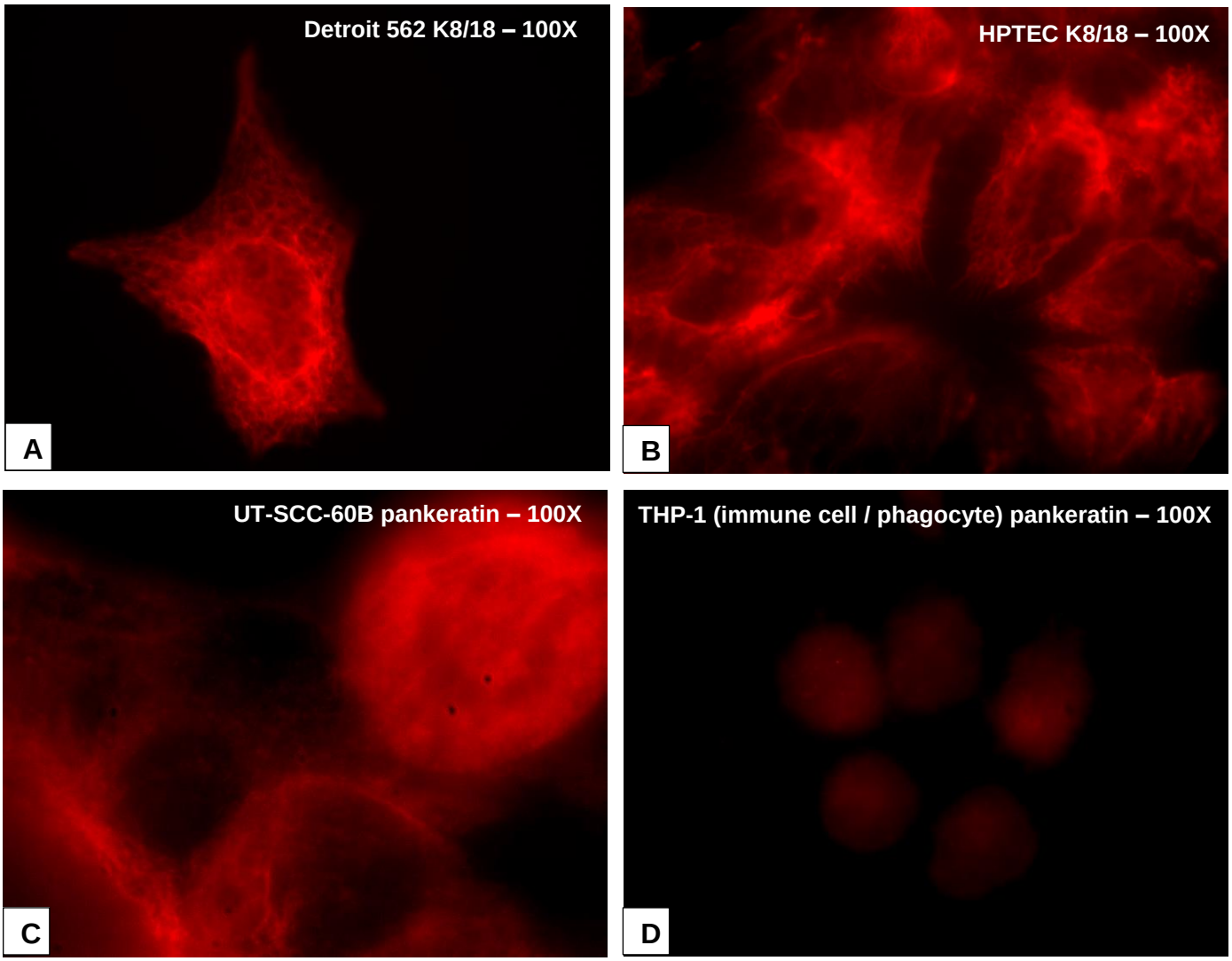
Detroit 562 K8/18 – 100X
A
HPTEC K8/18 – 100X
B
UT-SCC-60B pankeratin – 100X
C
THP-1 (immune cell / phagocyte) pankeratin – 100X
D

Appendix 6.1 Dye swap microarray between streptococci "associated" with Detroit 562 (nasopharyngeal) or UT-SCC-60B (palatine-tonsil) epithelial monolayers *Eight biological replicate experiments incorporating dye swaps [17] were performed to account for both biological and technical variability. Fluorophore-labeled c*DNA samples were hybridized to custom arrays *and scanned with an Agilent High-Resolution C Microarray Scanner at 5 μm per pixel resolution. The resulting images were processed using the GenePix Pro program. Panel (A) represents "standard" arrays with cDNA from GrAS associated with Detroit 562 is labeled with Cy3, while cDNA from GrAS associated with UT-SCC-60B is labeled with Cy5. Panel (B) is the opposite dye confirmation.*

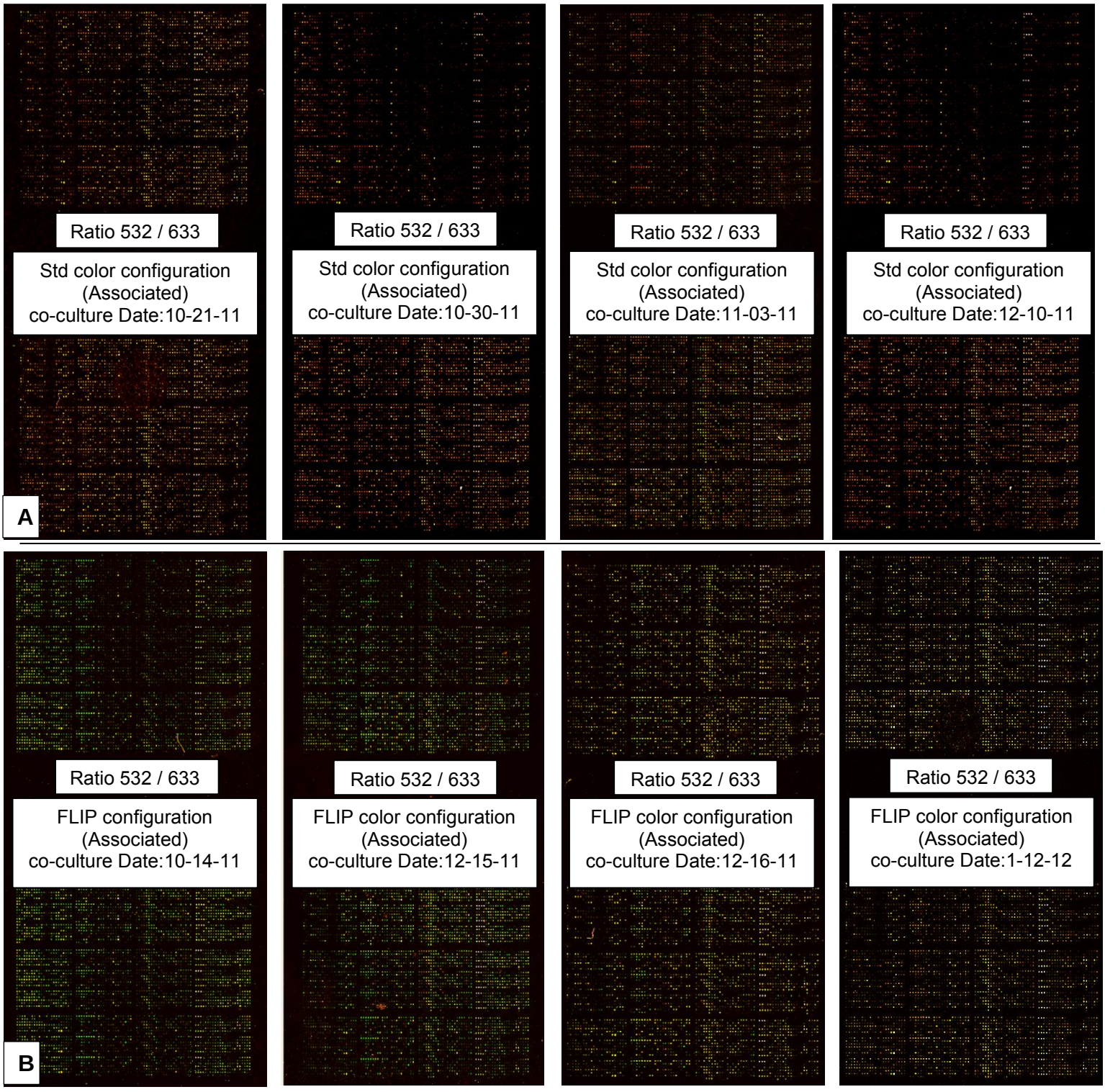
Ratio 532 / 633
Std color configuration
(Associated)
co-culture Date:10-21-11
Ratio 532 / 633
Std color configuration
(Associated)
co-culture Date:10-30-11
Ratio 532 / 633
Std color configuration
(Associated)
co-culture Date:11-03-11
Ratio 532 / 633
Std color configuration
(Associated)
co-culture Date:12-10-11
A
Ratio 532 / 633
FLIP configuration
(Associated)
co-culture Date:10-14-11
Ratio 532 / 633
FLIP color configuration
(Associated)
co-culture Date:12-15-11
Ratio 532 / 633
FLIP color configuration
(Associated)
co-culture Date:12-16-11
Ratio 532 / 633
FLIP color configuration
(Associated)
co-culture Date:1-12-12
B

§A8. *Supplementary Chapter.* IDENTIFYING STREPTOCOCCAL BINDING PARTNERS WITH HUMAN ORAL EPITHELIUM

A8.1 Introduction

The interactions between group A streptococcus with its human host has been extensively studied. In 2000, Cunningham reviewed at least 11 streptococcal adhesins and potential virulence factors that have been shown to bind host cell receptors in some direct fashion. Bacterial lipoteichoic acid (LTA), an amphipathic molecule, appears to account for approximately 60% of adhesion to epithelial cells via electrostatic interactions with positively charged host extracellular matrix components such as fibronectin (Hasty 1996, Cunningham 2000). Hasty and Courtney initially describes the action of LTA as the first step in their proposed 2-step model for streptococcal adherence. By this same model, it follows that the remaining 40% of the adhesion process is left to commence following LTA-mediated attachment, likely conferring receptor specificity with greater avidity. Their theory hinges on the idea of adhesin-host multiplicity where this interaction would require that multiple binding partners be engaged working in concert to promote GrAS adherence to the epithelial surface. Hasty and Courtney's two step mechanism may in part explain the ability for GrAS to interact and possibly attach to numerous cell types *in vitro*, at times in lieu of natural anatomic relevance to the bacterium.

Several extracellular host cell proteins have been implicated in as the pathogen's receptors or surface moiety principally involved in conferring specific attachment

and / or internalization by group A streptococci including: fibronectin, fibrinogen, collagen, vitronectin, a fucosylated glycoprotein, and integral membrane proteins including CD46, the membrane cofactor protein on keratinocytes, and CD44, the hyaluronate- binding receptor on keratinocytes. While it is undisputed by the evidenced presented to argue the case for these numerous adhesins playing significant roles in GrAS adherence in the respective models tested, deciphering relative significance for site specific pathogenesis remains a challenge for researchers to rectify.

Questions surrounding the contextual significance of one receptor/ligand pair over another have resulted in much contention in the field regarding definitive mechanisms. For example, the importance of CD46 as a cellular receptor for group A streptococci is uncertain. While CD46 binds M protein through factor H-like repeats, transfection of L cells with cDNA encoding human CD46 failed to increase binding of group A streptococci (Abbot 2007). Additionally, Abbot *et al*., recently confirmed that tonsil epithelium was replete with CD44 receptors (Abbot 2007), described by Cunningham to be the host receptor for the hyaluronic acid capsule of *S. pyogenes*. Abbot's group, however, noted that a ΔhasA capsule deficient SF370 strain did not alter adherence capabilities in their *ex vivo* tonsil system contradicting the relative importance of this described hyaluronic capsule – CD44 interaction as significant towards explaining the enhanced adherence phenotype seen clinically and *in vitro* towards the surface of the palatine tonsil.

We have described in previous chapters observations that demonstrate

significantly different adherence and invasion phenotypes by M type 1 GrAS strain SF370 during co-culture with nasopharyngeal and tonsil epithelium. Notably, the streptococcal adherence efficiency to our palatine tonsil derived tumor lines was statistically indistinguishable from human primary tonsil epithelium. Although purely circumstantial, we may speculate from these observations the possibility of retained similar surface topographies between our primary and tumor tonsil cell lines. Therefore, our UT-SCC-60A, UT-SCC-60B and HPTE cell cultures may provide contextually-applicable epithelial sources that may augment and facilitate the discovery of novel receptors earlier investigators missed due to sample limitations when exploring whole tonsil tissues or intrinsic inadequacies of the existing non-palatine tonsil cell *in vitro* models. Our described experimental findings from relevant tissue-specific association and adherence may also allow us to prioritize such exploration by key receptor-ligand pairs consistent with the gene expression profile during association at the tonsil surface.

To better understand the implications of our previous results, we have begun studies to describe host-pathogen interaction. Preliminarily, we sought to test our ability to identify the corresponding protein binding partner(s) between our tumor cell lines and a known streptococcal surface adhesins. We hypothesize that streptococci likely interact with unique surface proteins on UT-SCC-60B as compared to Detroit 562 cells, which may account for observed differences in adherence. This chapter provides our preliminary results, and introduces our data-informed future plans for additional screens to elucidate the cellular basis of

tonsil tissue tropism.

A8.2 Results

A*8.2.1 Identification of epithelial cell wall proteins that bind recombinant group A streptococcal M6 protein*

Our earlier described studies have consistently demonstrated that *Streptococcus pyogenes* M type 1 strain SF370 adhere to tonsil epithelial cells with greater efficiency than the Detroit 562 nasopharyngeal cell type. Due to the novelty of using UT-SCC-60A and UT-SCC-60B cells to model streptococcal pharyngotonsillitis, however, their cell surface receptor distribution remains largely uncharacterized in the context of any host-pathogen interaction. As a means to determine similarities between these tonsil tumor cell lines and the otherwise well characterized Detroit 562 cell line, we decided to test a GrAS adhesin known to have multiple defined epitopes on epithelial cells. Possibly the quintessential classic determinant of streptococcal virulence, M protein has been extensively studied by our lab and others as an important adhesion and invasion during streptococcal colonization of epithelial cells. Previous studies on the mechanism of M protein adherence have been conducted over the decades across numerous cell types yielding a cadre of putative receptors (Cunningham 2000, Nobbs 2009). Our lab recently highlighted the ability of recombinant M type 6 (rM6) protein to bind glucosaminoglycans (GAGs) and sialic acid containing cell surface proteins (Ryan 2001) during Detroit 562 epithelial cell adherence. Similar

to M type 1 strain SF370, the M type 6 is a member of the emm type pattern A-C described as a throat tropic.

Based on our expansive experience with M protein and the availability of purified recombinant protein material, we used M type 6 protein our initial probe (or “bait”) protein to perform comparative co-immunoprecipitation experiments. These studies would determine whether different “M6 protein – human epithelial receptor” complexes might be distinguishable between epithelial cell membrane associated proteins from nasopharyngeal and palatine tonsil cells.

Prior to the co-immunoprecipitation, we conducted preliminary co-culturing experiments using M type 6 strain D471 and the M6 isogenic knockout strain JRS75 respectively with Detroit 562, and UT-SCC-60B epithelial cell monolayers. As had been shown previously by our group and others, during co-culture with Detroit 562 cells, adherence was drastically diminished in the isogenic M6 protein knockout strain versus the wild type D471 strain. The adherence to the UT-SCC-60B was similarly decreased in the absence of M protein although variability between independent experimental replicates in the wild type will necessitate that repeat experiments be performed to assess statistical significance (data not shown).

Our co-immunoprecipitation experiments were performed as detailed in the methods. Briefly, recombinant M type 6 (rM6) protein was incubated with

epithelial surface proteins in mixed suspension from each respective cell line to encourage potential protein-protein interactions and identify natural binding partners. Protein complexes were captured by the 10.B6 mAb (α -M protein) bound to packed protein G beads. After washing away unbound proteins, rM6 protein with accompanying complexes were eluted from the protein G beads, and analyzed by SDS-PAGE.

We observed two unique protein bands at 30kD and 80kD, respectively, putatively representing components of complexes between Detroit 562 surface proteins and the streptococcal rM6 protein (Figure 8.1). These bands have yet to be analyzed by mass spectrometry for protein identification. Based solely on the molecular weights, however, these bands may indeed prove to be novel M protein binding partners as their weights are inconsistent with some of the known M protein ligands including: filamentous actin (MW = 42kD); CD46 (MW = 56 – 66 kD); and the fibronectin (MW = 240kD)- $\alpha_5\beta_1$ integrin (MW > 115kD) complex. This list of M protein receptors is not meant to be exhaustive (see Table 1.2), however, and final confirmation of identity will need to be performed by more rigorous LC-MS/MS analysis.

It may be significant that bands from known M protein binding partners were not evident following SDS-PAGE analysis. Based on the literature, it is evident that more M protein – host interactions with the Detroit 562 cells would be expected than what we observed following our co-immunoprecipitations. Notably, the UT-

SCC-60B cell surface proteins did not elute with any observable proteins in complex with the rM6 protein. We recognize a number of technical considerations that may account for these results. One observation is the low concentration of epithelial cell membrane associated proteins and rM6 protein in flow through / wash lanes 5 and 8 (Figure 8.1). Additionally, it is unclear whether there is observable rM6 protein in our eluted lanes (4 and 7), as the band at ~50 kDa may be the degraded heavy chain portion of our mAb, 10B6. Since we only used coomasie to visualize our bands, there is the possibility that we were unable to see fainter bands more readily observable following silver staining. In future iterations of this experiment, we may add more epithelial cell proteins as well as rM6 protein into our initial suspension to promote more interactions and potentially stronger banding patters. We may also consider a more stringent elution buffer or procedure to confirm our bound complexes do not remain in the column.

Our co-immunoprecipitation, though preliminary, would qualify as the first time the UT-SCC-60B cell line has been probed for M protein binding potential and may reflect something novel about their surface topography. We also note, however, that recombinant M type 1 protein may yield a more impressive yield of protein – protein complexes.

Figure A8.1. Identification of binding complexes between epithelial cell membrane-associated proteins (CMAP) and recombinant M6 protein. Detroit 562 and UT-SCC-60B human epithelial CMAPs were placed in suspension with recombinant M6 protein. Protein-protein complexes were then affinity purified using a μMACS^{TM} protein G MicroBeads column conjugated to 10.B6 (α-M protein) mAb. M protein-CMAP complexes were resolved by SDS-PAGE and stained with 0.1% (w/v Coomasie). *Lane 1)* Bands at 75, 100, 150, and 250kDa determined to be "carryover" dye from MW ladder. *Lane 4*) Green arrow: putative D562 – rM6 complex #1, White arrow: suspected rM6 +/- 10.B6 mAb heavy chain, Red arrow: putative D562 – rM6 complex #2, Blue arrow: suspected 10.B6 mAb light chain.

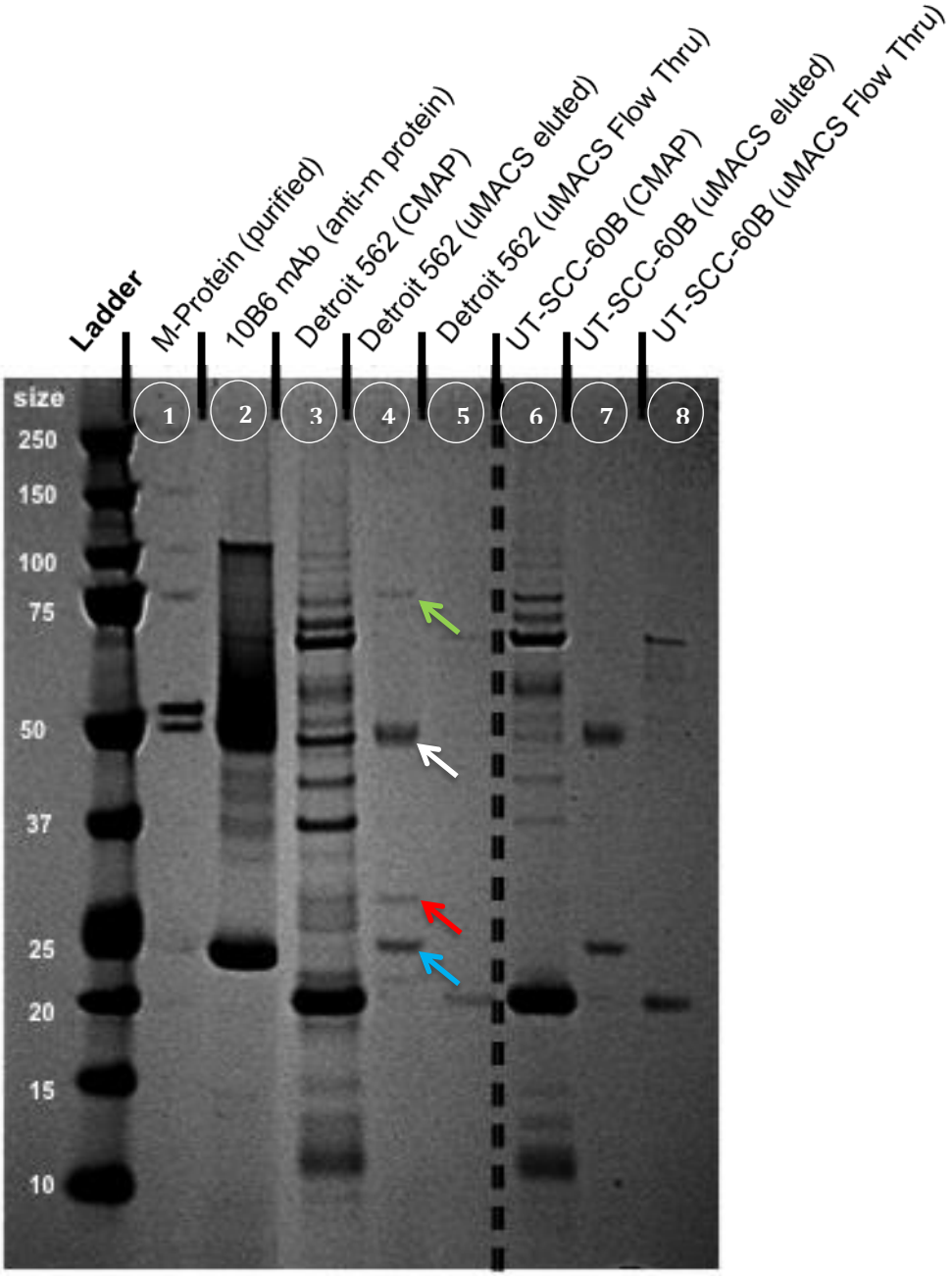
Ladder
M-Protein (purified)
10B6 mAb (anti-m protein)
Detroit 562 (CMAP)
Detroit 562 (uMACS eluted)
Detroit 562 (uMACS Flow Thru)
UT-SCC-60B (CMAP)
UT-SCC-60B (uMACS eluted)
UT-SCC-60B (uMACS Flow Thru)
size
250
150
100
75
50
37
25
20
15
10
1
2
3
4
5
6
7
8

A*8.2.2 Click Chemistry metabolically labels newly synthesized streptococcal proteins*

We have reported on comparative genomic and mutagenesis studies to revela bacterial genes that are important for infection, but their precise biochemical mechanisms and temporal expression patterns are difficult to measure or truly speculate as a result of posttranslational regulation. Direct biochemical analysis of bacterial proteomes during infection may be a useful measure to elucidate these mechanisms informed by microarray transcriptome analysis. New strategies for selectively enriched bacterial proteins from host proteomes during infection have recently been described, including the use of non-natural amino acids to distinguish bacterial proteins from the host. (Grammel 2010).

For example, Azide functionalized methionine surrogate, Azidohomoalanine (AHA) (Fiigure 8.2*A*) has been shown to be incorporated into the bacterial proteome by endogenously expressed methionyl-tRNA synthetase (MetRS) in *Escherichia coli*. The azide group is able to survive cellular metabolism and remains available to be subsequently reacted with a secondary reporter such as Alkyne-Rhodamine (Alk-Rho) detection tag by Cu1-catalyzed Azide-Alkyne Cycloaddition, also called “Click Chemistry”. This selective tagging can occur in mixed bacteria-host lysate solution and resolved by SDS-PAGE and in-gel fluorescence scanning.

To our knowledge, the ability of the streptococcal endogenous translational apparatus to incorporate alkyne- / azide-functionalized non-natural amino acids has yet to be tested. Additionally, the subsequent use of Click Chemistry to selectively label bacterial proteins during infective processes has yet be exploited for the study of streptococcal virulence.

As our first step towards utilizing these new tools, we successfully demonstrated *S. pyogenes* incorporation of Azidohomoalanine (AHA) (Figure 8.2). In our initial experiments, we added unlabeled streptococcal cell wall protein in excess to a well and resolved the band using SDS-PAGE. Previous investigators have reported levels of autofluorescence as a source of background signal and confounding noise during in-gel fluorescence analysis post Click Chemistry reactions. Similar to these previous reports, we also observed faint autofluorescence at 580nm, although the observed background remained distinguishable from AHA + Alk-Rho labeled samples (Figure 8.3*C*). Significantly, we also note that low expressing proteins that proved difficult to visualize by normal coomasie stain may be better analyzed with metabolic labeling and in-gel fluorescence (Figure 8*C*).

Figure A8.2. In-Gel Fluorescence distinguishes metabolically labeled Streptococcal proteins using Click Chemistry. *A*) Structures of methionine (Met) and azidohomoalanine (AHA). *S. pyogenes*.was cultured in THY media to late log phase, and then diluted into methionine-free minimal media supplemented with AHA. Protein Bacteria were lysed and extracted cell wall fractions were either (*B*) directly resolved by SDS-PAGE or (*C*) reacted with the clickable fluorophore Alkyne-Rhodamine (Alk-Rho) via Cu^{1}-catalyzed azide-alkyne cycloaddition ("Click Chemistry") immediately before resolving on SDS-PAGE. Resulting gels were visualized with 1% (w/v) Coomasie stain (CM) or by In-Gel fluorescence scan (Fluor) at 580nm. AHA/Alk-Rho samples were compared to normal treated samples.

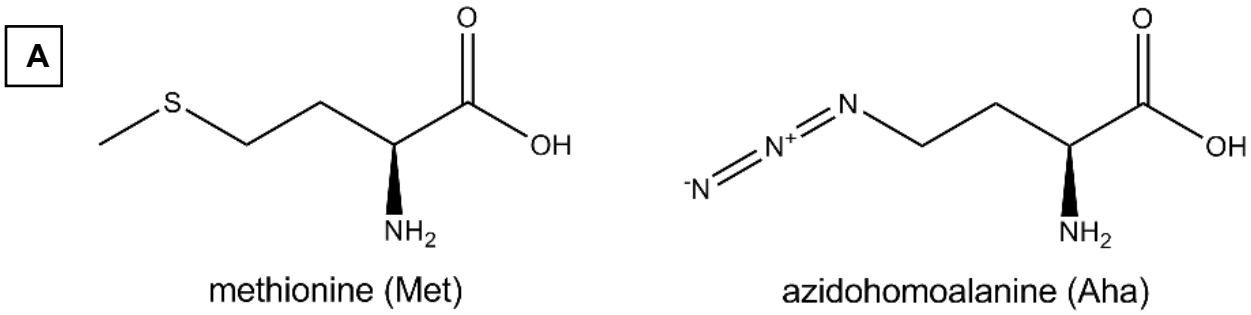
A
O
S
OH
NH2
methionine (Met)
O
N
N+
-N
OH
NH2
azidohomoalanine (Aha)

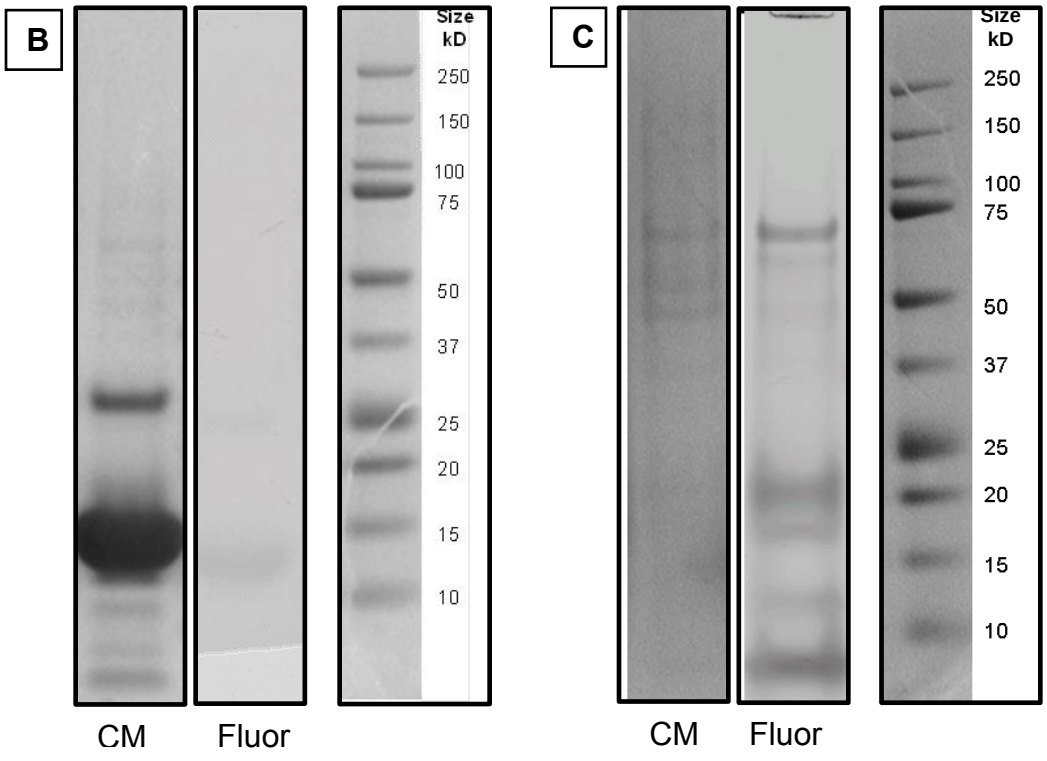
B
Size kD
250
150
100
75
50
37
25
20
15
10
CM
Fluor
C
Size kD
250
150
100
75
50
37
25
20
15
10
CM
Fluor

A8.3 Discussion

Most of our current methods to determine protein-protein interactions between host and pathogens, including our co-immunoprecipitation, require that one of the proteins in the pair be a known entity. This has limited the field to consider the current scope of known adhesins when searching for binding partners. Numerous reports have demonstrated that M protein binds multiple eukaryotic proteins in human serum and on macrophages, fibroblasts, and keratinocytes. Our preliminary search for unique interactions between tonsil cell surface proteins only captured identifiable interactions with the Detroit 562 cell line. Additional analysis of the two resulting bands on SDS-PAGE may offer insight on differences in streptococcal interactions between these neighboring epithelial surfaces, although this remains to be determined. Moving forward, however, we plan to modify our exploratory search in a more directed manner informed by our microarray and adherence phenotype data.

One area of immediate intended focus is on establishing tissue-specific roles for the components of the highly upregulated operon Spy0127 – Spy130. Our co-culture phenotype and transcriptional expression data support that pili are important during GrAS strain SF370 association with –, adherence to –, and invasion of – tonsil epithelial cells. Recently reported adherence studies using purified recombinant *S. pyogenes* pilus ancillary proteins encoded by Spy0125 (rSpy0125) and Spy0130 (rSpy0130) have shown that both of these SF370 pili subunits bind Detroit 562 (Manetti 2007) and HaCaT cell lines as well as intact

human tonsil epithelium (Smith 2010). Smith *et al* subsequently assigned subunit Spy0125 as the principle pili adhesin based on the ability for anti-rSpy1025 sera to inhibit adherence to tonsil epithelium (Smith 2010). Their report was unable to determine pili – host epithelial binding partners, leaving the exact mechanism for their observed adherence properties yet to be described. We would like to use these recombinant pili subunits, rSpy1025 and rSpy0130, and corresponding anti-sera to repeat co-immunoprecipitation and immobilized ligand assays comparing binding partners from UT-SCC-60A, UT-SCC-60B, HPTE, and Detroit 562 cell lysates.

As our M protein experiments may reveal, there may be tissue-specific or even bacterial –serotype differences in the engagement of particular bacterial adhesion-surface receptor complexes. This idea may be supported by Bessen *et al'*s recent characterization of throat tropic members of the emm pattern types A-C. The heterogeneity of genes imply horizontal gene transfers and mutations account for a convergence of adaptation for this oral niches, quite possibly by numerous mechanisms (Bessen 2011).

Though not fruitful as of yet, metabolically labeled proteins able to be visualized through Click Chemistry is a safe means of tagging epithelial proteins for experiments that are less linked to identifying the protein of interest at the onset. Our lab has recently attempted mixing epithelial cell membrane associated proteins with metabolically labeled, Mitomycin C-killed, intact bacteria in a suspension that encourages naturally-occurring protein-protein complexes to

form. Using the same principles of our earlier co-imunoprecipitation column, this has allowed for an unbiased approach to identifying binding partners (not shown). We may consider pre-incubating the bacteria in tonsil-conditioned media to assure expression of relevant surface proteins likely present within the intended tonsil niche. While elution methods may have so far presented a challenge in capturing all host-pathogen complexes formed during co-immunoprecipitation, crosslinking receptor-bound complexes using DTSSP (3,3´-dithiobis[sulfosuccinimidylpropionate]), as well as using Click Chemistry may provide us stronger results in the future.

§9.0 REFERENCES

Abbot EL, Smith WD, Siou GPS, Chiriboga C, Smith RJ, Wilson JA, Hirst BH, Kehoe MA. (2007). Pili mediate specific adhesion of *Streptococcus pyogenes* to human tonsil and skin, *Cellular Micro* 9 (7):1822–1833

Aziz RK, Kansal R, Aronow BJ, Taylor WL, Rowe SL, et al. (2010) Microevolution of group A streptococci in vivo: capturing regulatory networks engaged in sociomicrobiology, niche adaptation, and hypervirulence. *PLoS ONE* 5: e9798.

Ball SL, Siou GP, Wilson JA, Howard A, Hirst BH, Hall J. (2007). Expression and immunolocalisation of antimicrobial peptides within human palatine tonsils. *J Laryngol Otol.* Oct;121(10):973-8.

Banks DJ, Beres SB, and Musser JM. (2002). The fundamental contribution of phages to GrAS evolution, genome diversification and strain emergence. *Trends in Microbiology.* 10:515-521.

Banks, D.J., S.F. Porcella, K.D. Barbian, S.B. Beres, L.E. Philips, J.M. Voyich, F.R. DeLeo, J.M. Martin, G.A. Somerville, & J.M. Musser. (2004). Progress toward characterization of the group A Streptococcus metagenome: complete genome sequence of a macrolide-resistant serotype M6 strain. *Journal of Infectious Diseases.* 190: 727 – 738.

Barnham M, Weightman N, Anderson A, Pagan F, Chapman S. (1999). Review of 17 cases of pneumonia caused by *Streptococcus pyogenes*. *Eur J Clin Microbiol Infect Dis,* 18(7):506-509.

Beachey, EH, and Ofek I. **(**1976). Epithelial cell binding of group A streptococci by lipoteichoic acid on fimbriae denuded of M protein. *J. Exp. Med*. 143**:**759–771.

Beachey, EH. Courtney. (1987). Bacterial adherence: the attachment of group A streptococci to mucosal surfaces, *Rev. Infect. Dis.* 9 (Suppl. 5):475-481.

Bell S, Howard A, Wilson JA, Abbot EL, Smith WD, Townes CL, Hirst BH, Hall J. (2012). *Streptococcus pyogenes* infection of tonsil explants is associated with a human beta-defensin 1 response from control but not recurrent acute tonsillitis patients. *Molecular Oral Microbiology* 27:160–171.

Beres SB, and Musser JM. (2007) Contribution of exogenous genetic elements to the group A Streptococcus metagenome. *PLoS ONE.* 2:e800.

Bessen DE, Lizano S. (2010). Tissue tropisms in group A streptococcal infections *Future Microbiol.* 5(4): 623–638.

Bessen DE, Kumar Nikhil, Hall G, Riley DR, Luo F*, et al* (2011). Whole-Genome association study on tissue tropism phenotypes in group A Streptococcus. *J Bacteriology*. 193(23):6651-63.

Bessen DE, Sotir CM, Readdy TL, Hollingshead SK. (1996). Genetic correlates of throat and skin isolates of group A streptococci. *J Infect Dis* 173: 896–900.

Bisno AL, Rubin FA, Cleary PP, Dale JB. (2005). Prospects for a group A steptococcal vaccine: rationale, feasibility, and obstacles—report of a national institute of allergy and infectious diseases workshop. *Clin Infect Dis* 41: 1150–1156.

Bisno AL. (2001) Acute pharyngitis. *N Engl J Med*. 344:205-11.

Brock SC, McGraw PA, Wright PF, Crow JE. (2002). The Human Polymeric Immunoglobulin Receptor Facilitates Invasion of Epithelial Cells by *Streptococcus pneumoniae* in a Strain-Specific and Cell Type-Specific Manner. *Infect Immun*. 70(9): 5091–5095.

Broudy, T.B., V. Pancholi, & V.A. Fischetti. (2001) Induction of lysogenic bacteriophage and phage-associated toxin from group A streptococci during coculture with human pharyngeal cells. *Infection and Immunity.* 69:1440- 1443.

Broudy, T.B., V. Pancholi, & V.A. Fischetti. (2002) The *in vitro* interaction of *Streptococcus pyogenes* with human pharyngeal cells induces a phage- encoded extracellular DNase. *Infection and Immunity.* 70:2805-2811.

Carapetis JR, Steer AC, Mulholland EK, Weber M. (2005).The global burden of group A streptococcal diseases. *Lancet Infect Dis* 5: 685–694.

Chaussee MS, Watson, RO, Smoot, JC, and Musser, JM. (2001) Identification of Rgg-regulated exoproteins of *Streptococcus pyogenes*. *Infect Immun* 69: 822–831.

Clark MA, Wilson C, Sama A, Wilson JA, Hirst BH. (2000). Differential cytokeratin and glycoconjugate expression by the surface and crypt epithelia of human palatine tonsils. *Histochem Cell Biol.* 114(4):311–321.

Collin M, and Olsen A. (2001). EndoS, a novel secreted protein from *Streptococcus pyogenes* with endoglycosidase activity on human IgG. *EMBO J*. 20:3046–3055.

Courtney, HS, and Hasty, DL. (1991). Aggregation of group A streptococci by human saliva and effect of saliva on streptococcal adherence to host cells. *Infect Immun* 59**:** 1661–1666.

Cue D, Southern SO, Southern PJ, Prabhakar J, Lorelli W, Smallheer JM, Mousa SA, and Cleary PP (2000). A nonpetide integrin antagonist can inhibit epithelial cell ingestion of *Streptococcus pyogenes* by blocking formation of integrin α5β1-fibronectin-M1 protein complexes. *Proc Natl Acad Sci* 97(6): 2858–2863.

Cunningham, MW (2000). Pathogenesis of a group A streptococcal infections. C*lin. Microbiol. Rev.* 13:470–511.

Cunningham, MW (2012). Streptococcus and rheumatic fever. *Curr Opin Rheumatol.* 2012, 24:408-416.

Donnelly LE. (2001) Airway Epithelial Cells (Primaries vs Cell Lines) *Methods Mol Med* 56:127-36.

Ebell MH, Smith MA, Barry HC, Ives K, Carey M. (2000). Does this Patient Have Strep Throat? *J Amer Med Assoc.* 284(22):2912-2918.

Ellen RP and Gibbons RJ. (1974). Parameters affecting the adherence and tissue tropism of Streptococcus pyogenes. *Inf Imm* 9:84-91.

Effat KG and Milad M (2007). Comparative study of palatine tonsil histology in mammals, with special reference to tonsillar salivary glands. *J of Laryng & Otol* 121, 468–471.

Euler, C. (2010). The role of lysogenic bacteriophage in virulence and survival of *Streptococcus pyogenes.* Doctoral Dissertation, The Rockefeller University, New York, NY.

Facklam R, Beall B, Efstratiou A, Fischetti V, Johnson D, Kaplan E et al. (1999). Emm typing and validation of provisional M types for group A streptococci. *Emerg Infect Dis* 5: 247–253.

Falugi F., C. Zingaretti, V. Pinto, M. Mariani, L. Amodeo, A. G. Manetti, S. Capo, J. M. Musser, G. Orefici, I. Margarit, J. L. Telford, G. Grandi, and M. Mora. (2008). Sequence variation in group A Streptococcus pili and asso- ciation of pilus backbone types with Lancefield T serotypes. *J. Infect. Dis.* 198:1834–1841

Fischetti VA, Jones KF, Manjula BN, Scott, JR. (1984).Streptococcal M6 Protein Expressed in *Escherichia coli. J Exp Med.* 159:1083-1095.

Fischetti VA. (2000) in Gram-positive pathogens (Fischetti, V. A., Novick, R. P., Ferretti, J. J., Portnoy, D. A., and Rood, J. I., eds) pp. 11–24, ASM Press, Washington, D. C.

Fischetti VA. (2005). Bacteriophage lytic enzymes: novel anti-infectives. *Trends Microbiol.* 13:491–496.

Fischetti, VA, Gotschlich, EC, Bernheimer, AW. (1971). Purification and physical properties of Group C streptococcal phage-associated lysin. *J Exp Med* 133: 1105-1117.

Fluckiger U, Jones KF, and Fischetti VA. **(**1998). Immunoglobulins to group A streptococcal surface molecules decrease adherence to and invasion of human pharyngeal cells. *Infect. Immun*. 66**:**974–979.

Gates GA, Folbre TW. (1986). Indications for adenotonsillectomy. *Arch Otolaryngol Head Neck Surg*;112:501-2.

Greco R, DeMartino L, Donnarumma G, Conte MP, Seganti L, and Valenti P. **(**1995). Invasion of cultured human cells by *Streptococcus pyogenes*. *Res. Microbiol*. 146:5551–5560.

Hauser AR, Stevens DL, Kaplan EL, and Schlievert PM. (1991). Molecular analysis of pyrogenic exotoxins from *Streptococcus pyogenes* isolates associated with toxic shock-like syndrome. *J. Clin. Microbiol.* 29:1562– 1567.

Hokonohara M, Yoshinaga M, Inoue H, Haraguchi T, Miyata K. (1988).Experimental studies on the initial focus of invasion of group A streptococci. *Acta Otolaryngol Suppl*. 454:192-6

Jadoun J, Ozeri V, Burstein E, Skutelsky E, Hanski E, and Sela S. (1998). Protein F1 is required for efficient entry of *Streptococcus pyogenes* into epithelial cells. *J. Infect. Dis*. 178:147–158.

Johnson DR, Kaplan EL, VanGheem A, Facklam RR, Beall B. (2006). Characterization of group A streptococci (*Streptococcus pyogenes*): correlation of M-protein and emm-gene type with T-protein agglutination pattern and serum opacity factor. *J Med Microbiol* 55: 157–164.

Juncosa B. (2012). The dynamic *Streptococcus pyogenes* transcriptome in the host cell environment and contributions by phage. Doctoral Dissertation, The Rockefeller University, New York, NY.

Kaplan EL. (1996). Recent Epidimiology og Group A Streptococcal Infections in North America and Abroad: An Overview. Pediatrics 97:945-48.

Kaplan EL. (2009). Some Things Never Change! *Clin Inf Dis* 48:1220-1222.

Kiska DL, Thied, B, Caracciolo, J, Jordan, M, Johnson, D, Kaplan, EL, Gruninger, RP, Lohr, JA, Gilligan, P H and Denny, FW, Jr. (1997). Invasive Group A Streptococcal Infections in North Carolina: Epidemiology, Clinical Features, and Genetic and Serotype Analysis of Causative Organisms. *J. Infect. Dis.* 176, 992–1000.

Klenk M, Nakata M, Podbielski A, Skupin B, Schroten H and Kreikemeyer B. (2007). *Streptococcus pyogenes* serotype-dependent and independent changes in infected HEp-2 epithelial cells. *The ISME Journal* 1, 678–692.

Koltai PJ, Solares CA, Mascha EJ, Xu M. (2002). Intracapsular partial tonsillectomy for tonsilar hypertrophy in children'. *Laryngoscope* 112 (8 Suppl 100):17-9.

Kreikemeyer B, Nakata M, Oehmcke S, Gschwendtner C, Normann J, and Podbielski A. (2005). *Streptococcus pyogenes* collagen type I-binding Cpa surface protein: Expression profile, binding characteristics, biological functions, and potential clinical impact. *J Biol Chem* 280:
33228–33239.

Kunitomo E., Terao Y, Okamoto S, Rikimaru T, Hamada S, and Kawabata S. (2008). Molecular and biological characterization of histidine triad protein in group A streptococci. *Microbes and Infection.* 10:414-423.

Lancefield RC and Dole VP. (1946). The properties of T antigens extracted from Group A Streptococci. *J Exp Med* 71:449-471.

Lancefield RC and Perlmann. (1952). Preparation and properties of a protein (R antigen) occurring in streptococciof group A streptococci of group A, type 28, and in certain streptococciof other serological groups. *J Exp Med* 96:83-97.

LaPenta D, CRubens, E. Chi, and Cleary PP. (1994). Group A streptococci efficiently invade human respiratory epithelial cells. *Proc. Natl. Acad. Sci.* USA 91:12115–12119.

Lilja M, Silvola J, Räisänen S, Stenfors LE. (1994).Where are the receptors for *Streptococcus pyogenes* located on the tonsillar surface epithelium? *Int J Pediatr Otorhinolaryngol.* 15;50(1):37-43.

Little P and Williamson I. (1996). Sore throat management in general practice. *Fam Pract* 13: 317–321.

Livezey J, Perez L, Suciu D, Yu X, Robinson B, Bush D, and Merrill G. (2011) Analysis of group A Streptococcus gene expression in humans with pharyngitis using a microarray. *Journal of Medical Microbiology.* 60:1725**-** 1733.

Lory S, Jin S, Boyd JM, Rakeman JL & Bergman P (1996). Differential gene expression by *Pseudomonas aeruginosa* during interaction with respiratory mucus. *Am J Respir Crit Care Med* 154: S183–186.

Lyon W R, Madden JC, Levin JC, Stein JL, & Caparon MG. (2001). Mutation of *luxS* affects growth and virulence factor expression in *Streptococcus pyogenes. Molecular Microbiology.* 42:145-157.

Maher DM, Zhang ZQ, Schacker TW and Southern PJ. (2005) Ex Vivo Modeling of Oral HIV Transmission in Human Palatine Tonsil. *J Histoch and Cytoch* 53 (5):631-642.

Manetti AGO, Zingaretti C, Falugi F, Capo S, Bombaci M, Bagnoli F, Gambellini G, Bensi G, Mora M, Edwards AM, Musser JM, Graviss EA, Telford JL, Grandi G, and Margarit I. (2007). *Streptococcus pyogenes* pili promote pharyngeal cell adhesion and biofilm formation. *Mol Microb* 64(4), 968–983

Moutsopoulos NM, Nares S, Nikitakis N, Rangel Z, Wen J, Munson P, Sauk J, Wahl S. (2007). Tonsil Epithelial Factors May Influence Oropharyngeal Human Immunodeficiency Virus Transmission. *Am J Pathol* 171:571-579.

Nelson D, Loomis L, Fischetti VA (2001). Prevention and elimination of upper respiratory colonization of mice by group A streptococci by using a bacteriophage lytic enzyme. *Proc Natl Acad Sci* U S A 98: 4107–4112.

Nelson DC, Schuch R, Chahalez P, Zhu S,Fischetti VA. (2006). PlyC: A multimeric bacteriophage lysin. *Proc Natl Acad Sci* 103:-10765-10770.

Nelson, DC, Garbe J, & Collin M. (2011). Cysteine protease SpeB from *Streptococcus pyogenes—a* potent modifier of immunologically important host and bacterial proteins. *Journal of Biological Chemistry.* 392:1077-1088.

Nelson, K., P. M. Schlievert, R. K. Selander, and J. M. Musser. (1991). Characterization and clonal distribution of four alleles of the *speA* gene encoding pyrogenic exotoxin A (scarlet fever toxin) in *Streptococcus pyogenes. J. Exp. Med.* 174:1271–1274.

Nimishikavi S, Stead L. (2005). Images in Clinical Medicine: Streptococcal Pharyngitis. *New England Journal of Medicine*. 352;11, e10.

Nobbs, A.H., R.J. Lamont, & H.F. Jenkinson. (2009) Streptococcus adherence and colonization. *Microbiology and Molecular Biology Reviews.* 73:407-450.

Olsen RJ, Shelburne SA, Musser JM. (2009). Molecular mechanisms underlying group A streptococcal pathogenesis. *Cell Microbiol*. Jan;11(1):1-12.

Omary MB, Ku NO, Strnad P, Hanada S. (2009). Toward unraveling the complexity of simple keratins in human disease. *J Clin Inv.* 119(7):1794-1805.

Osterlund A, Popa R, Nikkila T, Scheynius A & Engstrand L (1997). *Laryngoscope* 107, 640–647.

Osterlund A, and Engstrand L. (1995). Intracellular Penetration and Survival of *Streptococcus pyogenes* in Respiratory Epithelial Cells In Vitro. *Acta Otolaryngol* (Stockh) 1 15: 685-688.

Paoletti LC, Madoff LC, Kasper DL. (2000). in *Gram-Positive Pathogens* (Fischetti, V A., Novick, RP, Ferretti, JJ, Portnoy, DA, and Rood J I, eds) p. 145, ASM Press, Washington, D. C.

Pancholi, V., & VA Fischetti. (1992). A major surface protein on group A streptococci is a glyceraldehyde-3-phosphate-dehydrogenase with multiple binding activity. *Journal of Experimental Medicine.* 176:415-426.

Pancholi, V., and VA Fischetti. (1993). Glyceraldehyde-3-phosphate dehydrogenase on the surface of group A streptococci is also an ADP-ribosylating enzyme. *Proc. Natl. Acad. Sci*. USA 90:8154–8188.

Park HS, Francis KP, Yu J, Cleary P. (2003). Membranous Cells in Nasal-Associated Lymphoid Tissue: A Portal off Entry for the Respiratory Mucosal Pathogen Group A Streptococcus*. J immunology* 171(5):2532-2537.

Pavone P, Parano E, Rizzo R, Trifiletti RR. (2006). Autoimmune Neuropsychiatric Disorders Associated with Streptococcal Infections: Sydenham Chorea, PANDAS, and PANDAS variants. *J Child Neurol* 21:727–736.

Pegtel DM, Middeldorp J, and Thorley-Lawson DA. (2004). Epstein-Barr Virus Infection in *Ex Vivo* Tonsil Epithelial Cell Cultures of Asymptomatic Carriers *Journal of Virology*, 78(22):12613-12624.

Perry ME. (1994) The Specialized structure of crypt epithelium in the human palatine tonsil and its functional significance. *J Anat* 185:111-127.

Perry ME and Whyte A. (1998). Immunology of the tonsils. *Immunol Today*. 19(9):414-21

Peterson WD Jr, Stulberg CS, Simpson WF. (1971). A permanent heteroploid human cell line with type B glucose-6-phosphate dehydrogenase. *Proc. Soc. Exp. Biol.Med.* 136: 1187.

Pichichero ME. (1991). The rising incidence of penicillin treatment failures in group A streptococcal tonsillopharyngitis: an emerging role for the cephalosporins? *Pediatr Infect Dis J* 10(Suppl):50S–5S.

Pichichero ME (2007). Systematice Review of Factors contributing to penicillin treatment failure in *Streptococcus pyogenes* pharyngitis, *Otolaryngology Head & Kneck Surgery* 137(6):851-857.

Pries R Wittkopf N, Trenkle T, Nitsch SM and Wollenberg B. (2008). Potential Stem Cell Marker CD44 is Constitutively Expressed in Permanent Cell Lines of Head and Neck Cancer *in vivo* 22: 89-92.

Ribardo DA and McIver (2003). amrR encodes a putative membrane protein necessary for maximal exponential phase expression of the Mga virulenceregulon in *Streptococcus pyogenes. Mol Micro* 50(2):673-685.

Roberts AL, Connolly KL, Kirse DJ, Evans AK, Poehling KA, Peters TR and Reid SD. (2012). Detection of group A Streptococcus in tonsils from pediatric patients reveals high rate of asymptomatic streptococcal carriage. *BMC Pediatrics* 12:3.

Ryan PA, Pancholi V, Fischetti VA (2001). Group A streptococci bind to mucin and human pharyngeal cells through sialic acid-containing receptors. *Infect Immun* 69: 7402–7412.

Ryan PA, Kirk BW, Euler CW, Schuch R, Fischetti VA (2007). Novel algorithms reveal streptococcal transcriptomes and clues about undefined genes. *PLoS Comput Biol* 3(7): e132.

Schappert SM, Rechtsteiner EA. (2011). Ambulatory medical care utilization estimates for 2007. National Center for Health Statistics. *Vital Health Stat* 13(169).

Schwaab M, Gurr A, Hansen S, Minovi AM, Thomas JP, Sudhoff H, and Dazert S. (2010). Human ß-Defensins in different states of diseases of the tonsilla palatina, *Eur Arch Otorhinolaryngol* 267:821-830.

Semino-Mora C, Doi SQ, Marty A, Simko V, Carlstedt I & Dubois A. (2003). Intracellular and interstitial expression of *Helicobacter pylori* virulence genes in gastric precancerous intestinal metaplasia and adenocarcinoma. *J Infect Dis* 187:1165–1177.

Shea PR, Virtaneva K, Kupko JJ, Porcella SF, Barry WT, Wright FA, Kobayashi SD, Carmody A, Ireland RM, Sturdevant DE, Ricklefs SM, Babar I, Johnson CA, Graham MR ,et al. (2010) Interactome analysis of longitudinal pharyngeal infection of cynomolgus macaques by group A Streptococcus*. Proceedings of the National Academy of Sciences.* 107:4693-4698.

Shelburne SA, Sumby P, Sitkiewicz I, Granville CN, DeLeo FR, and Musser JM. (2005). Central role of a two-component gene regulatory system of previously

unknown function in pathogen persistence in human saliva. *Proc Natl Acad Sci USA* 102: 16037–16042.

Shelburne SA, Granville C, Tokuyama M, Sitkiewicz I, Patel P, and Musser JM. (2005). Growth characteristics of and virulence factor production by group A Streptococcus during cultivation in human saliva. *Infect Immun* 73: 4723–4731.

Smith WD, Pointon JA, Abbot E, Kang HJ, Baker EN, Hirst BH, Wilson JA, Banfield MJ, and Kehoe M. (2010) *J. Bacteriol.*, 192(18):4651.

Spencer DJ and Jones JE. (2012). Complications of Adenotonsillectomy in Patients Younger than 3 Years. *Arch Head Kneck Surg.* 138(4):335-339.

Sumby, P, Tart, AH, and Musser, JM. (2008). A non-human primate model of acute group a Streptococcus pharyngitis. *Methods Mol Biol* 431: 255–267.

Sutcliffe et al. (2008) Bioinformatic insights into the biosynthesis of the Group B carbohydrate in *Streptococcus agalactiae* M*icrobiology* 154(5): 1354-1363.

Swift HF, Wilson AT, Lancefield RC. (1943). Typing group A hemolytic streptococci by M pecipitin reactions in pipettes. *J Exp Med*. 78:127-133.

Takebayashi S, Hickson A, Ogawa T, Jung KY, Mineta H, Ueda Y, Grénman R, Fisher SG, Carey TE. (2004). Loss of chromosome arm 18q with tumor progression in head and neck squamous cancer. *Genes Chromosomes Cancer* 41 (2) 145-154.

TeraoY, Kawabata S, Kunitomo E, Murakami J, Nakagawa I, and Hamada S. (2001). Fba, a novel fibronectin-binding protein from *Streptococcus pyogenes,* promotes bacterial entry into epithelial cells, and the *fba* gene is positively transcribed under the Mga regulator. *Mol. Microbiol.* 42:75–86.

Virtaneva K, Graham MR, Porcella SF, Hoe NP, Su H, Graviss EA, Gardner TJ, Allison JE, Lemon WJ, Bailey JR, Parnell MJ, and Musser JM. (2003). Group A Streptococcus gene expression in humans and cynomolgus macaques with acute pharyngitits. *Infection and Immunity*. 71:2199-2207.

Wang B, Li S, Southern PJ, and Cleary PP. (2006) Streptococcal modulation of cellular invasion via TGF-beta1 signaling. *Proc Natl Acad Sci* USA 103: 2380–2385.

Wang B, Yurecko RS, Dedhar S, and Cleary PP. (2006). Integrin-linked kinase is an essential link between integrins and uptake of bacterial pathogens by epithelial cells. *Cell Microbiol* 8: 257–266.

Wannamaker LW. (1970). Differences between streptococcal infections of the throat and of the skin. *N Engl J Med*. 282:23–31.

Want EI, Cravett, Siuzdak G. (2005). The expanding role of mass spectrometry in metabolite profiling and characterization. *ChemBioChem* 6:1941-1951

Weeks CR, and Ferretti JJ. (1986). Nucleotide sequence of the type A streptococcal exotoxin (erythrogenic toxin) gene from *Streptococcus pyogenes* bacteriophage T12. *Infect. Immun*. 52:144–150.

Wishart DS, Knox C, Guo AC, Eisner R, Young N, Gautam B, Hau DD, Psychogios N, *et al.* (2009). HMDB: a knowledgebase for the human metabolome. *Nucleic Acids Res*. 37(Database issue):D603-610

Yeates TO and Clubb RT. (2007). How Some Pili Pull. *Science*, 318:1558-1559.

Yesilkaya H, Manco S, Kadioglu A, Terra VS, Andrew PW. (2008). The ability to utilize mucin affects the regulation of virulence gene expression in *Streptococcus pneumoniae*. *FEMS Microbiol Lett* 278:231-235.

Zahner D, and Scott JR. (2008). SipA is required for pilus formation in *Streptococcus pyogenes* serotype M3. *Journal of Bacteriology.* 190:527-535.

Zhang X, Rimpiläinen M, Simelyte E, Toivanen P. (2001). Characterisation of Eubacterium cell wall: peptidoglycan structure determines arthritogenecity. *Ann Rheum Dis* 60:269-274.

www.cdc.gov/ncidod/dbmd/diseaseinfo/groupastreptococcal_t.htm